

personal buildup for

Force Motors Limited Library



mtzw 3/2015, as epaper released on 30.01.2015
<http://http://www.mtz-worldwide.com>

content:

page 1: Cover. p.1

page 2: Contents. p.2

page 3: Editorial. p.3

page 4: Dieseleinspritzung. p.4-9

page 10: Klopfsimulation. p.10-15

page 16: Pruefstand. p.16-21

page 22: Eisenguss. p.22-27

page 28: Hybrid_Virtual. p.28-33

page 34: Turbogeraeusche. p.34-39

page 40: Festigkeit. p.40-43

page 44: Imprint. p.44

page 45: Peer_Review. p.45

page 46: Elektrisch_uni_wien. p.46-52

copyright

The PDF download of contributions is a service for our subscribers. This compilation was

created individually for Force Motors Limited Library. Any duplication, renting, leasing, distribution and publicreproduction of the material supplied by the publisher, as well as making it publicly available, is prohibited without his permission.

MTZ

WORLDWIDE

03 March 2015 | Volume 76

personal buildup for Force Motors Limited Library

COVER STORY

Mixture Formation and Combustion

SHIFTING

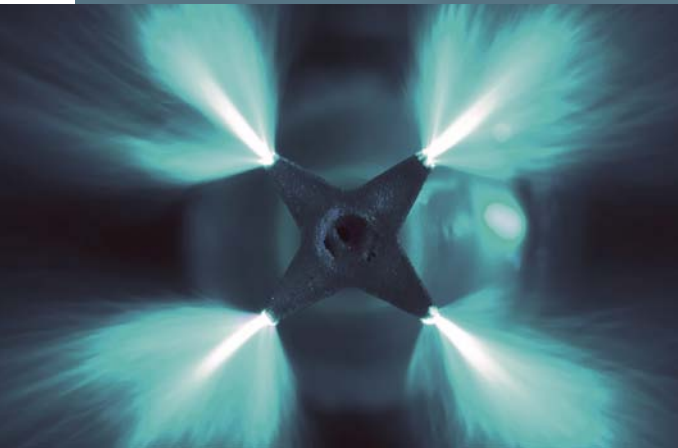
Chassis Dynamometer Tests
to the Engine Test Bench

LIGHTWEIGHT DESIGN

of Cast Iron Cylinder Blocks

NUMERICAL

Optimisation of Electro Hybrid
Powertrains



COVER STORY

Mixture Formation and Combustion

Work on the combustion process and upstream mixture formation will remain a key component of the further development of internal combustion engines in the future. The reasons for this include increasingly strict emissions standards that will apply to further engine operating ranges in future and ambitious CO₂ targets. Further developments of the engine and subsystems that result from this will not be able to achieve their full potential until the combustion process has been suitably adapted. Our cover story describes measures to optimise mixture formation and combustion in diesel and spark-ignition engines.

4 Improved Combustion in Diesel Engines by Injection Rate Shaping

Barbara Graziano, Benedikt Heuser [RWTH Aachen University], Paul Grzeschik [FEV]

10 New Approach to Determine the Knock Onset Angle

Andrea Marchi, Ioannis Vlaskos, Georgios Bikas [Ricardo]

DEVELOPMENT

ON-BOARD DIAGNOSTICS

- 16 Shifting Chassis Dynamometer Tests to the Engine Test Bench
Stephan Krämer, Christian Landgraf, Gianni Di Martino, Martin Meiß [APS-technology]

CYLINDER BLOCK

- 22 Lightweight Design of Cast Iron Cylinder Blocks
Helfried Sorger, Wolfgang Schöffmann [AVL], Wilfried Wolf, Wilhelm Steinberg [Fritz Winter Eisengießerei]

ACOUSTICS

- 28 Analysis of Vibrations in Powertrains Using Simulation Support
Josef Girstmair, Anton Fuchs [Virtual Vehicle]
- 34 Appearance and Effects of Turbocharger Noise
Robert Hanisch [Mann+Hummel]

SUPERCHARGING

- 40 Optimising Thermomechanical Strength of High-load Turbochargers
Michael Werner, Florian Jurecka [Dassault Systèmes]

RESEARCH

- 45 Peer Review

SOFTWARE

- 46 Numerical Optimisation of Electro Hybrid Powertrains
Thorsten Krenek, Christopher Bacher, Günther Raidl, Thomas Lauer [Vienna University of Technology]

RUBRICS | SERVICE

- 3 Editorial
44 Imprint, Scientific Advisory Board

COVER FIGURE © Bosch
FIGURE ABOVE © Federal-Mogul

Shaping the Transition

Dear Reader,

Legislation will dramatically change the automotive landscape in the medium and long term, with increasing requirements concerning exhaust aftertreatment, the phasing out of the reduced mineral oil tax rate by the end of 2018 and above all due to progress in fully electric or electrified vehicles.

The Shell Passenger Car Scenarios predict that the fleet of vehicles with an electric propulsion system will grow to a total of 10.1 million by 2040, while the number of petrol- or diesel-powered vehicles will fall to 30.7 million in the same period. McKinsey's report even includes one scenario predicting that only around 5 % of vehicles will have an internal combustion engine in 2050. So does that mean that everything speaks in favour of electric powertrains? Not really, because added to the 31 million internal combustion powertrains of the Shell study are a further 5.5 million plug-in hybrids, while McKinsey forecasts a share of 35 % for PHEVs. Internal combustion powertrains will therefore significantly determine our mobility even in three decades' time. Hydrogen fuel cell powertrains are at best still a distant vision, even though some analysts might be more optimistic. What is clear is that emissions of below 90 g CO₂/km are hardly possible without electrification or alternative fuels.

This means that, when it comes to the powertrain of the future, the fuel will be increasingly relevant. Even CNG, which is already on the market, is only a niche product in many countries – it makes up a mere 0.41 % of the fuel mix throughout Europe, as reported in ATZ 2/2015. To make matters worse, the clear benefit of CNG in a monovalent configuration can hardly be exploited, as CNG powertrains are generally designed as bivalent systems for cost reasons. Wouldn't it therefore make more sense to use LNG?

In addition to the development of alternative fuels from fossil energy sources or biomass, such as methanol, DME, OME, ethanol or PME, there is also the important question of whether power-to-gas can be the best solution. The environmental performance of CNG with and without additives or bioethanol speaks for itself, although the environmental impact of fuels produced by power-to-liquid technology using the same raw materials is not worse. These fuels have the further advantage that they can be globally distributed faster, more cheaply and more sustainably.

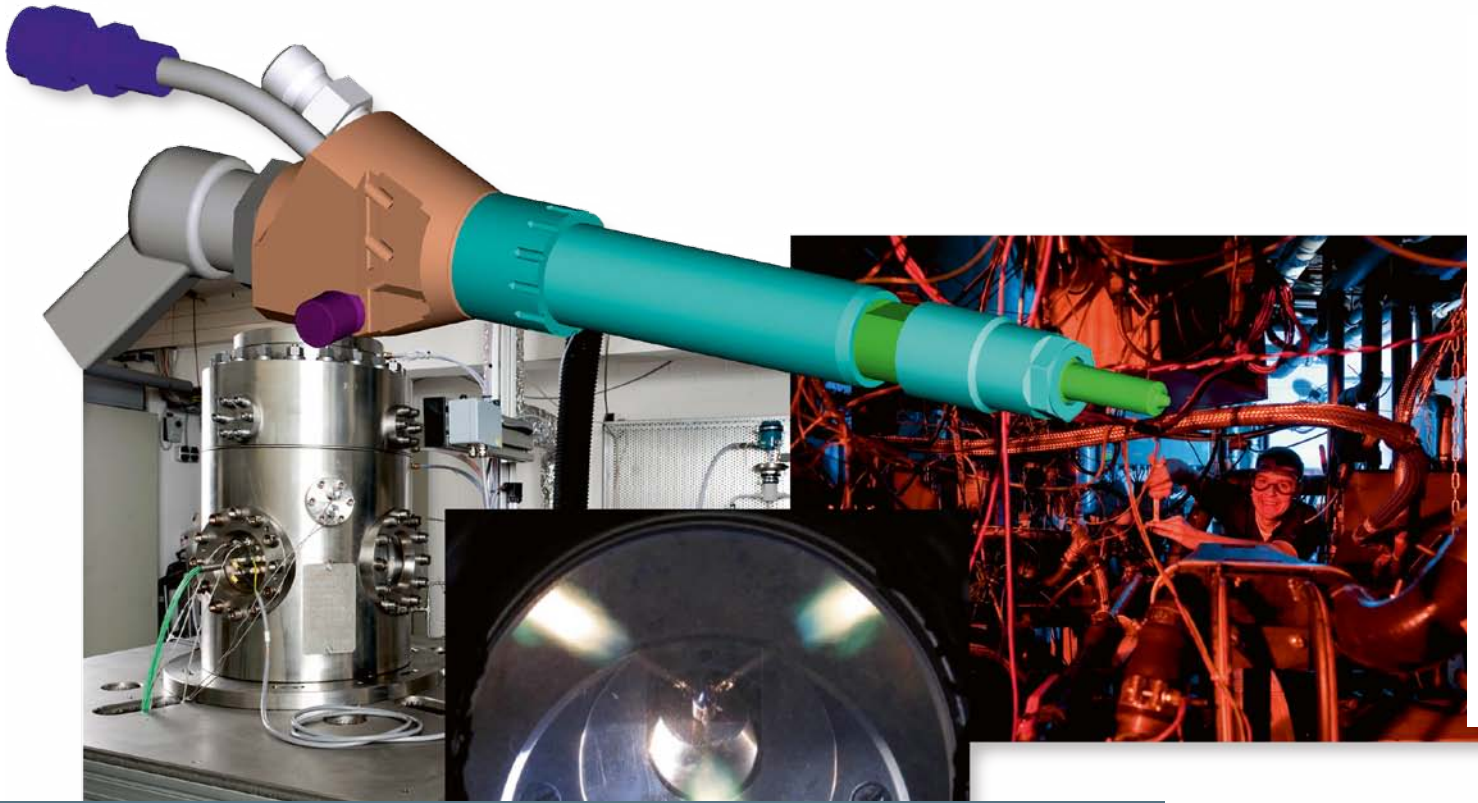
Fundamental decisions need to be taken to ensure that this intermediate step on the path towards electric mobility is successful, as a large number of different fuels would not be cost-effective for the industry and would hardly be accepted by consumers.

Best regards,



Dr. Alexander Heintzel, Editor in Chief
Wiesbaden, 8 January 2015





Improved Combustion in Diesel Engines by Injection Rate Shaping

The optimisation of fuel injection parameters remains a focal point in the further development of diesel engines. The Institute for Combustion Engines at RWTH Aachen University has developed a prototype injector that allows completely flexible injection rate shaping. Tests on the injector in a pressure chamber and on a single-cylinder research engine have shown the potential of improved injector needle opening times for achieving further reductions in emissions.

AUTHORS

**M. Sc. Barbara Graziano**

is Research Assistant at the Institute for Combustion Engines (VKA) at the RWTH Aachen University (Germany).

**Dipl.-Ing. Benedikt Heuser**

is Research Assistant at the Institute for Combustion Engines (VKA) at the RWTH Aachen University (Germany).

**Dipl.-Ing. Paul Grzeschik**

is Team Leader Engine Design at the FEV GmbH in Aachen (Germany).

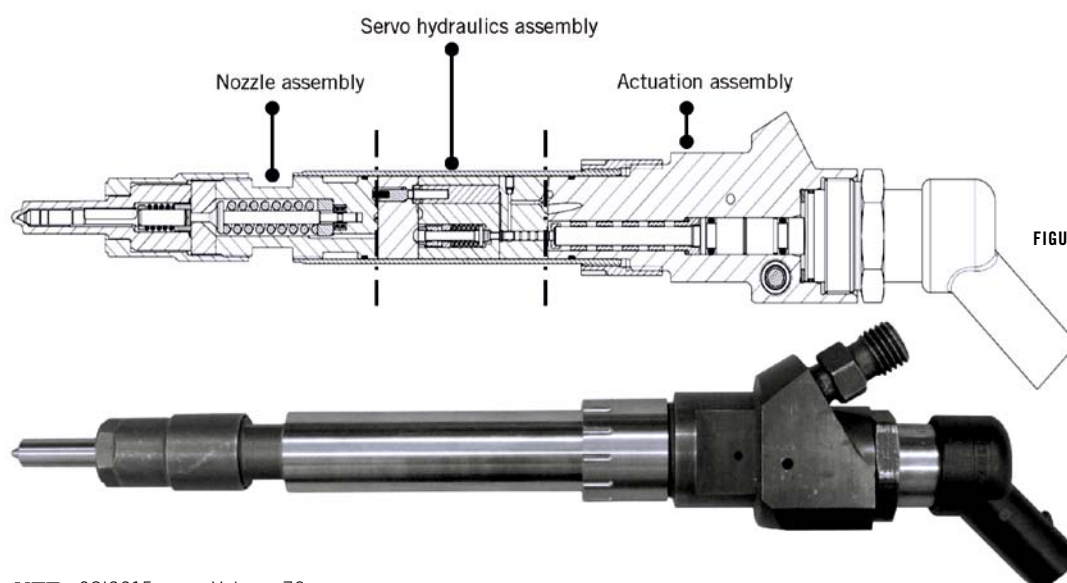
MOTIVATION

Efficient powertrain concepts represent an optimal solution to cope with the straightening of emission standard regulations regarding CO₂ emission and soot/NO_x trade-off. The intrinsic pollutant emissions of diesel engine pose a great challenge to meet present and future European emission standards. As an alternative to using complex and costly exhaust gas after treatment systems, pollutants can be reduced to a great extent by in-cylinder emission reduction. A substantial measure to reduce emissions is the improvement of mixture formation. This measure includes both air- and fuel-path optimisation. Optimised injection strategy coupled with digital rate shaping has led to a synergic reduction of both combustion noise and PM emissions [1, 2]. It was shown by Matsumoto et al. that the fuel injection system is one of the main determining factors in achieving these targets [3]. The present study aims at integrating a pressure modulation system into a standard-sized passenger car injector to overcome the challenge to realise rate shaping, maintaining the complexity of the injection system low. At the Institute for Combustion Engines of the RWTH Aachen University (VKA) a prototype injector, the HiFORS injector (High Pressure/Fast Opening/Rate Shaping), was designed to cope with a maximum injection pressure of 2500 bar, continuous rate shaping and fast needle opening. The HiFORS injector was designed

for completely flexible continuous rate shaping and shortest needle opening and closing times, in order to avoid needle seat throttling. Although the automotive industry goes towards discontinuous injection processes, a modular design overcomes the drawbacks of needle seat throttling on mixture formation, which are present in directly controlled injectors [4].

MODULAR CONCEPT OF THE HIFORS INJECTOR

The design of the HiFORS injector aimed at coupling a modular concept providing high layout flexibility for the use of the individual components with the functional flexibility of the injector. Thus, the individual injector functions were carried out by separate modules, **FIGURE 1**. The HiFORS injector is subdivided into three main parts: the actuation, the servo-hydraulics and the nozzle assembly. Each module is connected to the others with a clamping sleeve, ensuring a high contact pressure even at the maximum pressures. The actuation assembly is held by the connector body which carries the hydraulic fittings for high pressure inlets and drains, the electrical connections of the integrated sensors, and a piezo module as well. It is important to notice that the nozzle was taken from a serial production injector. Inside the connector body, the extension of the piezo-electric element is transmitted to the subsequent servo-hydraulics assembly by a transmission module.

**FIGURE 1** HiFORS injector [1]

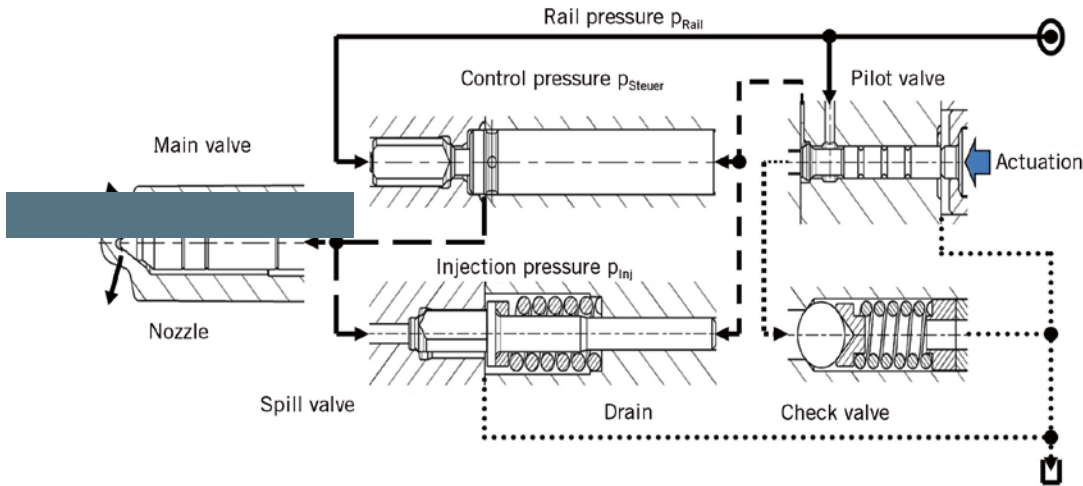


FIGURE 2 Servo-hydraulics assembly of the HiFORS injector [1]

The servo-hydraulics assembly depicted in **FIGURE 2** realises the injection free rate shaping. A pilot valve transmits the movement of the piezo module into a control volume, determining the control pressure (P_{ctrl}). The control pressure actuates the main valve, which supplies the injection pressure (P_{inj}) delivered into the nozzle assembly. The nozzle assembly consists of the nozzle module, the adapter plate and the nozzle holder including the nozzle spring. In addition, the nozzle holder has an integrated inductive needle lift sensor and a strain gauge based pressure sensor, enabling the rate shaping on the base of defined algorithms. The needle of the HiFORS always opens and closes very fast. In order to increase spray momentum and improve the mixture formation in particular at high load operating conditions, the throttle is located upstream of the needle.

MERITS OF FAST NEEDLE OPENING

The HiFORS injector was tested both in a high pressure vessel (HPV) and single

cylinder diesel engine (SCDE) for research applications. In **FIGURE 3**, a schematic of the HPV setup is given. Details of the optical experimental setup are given in former publications [5, 6].

The rate shaping experiments were conducted at an air pressure of 50 bar and at an air temperature of 800 K, reproducing diesel-like engine boundary conditions at the begin of injection during part load (PL) operations. Ramp, boot and squared injection profiles were tested for the HiFORS injector at different pressure levels of 1200 and 1800 bar. The ramp profiles were shaped for a fixed ramp duration of 1 ms independently of injection duration.

The optical technique adopted consisted of simultaneous OH*-chemiluminescence and shadowgraphy imaging in order to detect the Liquid Penetration Length (LPL), the Gaseous Mixing Length (GML) and the Lift-off Length LOL (i.e. the distance of the first ignition kernel downstream the injector nozzle). The HiFORS injector was tested against a reference series production piezo injector.

Thus, it was possible to point out the different injection performances of a standard needle seat throttling and the upstream throttling featured by the HiFORS injector. The results are presented in **FIGURE 4**. On the left side a variation of the injection profile is given for each measurement, whereas on the right side a variation of the injection pressure and boundary conditions is displayed. The energising duration for the HiFORS was calibrated to match the same fuel mass of the reference injector.

On the top in **FIGURE 4**, the LPL at time of ignition is given. With small amounts of fuel injected, the ignition occurs after the end of injection and no liquid fuel is present anymore. Generally for the same injected mass, the duration of injection increases at given rail pressure when shifting from a rectangular to the boot shape. When looking to the 1800 bar curves, all the different injection profiles allow a comparable penetration of the spray, with the exception of the boot shaped profile. This is due to the significantly reduced nozzle pressure at Start

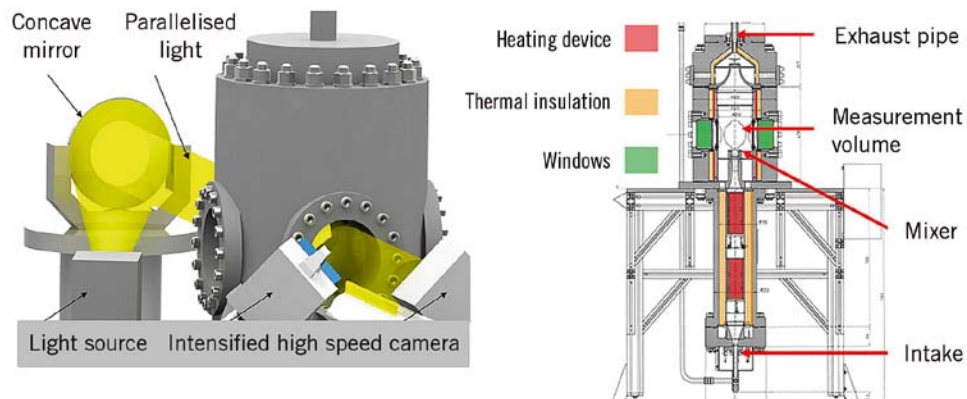


FIGURE 3 HPV set-up [5, 6]

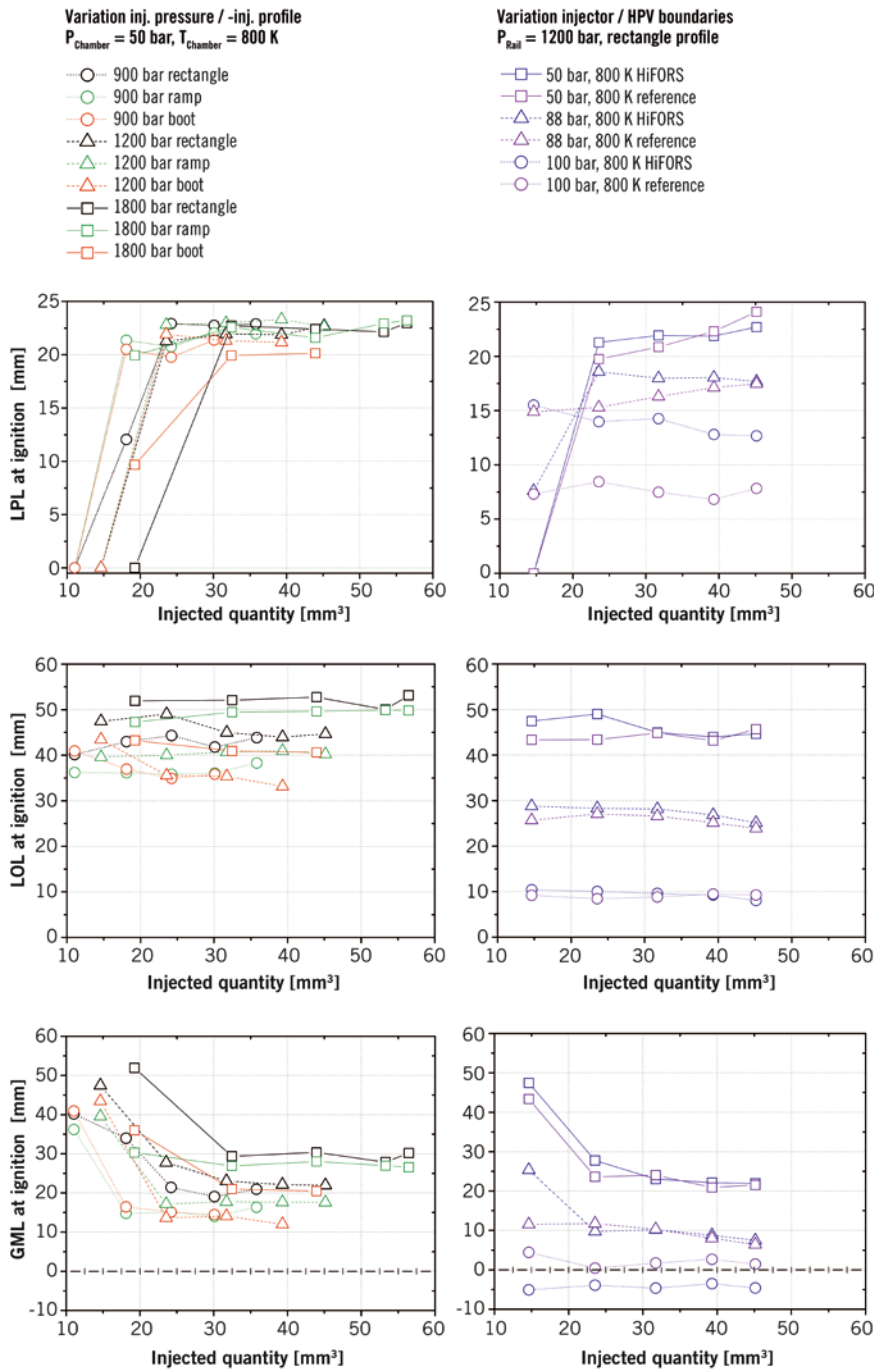


FIGURE 4 HPV test results: LPL, LOL and GML at time of ignition

of Injection (SOI) which lowers the nozzle outlet velocities. This trend is not observable at lower rail pressures, where the different injection strategies show same results. On the right hand side the LPL is analyzed for the same operating point, same injection profile and 1200 bar injection pressure over different operating conditions for a rectangular shaped injection rate. The first operating point (i.e. 50 bar at 800 K)

corresponds to a PL engine-like operating condition at event of injection, while the others correspond to high PL operating conditions. Both injectors perform similarly in terms of LPL of the spray, but the faster needle opening of the HiFORS allows the spray plume to develop faster for the same injected mass. This trend is more remarkable at higher loads.

On the middle plot in FIGURE 4 the LOL is depicted. In the first plot, the influ-

ence of the rate shaping on the LOL at different rail pressures is given. For the highest rail pressure, the rectangle injection profile shows the longest LOL, due to the higher nozzle pressure. When adopting the other injection profiles a reduction in LOL is observed; with decreasing injection pressure, the LOL becomes less sensitive to the injection profile chosen. As it can be concluded from the second plot from the left, the total LOL is predominantly influenced by the thermodynamic boundary conditions in the HPV; behaviour observed also in former works [5, 6, 7]. An increase in the LOL with the HiFORS injector is observable only in the lowest load condition. At higher pressures and temperatures, the spray of both injectors behaves almost equally. These measurements also prove that the LOL is rather independent of the injected fuel amount and injection duration.

The GML, namely the difference between LOL and LPL is plotted in the FIGURE 4 (bottom). According to the third graph from the left, high injection pressure and the rectangular shaped injection promote an increase in the GML, enhancing the air/fuel mixing process. This is due to the higher LOL achievable with the rectangular injection profile. As depicted by the graphs on the right, the HiFORS-injector contributes to higher GML at small amounts of injected fuel and low boundary conditions compared to the reference injector. This is caused by the faster needle opening and closing. However, at higher boundary conditions in the HPV, the difference between both injectors is negligible. Only at the highest boundary conditions the reference injector behaves slightly better in terms of GML due to its throttle in the needle seat.

BENCH TESTS ON A SINGLE-CYLINDER ENGINE

Based on these optical measurements it is expected that the HiFORS-injector has advantages at low engine load conditions compared to the reference injector with regards to the mixture formation process. At higher engine loads, the reference injector will benefit from the throttle in the needle seat, because of the shorter LPL at beginning of the injection event. Shorter LPL has the

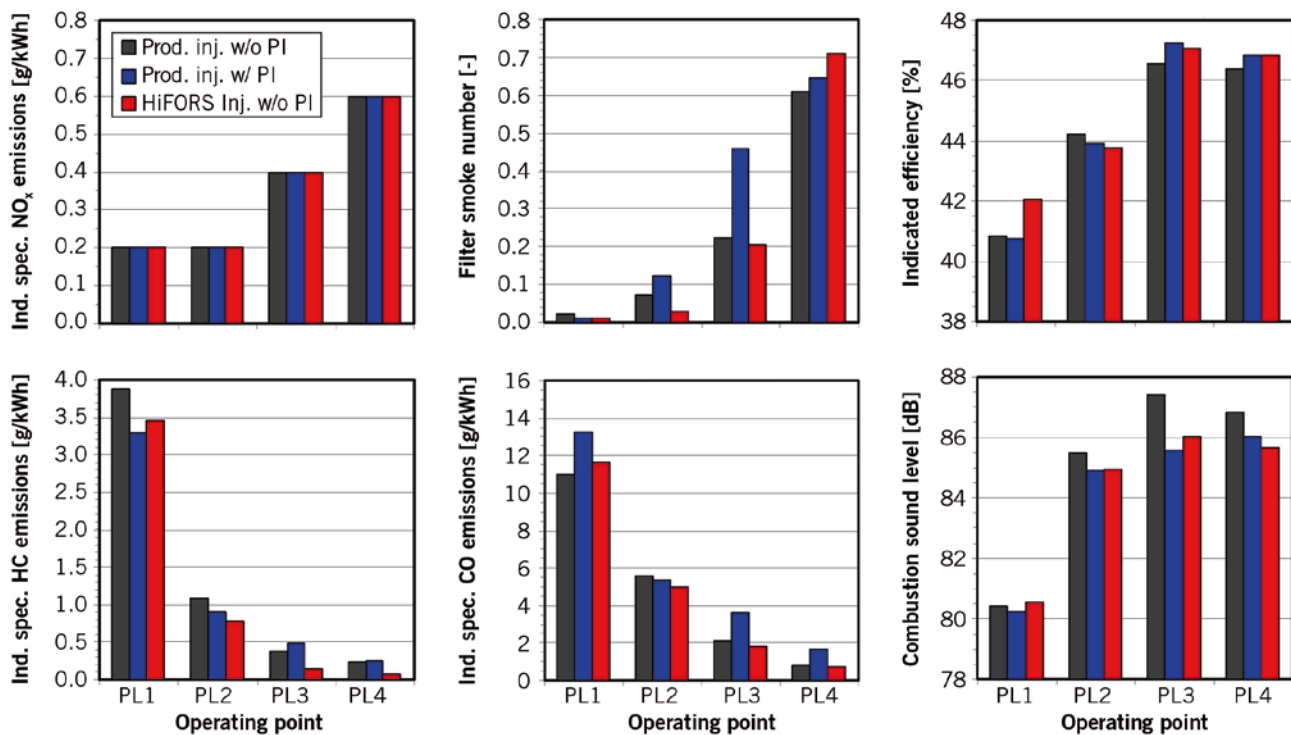


FIGURE 5 SCDE results at PL operation: HiFORS and reference injector compared for rectangular shaped injection profile

benefit that the liquid core does not extend into the combustion region, leading to a greater GML. If that compensates the advantages of a shorter injection duration with the HiFORS-injector cannot be stated on the basis of these optical measurements. For that reason, engine tests were carried out in succession. The engine investigations were carried out on a four-valve SCDE, 390 cm³ engine with a compression ratio of 15. The HiFORS injector was tested over four engine operating conditions representative of PLs within the New European Driving Cycle (NEDC) for a C-class vehicle. The engine calibration featured fixed centers of combustion of the engine's reference calibration with a close-to-production piezoelectrically driven servo injector, meeting EURO 6 NO_x emissions. The details of the engine calibration are described in former authors' works [7, 8]. The base

investigations were carried out in form of EGR sweeps at the four PLs, where the piezoelectrically actuated reference servo injector was tested with and without pilot injection (w/ PI and w/o PI) and the HiFORS injector w/o PI. The control of the reference injector was done by an open Engine Control Unit (ECU). **TABLE 1** lists the main engine calibration parameters.

As **FIGURE 5** summarises, the soot/NO_x trade-off could be improved compared to the reference injector without having drawbacks in terms of combustion noise or indicated efficiency by utilising a rectangle shaped injection profile. At the same NO_x level, the filter smoke number was reduced by up to 50 % with respect to those found with the reference injector. The emissions of unburned hydrocarbons (HC) and carbon monoxide (CO) could be reduced up to 70 % at medium to high PL operation. In the

trade-off of soot emissions and combustion noise a more favourable calibration was obtained without forfeiting low NO_x, HC and CO emissions and low fuel consumption.

CONCLUSIONS

The HiFORS injector is a highly flexible research tool to develop and test modern diesel combustion processes. The influence of injection rate profiles at different rail pressure on mixture formation and combustion was investigated at the HPV. The result of this investigation can be summarised as follows:

- The HiFORS injector allows a faster development of the spray at same injected mass.
- The HiFORS injector shows a positive influence of the fast needle opening on the mixture formation at 50 bar and 800 K.

| Operating point [-] | Engine speed [rpm] | IMEP [bar] | Rail pressure [bar] | Intake pressure [bar] | Center of combustion [°KW nZÖT] | NO _x target [g/KWh] |
|---------------------|--------------------|------------|---------------------|-----------------------|---------------------------------|--------------------------------|
| PL1 | 1500 | 4.3 | 720 | 1.07 | 5.8 | 0.2 |
| PL2 | 1500 | 6.8 | 904 | 1.50 | 6.6 | 0.2 |
| PL3 | 2280 | 9.4 | 1399 | 2.29 | 9.2 | 0.4 |
| PL4 | 2400 | 14.8 | 1800 | 2.60 | 10.8 | 0.6 |

TABLE 1 Engine load points of the SCDE [7, 8]

- High injection pressure coupled with square shaped profile enhances the air/fuel mixing for the HiFORS injector.
- HiFORS injector contributes to higher gaseous mixing length at small amounts of injected mass.

The impact of the HiFORS injector on engine operation was analysed at a SCDE against a piezoelectrically actuated servo injector with identical nozzle layout. The engine testing has proved that the new injector has a NO_x /soot trade-off on the level of production piezo injector with a single main injection, a combustion sound level similar to production piezo injector with pilot injection and reduced HC and CO emissions.

REFERENCES

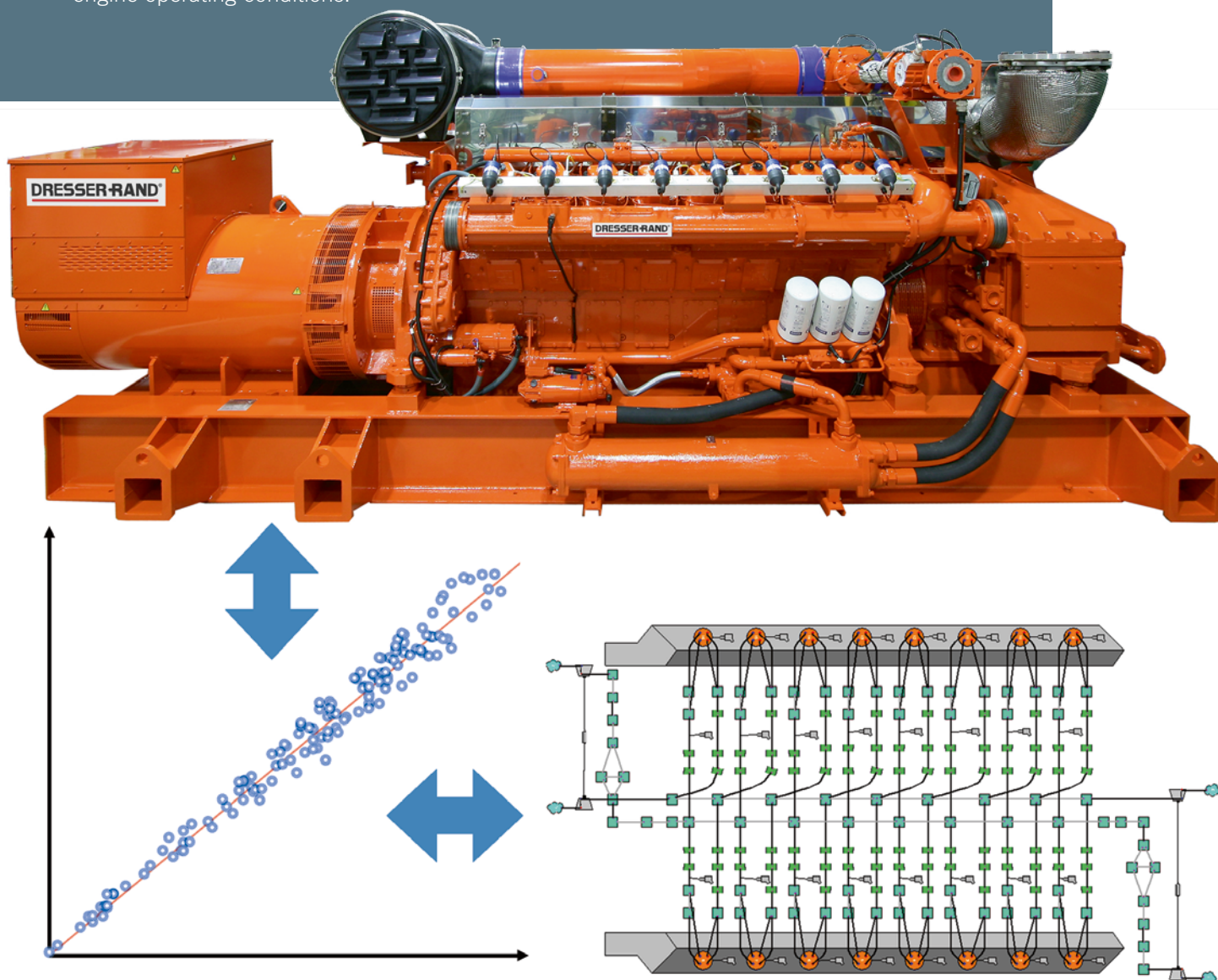
- [1] Grzeschik, P.: Dissertation, submitted internally at Institute for Combustion Engines, RWTH Aachen University, 2014
- [2] Kremer F.: Verbrennungsratenregelung durch Mehrfacheinspritzung im Dieselmotor. Dissertation, RWTH Aachen University, 2013
- [3] Matsumoto S.; Date, K.; Taguchi, T.; Herrmann, O. E.: Der neue Diesel-Magnetventil-Injektor von Denso. In: MTZ 74 (2013), No. 2, pp. 146-150
- [4] Predelli, O.; Gratzke, R.; Sommer, A.; Marohn, R.; Atzler, F.; Schüle, H.; Kastner, O.; Nozeran, N.: Kontinuierliche Einspritzverlaufsformung in Pkw-Dieselmotoren – Potenziale, Grenzen und Realisierungschancen. 31th International Vienna Motor Symposium, 2010
- [5] Graziano, B.; Jakob, M.; Kremer, F.; Pischinger, S.; Lee, C.; Fernandes, R. X.: Investigation on the Ignition Sensitivity of 2-MTHF, Heptane and Di-n-butylether. Proceedings "European Combustion Meeting", Lund, 2013
- [6] Jakob, M.; Klein, K.; Graziano, B.; Kremer, F.; Pischinger, S.: Simultaneous Shadowgraphic and Chemiluminescent Visualization to Determine the Mixture Formation Quality and Ignition Stability of Diesel Engine Related Surrogate Fuels. 14th congress "Der Arbeitsprozess des Verbrennungsmotors", Graz, 2013
- [7] Heuser, B.; Kremer, F.; Pischinger, S.: Optimization of Diesel Combustion and Emissions with Tailor-Made Fuels from Biomass. SAE paper 2013-24-0059, 2014
- [8] Grzeschik, P.; Laumen, H.-J.: A new passenger car Diesel injector with continuous rate shaping for 2500 bar injection pressure. In: PTNSS Combustion Engines 157 (2014), No. 2

THANKS

The research leading to these results has received funding from the European Union 7th Framework Program [FP7/2007-2011] under grant agreement No. 234032. The authors would like to thank Dr.-Ing. Markus Jakob, FEV, for his support during the high pressure vessel investigations.

New Approach to Determine the Knock Onset Angle

In the concept design phase and during the optimisation process of gasoline engines 1D gas exchange simulation techniques are extensively employed. This study by Ricardo shows a method to correlate the knocking intensity extracted from sets of cylinder pressure traces with the knock submodel. After correlating the model in a limited subset of experimental data, its predictive capability has been confirmed in a wide range of engine operating conditions.



AUTHORS

**Dr. Andrea Marchi**

is Principal Engineer of CAE Fluid Dynamics at the Ricardo Deutschland GmbH in Schwäbisch-Gmünd (Germany).

**Dr. Ioannis Vlaskos**

is Director Engines Business Unit and Global Market Sector Director Marine at the Ricardo Deutschland GmbH in Schwäbisch-Gmünd (Germany).

**Dr. Georgios Bikas**

was Chief Engineer Large Engines till September 2014 at the Ricardo Deutschland GmbH in Schwäbisch-Gmünd (Germany).

system still several sub-models are non-predictive and therefore limiting the model accuracy. The autoignition model currently implemented in Ricardo Wave platform, based on Douaud and Eyzat induction time correlation [1], captures with good approximation the dependency of the knocking intensity as a function of in-cylinder parameters and fuel properties. Nevertheless a direct correlation of the sub-model against test bench results can be challenging. This difficulty derives from the fact that the experimental determination of the crank angle and the unburned fuel fraction at knocking onset as well as the transfer of this information to the sub-model is not straightforward. Once the knocking onset has been determined it is possible to identify the knocking intensity as the rate of unburned fuel over the total fuel mass.

The model has been proven working well in gasoline engine for homogeneous charge (or fixed lambda) and low level of residual throughout the whole operating conditions. However when the considered operating range includes changes in oxygen concentration or EGR the model constants would vary as a function of these concentrations.

The proposed approach will take in consideration the correlation from the Douaud and Eyzat model although it is not limited to the knocking model used. A more complete induction time correlation based on a three-stage Arrhenius model was proposed by Sasaki et al. [2].

OVERVIEW ON KNOCKING ONSET ANGLE DETERMINATION

An aspect of knocking that has been object of multiple interpretations is the attempt to formulate a representative way to express the knocking intensity. A much widespread application consists of the signal amplitude output from accelerometers placed on the engine block which acquires the vibration produced by the knocking event. For scientific investigation of the phenomenon, more intrusive methods are required which can be based on post processed signal from fiber-optical spark plugs through boroscopes [3]. However due to the wide application of cylinder pressure sensors in engine test beds, the most common methods to detect knocking consist of several post processing methodologies which exploit the intrinsic

information content of the indicated pressure signal. The pressure spike which characterises the onset of knocking is often mixed with other high frequency noise generated by the main combustion event. This makes the identification of the knocking onset difficult, especially in case of a mild knocking. To avoid determining the knocking onset angle (KOA) due to the difficulty mentioned above, many of the widely applied methods aim to calculate a knocking intensity instead. They rely on the high-pass filtered pressure signal which is integrated for the entire engine cycle over crank angle. Although the criterion of knocking intensity has significant practical meaning it cannot be used for the correlation of a knocking sub-model embedded in a 1D gas exchange simulation environment. This is due to the fact that most of the knocking models used in almost all 1D commercial software packages rely on the calculation of an ignition delay time and not on a knocking intensity itself.

A common algorithm to detect the KOA is based on the detection of the highest peak in the high-pass filtered pressure signal. An alternative algorithm is based on the gradient of the net heat release rate [4]. The slope of the heat release curve of a knocking cycle is steeper compared to a non-knocking one. On the same principle another method for onset detection consists of a combination of the heat release and pressure signal analysis [5]. All heat released based methods make indirectly use of the derivative of the measured pressure exploiting the shape properties of a knocking pressure signal. In the same line with those methods a third derivative of the indicated pressure signal has been utilised [6, 7]. It is thought that most of the useful information on knocking is hidden in the raw signal and consequently in the high-pass filtered pressure curve. For that reason the KOA detection employed in the current study is based on the third derivative of the high-pass filtered pressure signal. The knocking event consists of a rapid positive-to-negative curve gradient. The mathematical quantification of the pressure trace curvature is given by the second derivative and therefore its rapid variation is associated with the third derivative for which intensity can be interpreted as knocking intensity, **FIGURE 1**.

CALCULATION OF THE KNOCK LIMIT

One of the most restrictive factors in increasing the efficiency of gasoline engines is knocking. Knowledge of the knocking limits of an engine and considering this information in the 1D simulation model for performance optimisation is essential. Knocking is a very complex phenomenon and is macroscopically characterised by the autoignition tendency of the fuel/air mixture prior to flame propagation.

1D performance simulation is a powerful tool which enables the prediction and performance optimisation of internal combustion engines. Despite the good accuracy achieved in the gas exchange

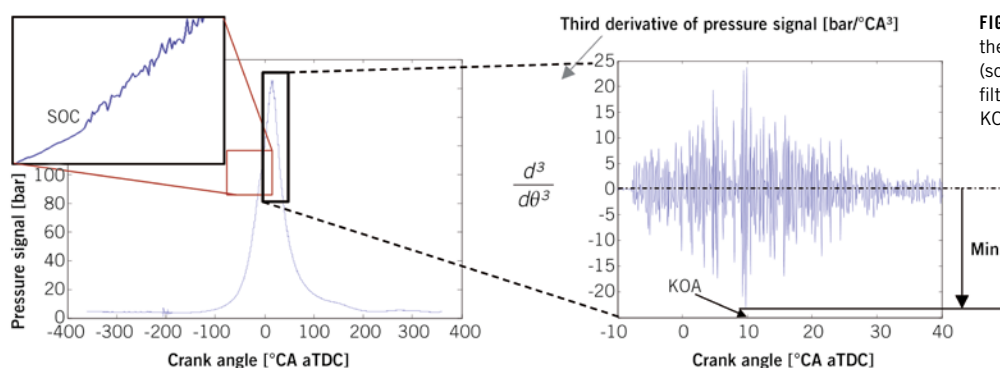


FIGURE 1 Graphical description of the third derivative KOA determination (schematically, after high pass filtering; SOC: start of combustion; KOA: knocking onset angle)

POST PROCESSING DESCRIPTION

The validation of the knocking model was performed on a lean burn CNG engine for stationary steady state operation. The operating range was at two different regimes for two boost pressure levels each of which was swept through a range of ignition timing from light to heavy knocking. For each measurement point 500 cycles were collected with angle resolution of 0.1 °CA.

To understand which algorithm for angle onset detection was the most representative, the criterion of the minimum third derivative was compared against the maximum peak pressure fluctuation method. The vertical axis in the graph in **FIGURE 2** represents a knocking intensity in bar defined as the amplitude of the oscillating high-pass filtered pressure

signal. The x-axis in the same graph outlines the value of the third derivative of the same signal. Despite the good correlation coefficient between the two criteria, **FIGURE 2**, a clear relation between the intensities and the respective onset angles was not observed. The missing link is due to the highly stochastic nature of the onset angle caused by the cycle to cycle variation in the phase of the burn rate. Nevertheless, by plotting the KOA of both detection criteria against each other, **FIGURE 3**, it is clearly visible that a large number of cycles lay on the bisector from which it could be observed that for a portion of the 500 cycles the angle from the two methods matches. Such a portion of matching cycles which are mutually confirmed by the agreement of both criteria will be referred as “two-criterion subset”.

The method based on the matching of the two criteria (peak pressure and minimum third derivative) will be referred as “double verification method”.

Due to the highly stochastic nature of knocking phenomenon, the full measurement set of 500 cycles comprehends a high number of non-knocking cycles for which the angle detection of the two methods does not match. The double verification method gives therefore the possibility to remove all the irrelevant points (non-knocking cycles) and analyse only the matching onset angles of the two-criterion subset. The comparison between the onset angle from the two criteria and for the common subset is shown in **FIGURE 4** for each assessed cylinder which reveals that the minimum third derivative criterion detects approximately the same KOA as the two-crite-

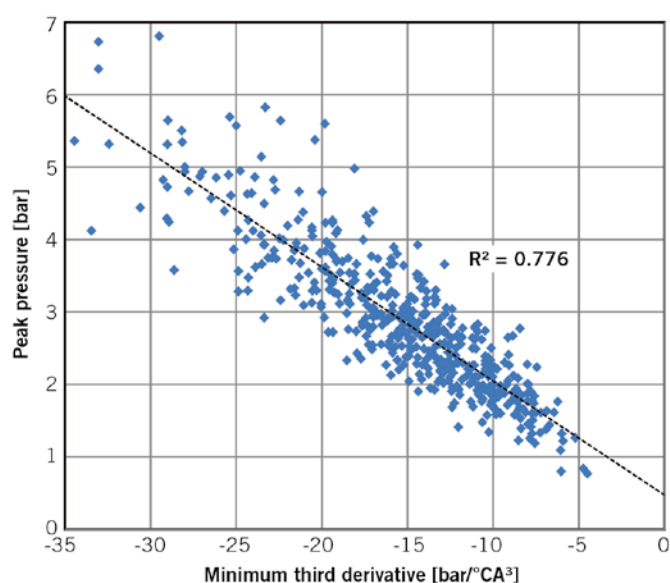


FIGURE 2 Comparison of knock intensity from third derivative method vs. maximum peak pressure method shows a direct proportionality relation

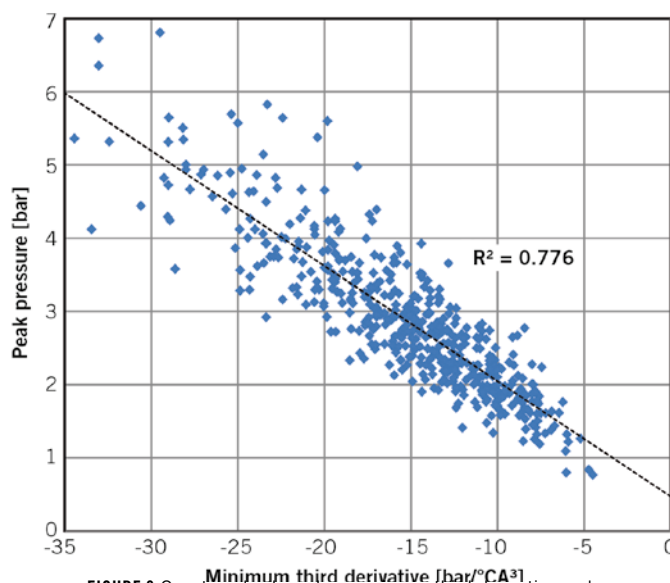


FIGURE 3 Onset angles based on minimum third derivative and maximum peak pressure methods show a large number of common points laying on the bisector: two-criterion subset

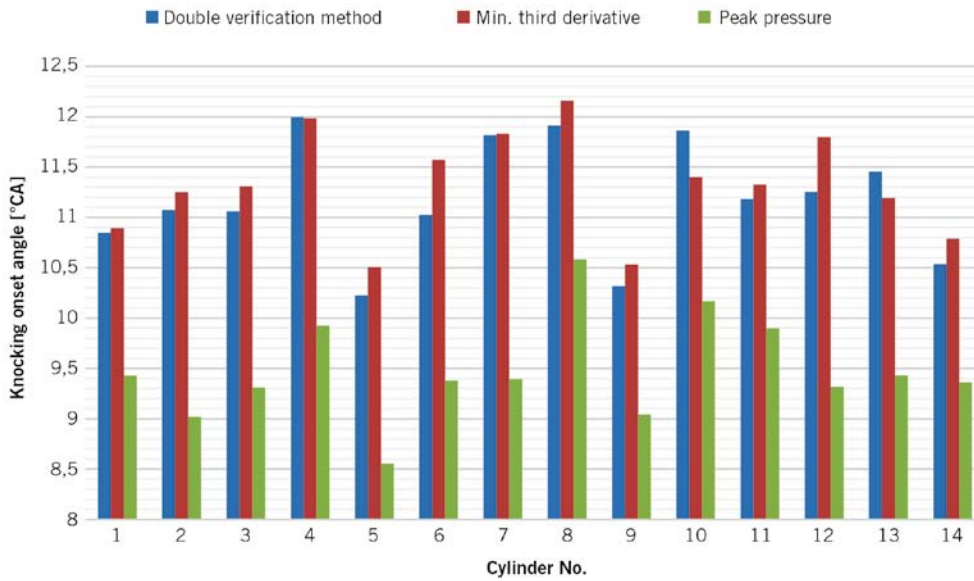


FIGURE 4 Comparison of the onset angle for the minimum third derivative, peak pressure and the double verification methods: the latter matches very well with the minimum third derivative method

rion subset. Therefore, with the assumption that the onset angle of the two-criterion subset is correct, it can be concluded that the minimum third derivative method can alone be used as a reliable KOA detection method.

CORRELATION AND VERIFICATION OF THE PRE-IGNITION SUBMODEL

To adapt the autoignition relation to a generic fuel (in this case CNG) and engine the proportional and exponential terms were corrected by a pre-exponential and activation temperature multipliers. After having validated the full gas handling system and the performance of the Wave model against test measurement data the multipliers were tuned to

match the KOA for each of the ignition time sweep at two different boost levels. The submodel response against test data is compared in **FIGURE 5** and it shows a good matching trend with a deviation range of 2 °CA.

To verify that the submodel is well correlated also in different operating conditions a new set of measurements at a different speed and for further sweeps of boost pressure and ignition timing was assessed. The knock onset angle comparison between Wave prediction and post-processed test data is shown in **FIGURE 6**. The correlation still follows well the trend and the absolute values of the swept measurement points except at low knocking conditions where a deviation up to 2.5 °CA is observed. Overall

the correlation provided a satisfactory matching and it could be successfully implemented in the performance optimisation including all the operating parameters which affects in-cylinder pressure and temperature such as valve timing, compression ratio and air/fuel ratio.

CONCLUSION

To carry out a performance optimisation by mean of 1D CFD gas exchange model a reliable pre-ignition submodel is essential to limit the ignition timing or any of the operating parameters affecting in-cylinder pressure and temperature. The simple knock model based on Douaud and Eyzat implemented in the commercial software Wave is cali-

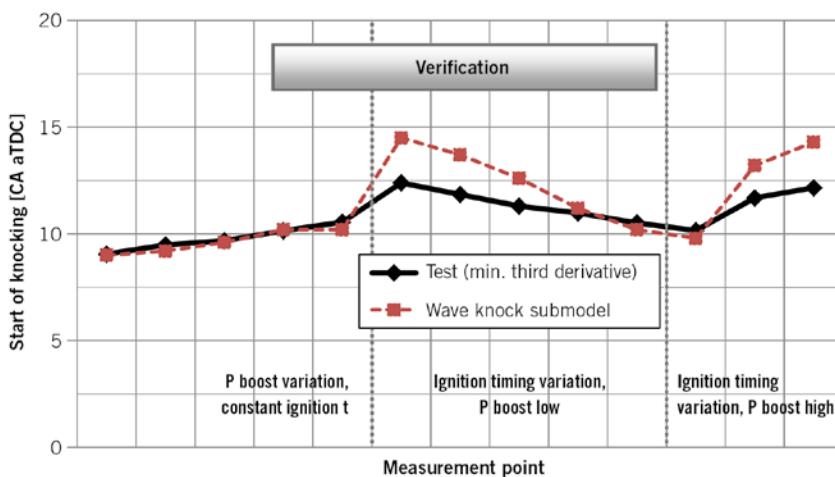


FIGURE 5 Correlation of the predicted knock onset angle against test data

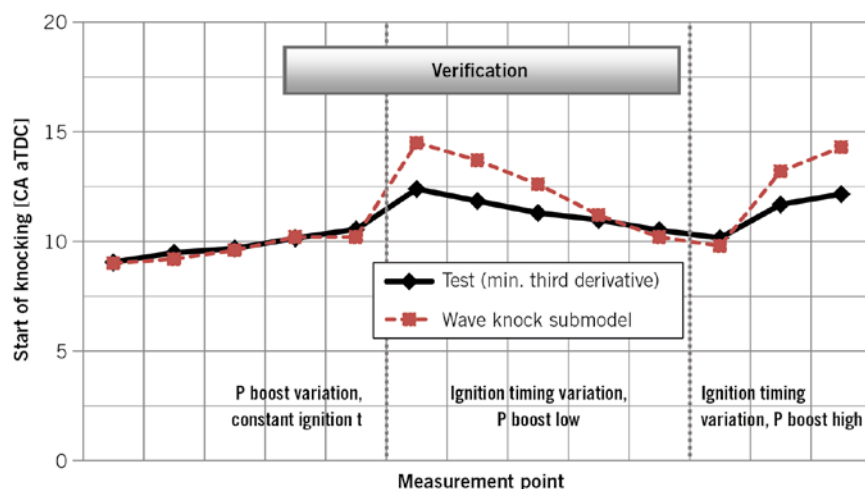


FIGURE 6 Verification of the validated knock submodel at a different engine speed for different operating conditions

brated based on post processed indicated cylinder pressure.

An overview of several criteria to detect the knocking onset angle was given. More specifically, the comparison between the crank angle detection based on maximum peak pressure fluctuation of the high pass filtered indicated data and of the minimum third derivative shows a subgroup of corresponding angles out of a set of 500 cycles for each measurement point. The comparison between the double verification method and of the third derivative criterion alone has shown similar results confirming the latter method as a reliable algorithm for the KOA detection. The established post processed onset angles could be then used to calibrate the coefficients of the ignition delay model. The response was then verified at a different speed and for sets of different operating conditions of ignition time and compressor pressure ratio showing a good match of the post processed KOA.

Overall the described approach proved to give good results in terms of post processing KOA and a fast and sufficiently reliable knock model calibration method especially for engines characterised by a limited operating range.

REFERENCES

- [1] Douaud, A. M.; Eyzat, P.: Four Octane Number Method for Predicting the Anti-Knock Behavior of Fuels and Engines. SAE 780080, 1978
- [2] Yates, A. D. B. et al.: Correlating auto-ignition delays and knock-limited spark-advance data for different types of fuel. SAE 2005-01-2083
- [3] Ra, Y. et al.: Combustion model for IC engine combustion simulations with multi-component fuels. In: Combustion and Flame 158, No. 1, pp. 69-90
- [4] Ohler, S.: New approach to the determination of knock onset. Conference "Knocking in Gasoline Engines", 2014
- [5] Wimmer, A. et al.: LEC-GPN – a new Index for assessing the knock behavior of gaseous fuels for large engines. Conference "Knocking in Gasoline Engines", 2014
- [6] Checkel, M. et al.: Testing a Third Derivative Knock Indicator on a Production Engine. SAE 861216, 1986
- [7] Rogers, D. R.: Engine Combustion: Pressure Measurement and Analysis. SAE 2010-08-19

chassis.tech^{plus}

6th International Munich Chassis Symposium

16 and 17 June 2015

Munich | Germany

CAR-TO-X COMMUNICATION

Benefits for ride comfort,
safety and efficiency

NEW CHASSIS SYSTEMS

Demands on the chassis
of tomorrow

CHASSIS TECHNOLOGY FOR COMMERCIAL VEHICLES

Innovations and requirements

//// SCIENTIFIC DIRECTOR

Prof. Dr. Peter E. Pfeffer
Munich University of
Applied Sciences

/// ONE FOR ALL

**Four congresses
in one event**



/// KINDLY SUPPORTED BY

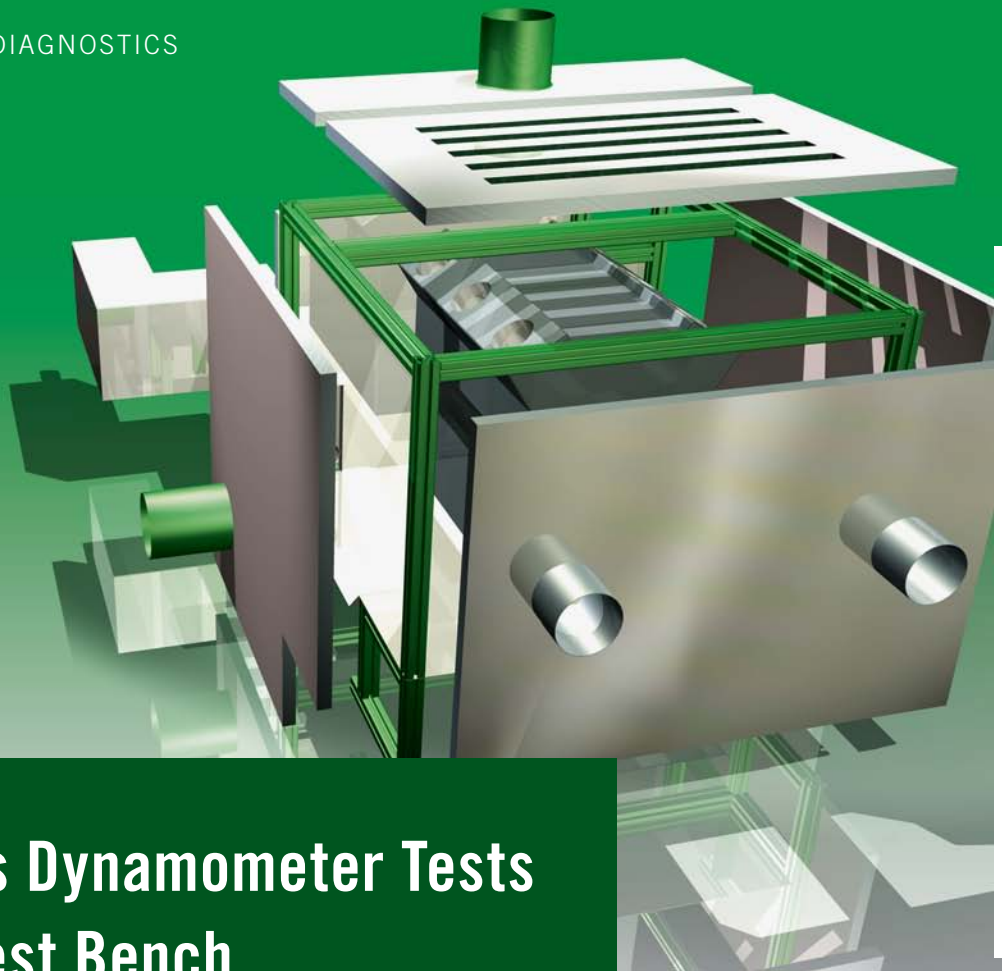


ATZ live
Abraham-Lincoln-Straße 46
65189 Wiesbaden | Germany

Phone +49 611 7878-131
Fax +49 611 7878-452
ATZlive@springer.com

MTZ 03|2015 Volume 76

PROGRAM AND REGISTRATION
www.ATZlive.com



Shifting Chassis Dynamometer Tests to the Engine Test Bench

APS-tech has developed a process to transfer chassis dynamometer tests to determine the emissions on an engine test bench. Main focus of the procedure is the effective design of an encapsulation for the engine and the underbody in order to realise similar vehicle conditions at the engine test bench. Particular attention was given to the transferability from vehicle to test bench concerning the temperature characteristic of exhaust aftertreatment components. The performance of this tool is being demonstrated in this article by considering the example of a diesel on-board diagnostics calibration.

MOTIVATION

The increase of variant diversity concomitant increase of legislative requirements leads to greater complexity in the field of powertrain development. Methods are in demand to move the process of development into higher flexibility and thus increasing efficiency. Not only the manufacturers see themselves as being faced with this challenge, but also service suppliers are optimising their methods and work flows. The aim is to

AUTHORS



Dr.-Ing. Stephan Krämer
is Executive Vice President of the APS-technology GmbH in Fellbach-Schmiden (Germany).



Dr.-Ing. Christian Landgraf
is Head of Calibration at the APS-technology GmbH in Fellbach-Schmiden (Germany).



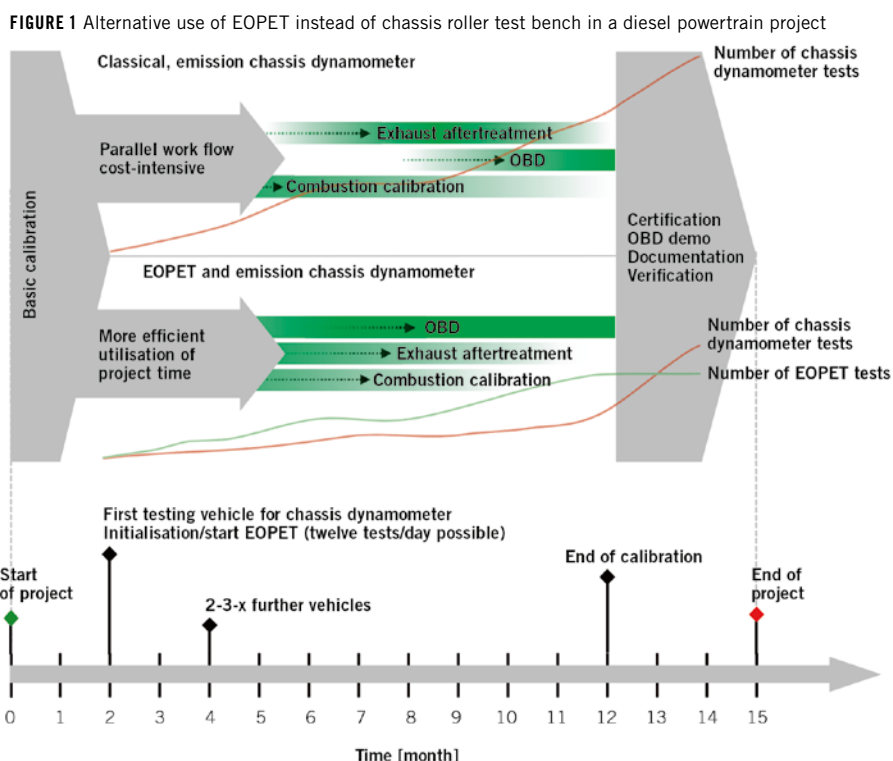
Dipl.-Ing. (FH) Gianni Di Martino
is Manager of Calibration On-Board Diagnostic at the APS-technology GmbH in Fellbach-Schmiden (Germany).



Dipl.-Ing. (FH) Martin Meiß
is Calibration Engineer On-Board Diagnostic at the APS-technology GmbH in Fellbach-Schmiden (Germany).

provide efficient and best possible tools for the development engineers. In the field of engine calibration, potential can be determined through the reduction or transition to flexible roller dynamometer tests for emission configuration and verification, for example at OBD (on-board diagnostics) calibration.

For this purpose, APS-tech has developed the method EOPET (end of pipe emissions on test bench). With this method, a part of all the required emission tests during today's development process can be shifted to a conventional engine test bench with minor expenses due to exorbitant higher output of tests per time. This method applies for example in the development of variants which react more flexibly to the availability of vehicles and roller dynamometer tests. In this context, the quality of calibration can be increased and associated costs can be reduced. **FIGURE 1** shows the possible use of EOPET in a variant calibration.



EMISSION TESTING IN DIESEL CALIBRATION

Up until now, the most often used diesel calibration work flow is that the combustion adjustment for raw emissions has to be done before the adjustment of exhaust aftertreatment systems. The adjustment of exhaust aftertreatment diagnostics for an engine calibration can mostly be found at the far end of the line. Due to such a sequential flow, delays of each subsection are passed through during the whole project plan. For this reason, nowadays it is mainly attempted in the field of engine calibration in order to calibrate in a parallel work flow. Unfortunately, the limits on the availability of resources such as testing vehicles are reached quickly.

In determining the emissions at a passenger car calibration is the roller dynamometer test bench still the measure of all things. This fact has technical and legal reasons. According to a rule of thumb: One test per day. If the vehicle needs to be preconditioned, two days will be needed for one valid emission test. During this time the vehicle is not available for any other purpose. Much higher is the availability of engines, exhaust systems and engine test benches during the project duration. The main idea is to achieve high-quality and comparable results by using these simple means.

REALISATION ON THE ENGINE TEST BENCH

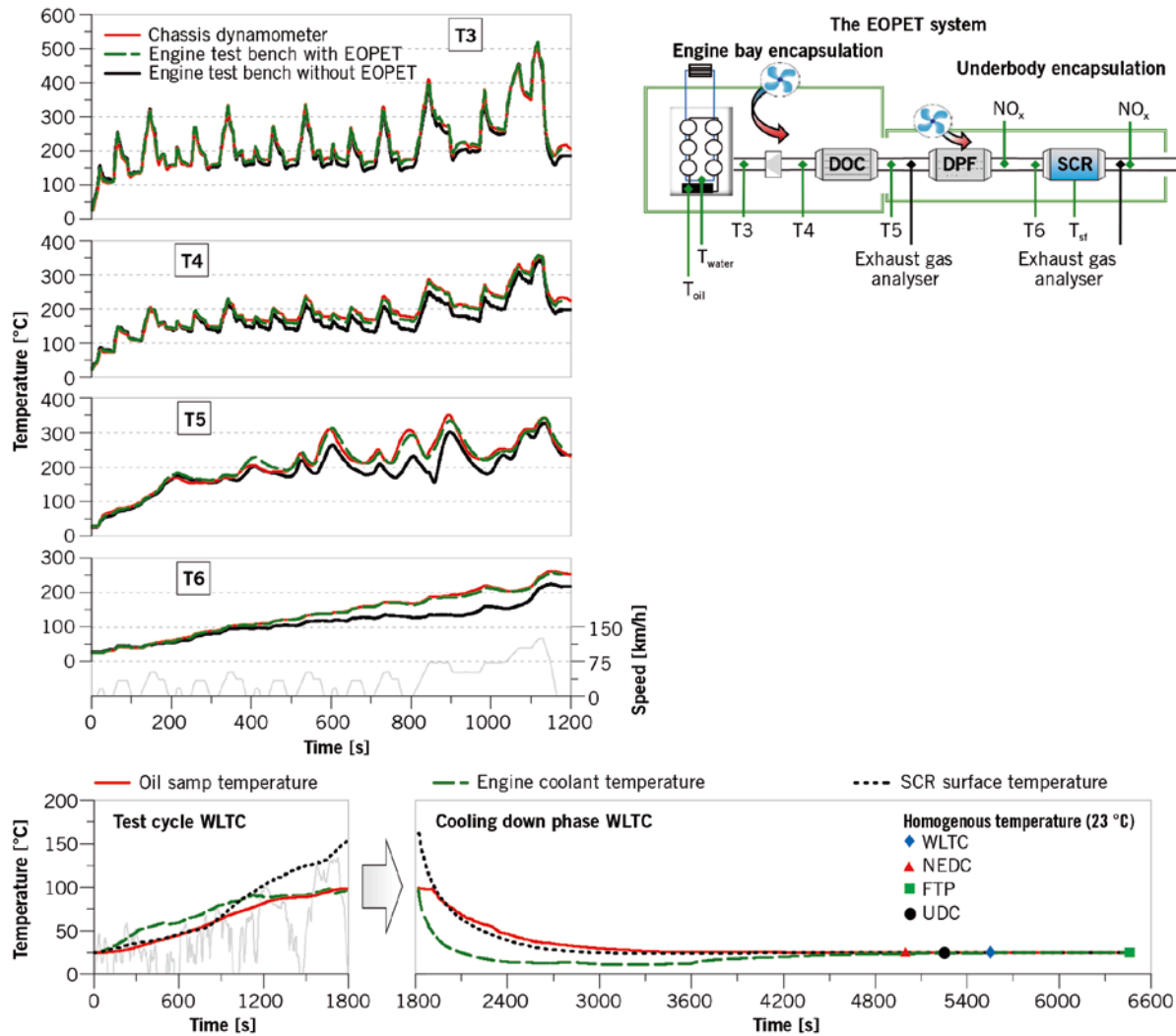
The engine test bench holds a high dynamic engine brake with appropriate automation system as standard specification. Premises in the test bench are arranged to mount a close-to-production exhaust system. All emissions and measurements can be recorded transient. This setup will not allow a proper comparison of emission results between the engine test bench and the roller dynamometer test bench. In particular, this is due to the escape of thermal energy of engine and exhaust system through the room conditioning. The functional capability of the different catalyst systems like DOC (diesel oxidation catalyst) or SCR (selective catalytic reaction) catalyst is strongly dependent on the catalyst and engine temperature. These facts lead to the idea of reproducing the functionality of the vehicle body. Therefore, the real test vehicle temperature curves measured on a roller test bench are used.

DESIGN AND SETTING OF THE CAPSULE MODULES

A simplified reflection of a vehicle body separates the engine bay and underbody. Components in a real vehicle sitting next

to the engine are allocated in the engine bay enclosure, **FIGURE 2**. In the same way, components from the underground are placed into the underbody enclosure. To obtain comparable temperatures a simple trick can be used. The temperature level is minimally increased compared to the baseline measurement of the vehicle. The installed engine fan unit is controlled in such way that compensates for the temperature difference. All temperatures behind will converge to the real system. The final touch can be achieved with a second fan unit installed in the underbody enclosure. In simple terms, the system shows the same reaction as the real vehicle. Without airstream the underbody and the engine bay heat up much more. The fan units just simulate the influence of the airstream. With these features, the relevant emission characteristics are technically and physically simulated, consequently so are the emission test results. Calibrating this configuration is made by a special feedback control that results in a setpoint track. This setpoint track represents the physical characteristics of the combination between cycle, vehicle and roller dynamometer test bench. This allows temperature changes caused by data set modification to result in the same effect at both test bench systems.

FIGURE 2 Principle of EOPET and benchmark to the chassis dynamometer



Without further optimisations just one to two tests per day are possible because of thermal conditioning reasons. The purpose of further development is to achieve a homogeneous cooled down test assembly. Initial temperatures, in the shown example 23 °C, are equal to the roller dynamometer tests and reproducible at the beginning of each test.

FIGURE 2 shows cooling down curves of four development-related tests with different thermal loads. The results show that the testing equipment and the proband are ready for the next cycle after at least two hours. The test procedure can be made fully automatic to reach up to twelve emission tests per day (24-h operations). With such an approach, a drastic increase of efficiency is achieved. A target vehicle roller dynamometer test including all temperatures is needed to

initialise the described method on the engine test bench. The engine and exhaust system encapsulation will be unchanged during the whole duration of the project. This is due to the fact that the encapsulation describes the total system characteristics and not the engine calibration characteristics.

PRACTICAL EXAMPLE OF DIESEL OBD CALIBRATION

The following OBD project example of a passenger car diesel variant calibration for the European market shall clarify the importance of emission tests in cycles for the calibration. The emissions are calibrated in the New European Driving Cycle (NEDC) and verified with the emission level Euro 6c: Threshold for NO_x emissions 80 mg/km, appropriate

OBD level Euro 6-2 with an OBD threshold for NO_x of 140 mg/km. The system consists of a six-cylinder diesel engine with single-stage turbocharging and exhaust system with DOC, diesel particulate filter (DPF) and SCR catalyst. The objective of on-board diagnostic is an early detection of excess emissions.

The legislation dictates a limit for each emission monitor and system. When exceeding these limits a fault type related entry must be set and the malfunction indicator lamp (MIL) must be switched on after a certain number of cycles. The detailed regulations would break this mould. Emissions and OBD limit in Europe are still verified in the NEDC up to the launch of worldwide Harmonized light vehicles test procedures (WLTP). At this point the EOPET method can be useful.

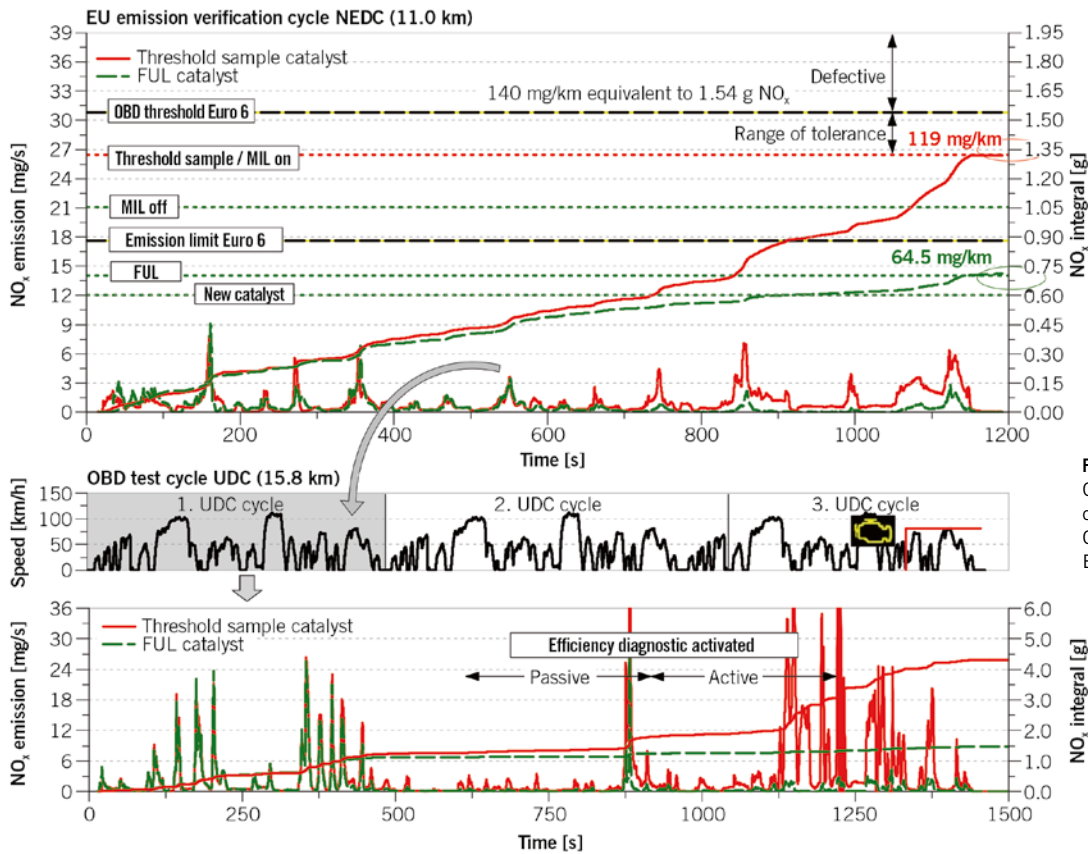


FIGURE 3 Verification of OBD threshold sample catalysts in NEDC and OBD test cycle at the EOPET test bench

A catalytic aging of the SCR catalyst is made for threshold sample generation. Verification measurements are made in the NEDC cycle to determine the NO_x OBD threshold. This threshold sample catalyst (MIL ON) is assembled in a full useful lifetime (FUL) exhaust system. A European FUL exhaust system represents

an aging of 160.000 km. The aim of the diagnostic is to identify the damaged catalyst. For that reason, in Europe exists a special recognition cycle (UDC: CARB Unified Driving Cycle) which can be used with special approval. The advantage of this cycle is the higher diagnostic possibility compared to the NEDC, **FIGURE 3**.

The diagnostic principle is based on the NO_x efficiency, calculated continuously during real-life operation. NO_x values are measured by two sensors, located upstream and downstream the SCR catalyst. The upstream one could be replaced by a model calculation. A damaged catalyst is indicated by the loss of

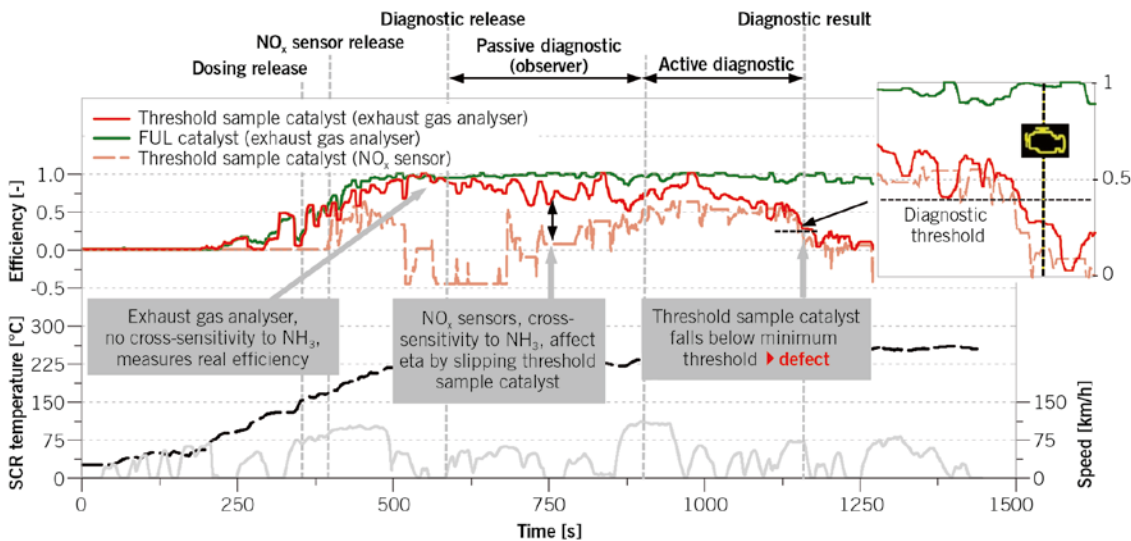


FIGURE 4 SCR diagnostic sequence in the UDC cycle, verified at the EOPET engine test bench

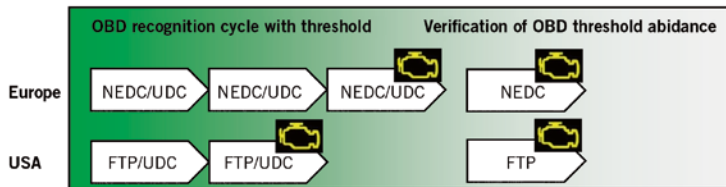
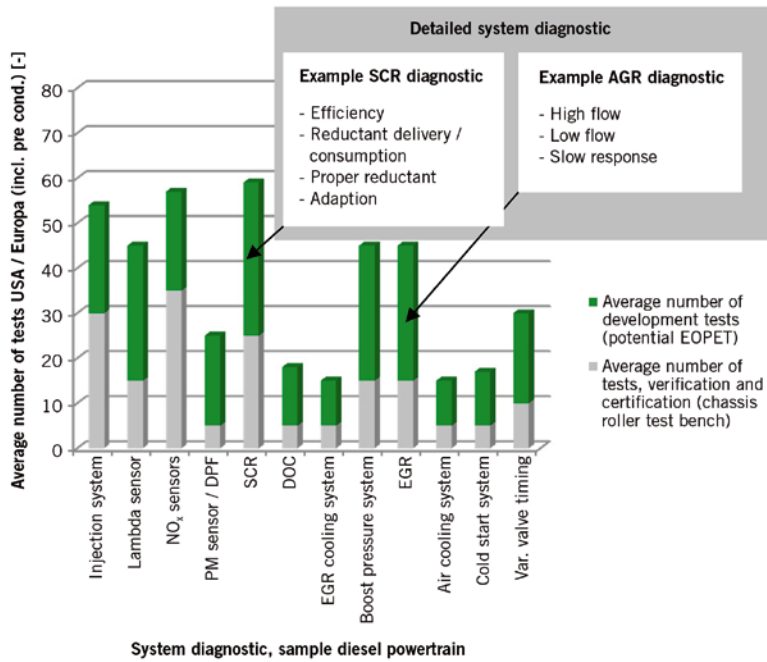


FIGURE 5 Estimated potential of an average OBD project

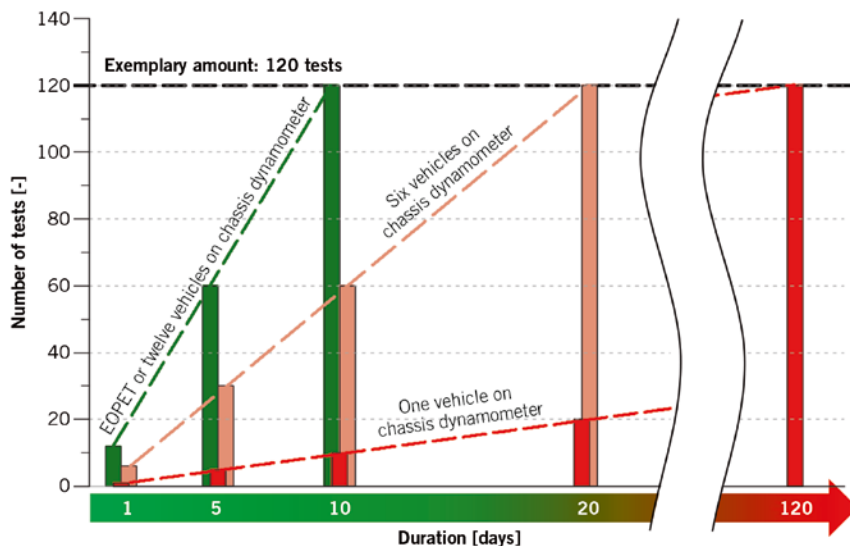


FIGURE 6 Theoretical saving potential and gain in flexibility by the use of EOPET

strong temperature gradients, model inaccuracies, sensor releases or adaptations have to be taken into account and calibrated for each variant. An average efficiency is determined to weaken the impact of short time disturbances. This performance is compared to an efficiency model that represents the threshold sample catalyst. When the actual efficiency result falls under the simulated threshold sample a fault is noticed. Several reasons, such as defective catalytic coating, defective dosing system, insufficient dosing, NH₃ slip (overdose), sensor drift, adverse operating points or model inaccuracy can lead to decline of NO_x conversion in the passive diagnostic. To sort out and distinguish between these causes of faults, the result is once more verified through an active diagnostic intrusion. During the active diagnostic the metering quantity is increased (overdosing) to obtain the best possible efficiency result. The appropriate evaluation of the cross sensitivity concerning NH₃ of the NO_x Sensors can be used for the overdosing and slip detection. The conversion efficiency is verified again after a certain time has passed by and no NH₃ tampers. Results the actual efficiency below a threshold, is this an indication for a damaged catalyst, **FIGURE 4**.

CONCLUSION AND EXPERIENCE

In the above described example of the SCR diagnostic, 15 to 25 % of the emission tests can be moved from the chassis dynamometer test bench to the engine test bench by means of the presented method. An average diesel variant calibration contains more than 400 diagnostics. More than 40 are similar to the described SCR diagnostic. **FIGURE 5** shows the estimated ratio between EOPET and real chassis dynamometer emission tests at the calibration of emission relevant diagnostic. The shown use of EOPET in the OBD example is exemplary for all other developing subsections such as exhaust aftertreatment or combustion calibration. Each subsection can achieve a higher efficiency in the field of flexibility, availability and cost saving, **FIGURE 6**. Cleverly used, this method can furthermore help early on in projects in order to gain emission-related knowledge, to perform quicker iterations and thereby increasing the quality early on in the development stage.

efficiency below a calibrated threshold. The diagnostic starts if electrical faults can be excluded. Not every engine operating point that occurs during real driving cycles as well as synthetically generated ones is ideal to detect a loss of effi-

ciency. Therefore release conditions for every diagnostic exist. Typical values for release conditions are exhaust temperature, exhaust mass flow, NO_x concentration, NH₃ filling level and metering quantity. Moreover, system events like

Start your day with the right magazine for your job!

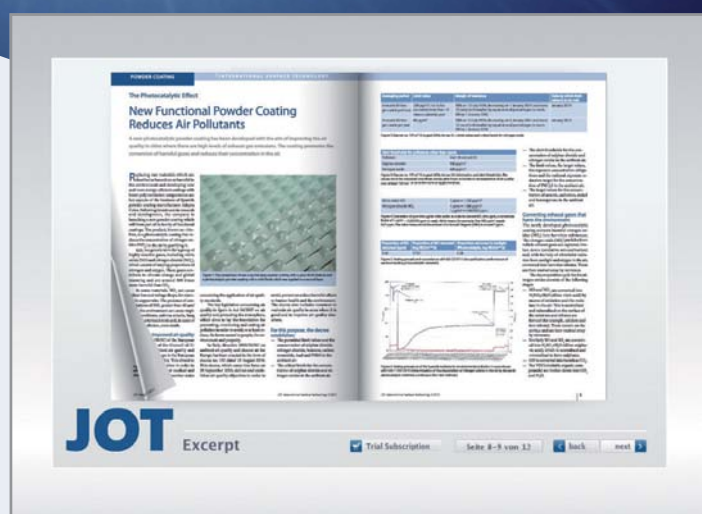
personal buildup for Force Motors Limited Library



JOT-IST print version (3 issues)

71,- EUR annual subscription for private persons

101,- EUR annual subscription for institutions




JOT-IST e-magazine (3 issues)

71,- EUR annual subscription for private persons

101,- EUR annual subscription for institutions

Subscriptions, mediadates and for more information:

www.jot-oberflaeche.de 

JOT



Lightweight Design of Cast Iron Cylinder Blocks

Reducing the weight of components will have to make a significant contribution

to the tasks of minimising CO₂ and fuel consumption. The cylinder block, the heaviest individual part of the engine, is worthy of particular attention. Fritz Winter and AVL investigated in this project the lightweight design of engine blocks out of cast iron materials. The objective was to replace the aluminium engine block of a four-cylinder turbocharged gasoline engine by a newly developed lightweight cast iron one.

AUTHORS



Dr. Helfried Sorger
is Executive Chief Engineer Design, Simulation and Mechanical Development, Engineering and Technology Powertrain Systems, at the AVL List GmbH in Graz (Austria).



Dr. Wolfgang Schöffmann
is Head of Design Passenger Car Powertrain, Engineering and Technology Powertrain Systems, at the AVL List GmbH in Graz (Austria).



Wilfried Wolf
is Director Product Engineering and Development at the Fritz Winter Eisengießerei GmbH & Co. KG in Stadallendorf (Germany).



Dipl.-Ing. (BA) Wilhelm Steinberg
is Product Engineer – Development Department at the Fritz Winter Eisengießerei GmbH & Co. KG in Stadallendorf (Germany).

OBJECTIVES

The continuing downsizing trend in diesel and gasoline engines has led to a steady increase in engine structural stress [1]. Cast iron engine blocks offer a better platform upon which to base future increases in performance. These characteristics will be retained in the subsequently described lightweight design just as much as the more favourable prerequisites for cylinder roundness, frictional performance, oil consumption, costs and NVH [2]. The product selected as reference was a gasoline engine that can be regarded as a benchmark in the price-sensitive middle segment, **TABLE 1**. The production version of the four-cylinder 1.6-l engine is manufactured with an aluminium cylinder block using high-pressure die-casting.

CONCEPT DEVELOPMENT AND COMPONENT DESIGN

Different design variants were judged in the concept phase with respect to the weight, cost, manufacturability and impacts on engine operation. In a first variant, the architecture of the aluminium cylinder block was transferred to a thin wall cast iron concept. In addition to the optimisation of thin wall concept, further variants with different layouts of cylinder head bolts have been reviewed. The main bearing integration into the block was investigated in the variants deep skirt, short skirt with raised aluminium oil pan upper section, and aluminium bedplate with and without main bearing inlays, **FIGURE 1**. A comparison of the concepts showed that variant 5, an optimised thin wall cast concept with deep skirt and short cylinder head bolts achieved the best overall rating of target criteria.

Due to the higher tensile strength of cast iron and the parent bore cylinder liners, the cylinder distance could be reduced from 87 to 84.5 mm. Together with other design measures, the total engine length could be reduced by 12.0 mm. The block shown in **FIGURE 2**, at this stage of development, has a weight difference to the cast iron reference component of 4.4 kg.

By reducing the engine length, a reduction in weight in other engine components could be achieved with the additional effects of creating cost saving

| Technical Data | |
|---------------------------------|-----------------|
| Power [kW at rpm] | 132 at 5700 |
| Torque [Nm at rpm] | 240-270 at 1600 |
| Displacement [cm ³] | 1596 |
| Bore [mm] | 79 |
| Stroke [mm] | 81.4 |
| Bore spacing [mm] | 87 |
| Block height [mm] | 204 |
| Main bearing Ø [mm] | 48 |

TABLE 1 Technical data of the reference engine

potential. By reducing the weight of components such as the crankshaft, oil pan, cylinder head and camshafts, the difference in weight could be reduced further to just 1.9 kg according to DIN 70020, **FIGURE 3**.

VIRTUAL DEVELOPMENT LOOPS

The thin wall block variants were optimised in simulation loops under operational load with respect to structural stiffness, cylinder bore deformation and thermal behaviour. The load conducting main bearing area was systematically developed with the aim of reducing weight. The key optimisation criteria were minimum cylinder bore deformations under assembly and thermal load, together with surface pressure distribution of the cylinder head gasket. Variant 5 was able to reach or exceed the targets in all criteria.

NUMERICAL SIMULATION – SOLIDIFICATION, FILLING AND STRESS BEHAVIOURS

The simulation of the casting process is the most time and cost effective possibility to determine the most appropriate casting and manufacturing parameters. Prerequisites for the application of such simulation programs were reliable material and process data obtained with a test procedure developed by Fritz Winter and adapted with measurements taken on real castings. Insights from the test procedure for material and process data:

- influence of the solidification speed on the microstructure
- effectiveness of inoculation practice and amount on the microstructure and in particular on the avoidance of chilled iron
- local temperature change of the mould to determine the thermal conductivity

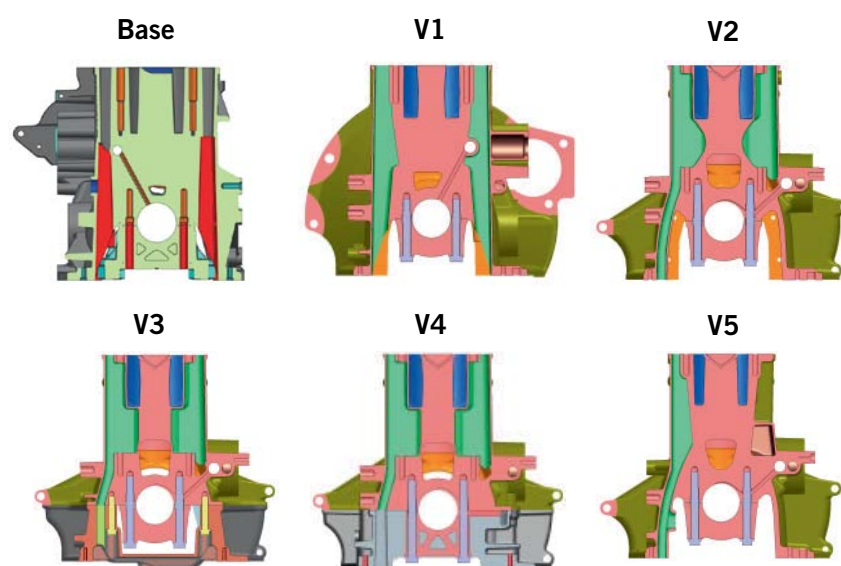


FIGURE 1 Overview of concept variants

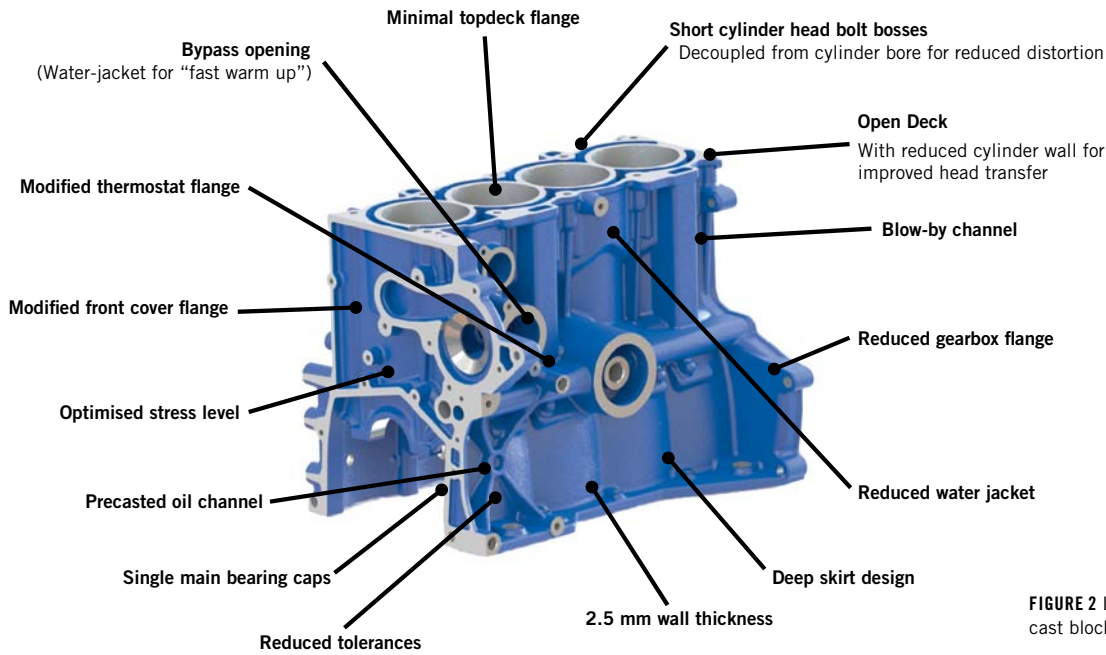


FIGURE 2 Lightweight thin cast block features

- influence of the chemical composition on the local microstructure characteristics and tensile strength
- analysis of pouring features as time and temperature on the filling behaviour and the above-mentioned characteristics.

Based upon these parameters, the numerical simulation software could be used to determine an optimum process window with regards to gating system, inoculation type and amount, and chemical composition. Numerous local optimisations on the geometry with respect to thermally induced stresses made it possible to reduce the residual stresses to

the target level. The virtual pouring on the computer enabled the process parameters to be chosen in such a way, that the first real castings were immediately successful.

NEW METHODS OF MANUFACTURING/CASTING PROCESS

Apart from the design and simulation aspects, a fundamental element of the implementation of the lightweight concept [3] was the development of the process with the following product-relevant objectives:

- minimisation of the general casting tolerance (± 0.8 mm)
 - minimisation of the wall thickness tolerance (± 0.5 mm)
 - increase casting quality
 - achieving nominal data weight targets.
- The most important process-specific objectives were:
- sustainability to protect resources
 - global availability
 - standardisation of processes and tools
 - cost efficiency.

These objectives require a minimisation of the process steps and their influences. Passenger car cast iron cylinder blocks are normally manufactured using conventional greensand moulding methods either horizontally or vertically. The new casting method for cast iron blocks eliminates the need for a greensand moulding line and uses a sophisticated core concept which enables a significant increase in product quality and process stability. The result is a modular foundry that permits manufacturing with globally homogenous quality, without greensand moulding line, their associated high investment costs and the dependency on raw material quality.

CLOSE-TO-PRODUCTION PROTOTYPING

In order to validate the development results, completely processed prototypes were produced. The challenge here was a

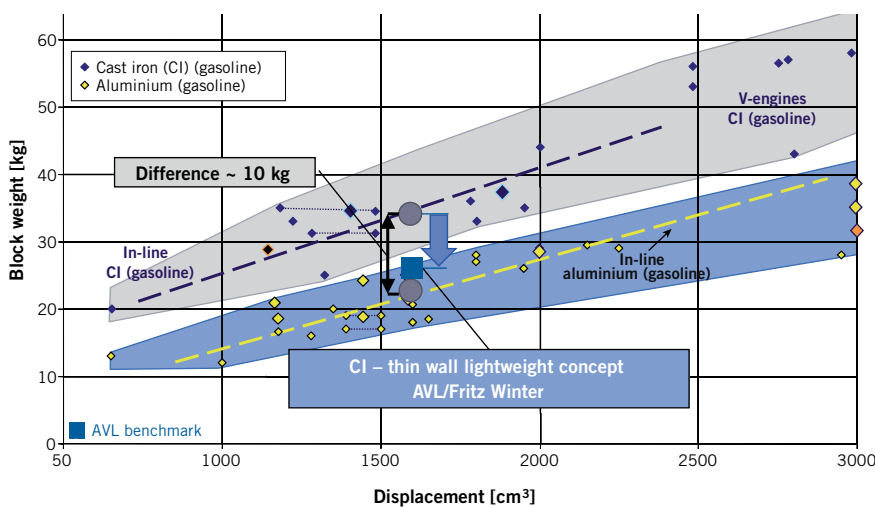


FIGURE 3 Weight benchmark aluminium and cast iron cylinder blocks

Driver Assistance Systems

From Assistance to Automated Driving

1st International ATZ Conference

28 and 29 April 2015

Frankfurt am Main | Germany

HIGH-LEVEL AUTOMATION

Technical risks and opportunities

THE CONNECTED CAR

Safe control of connected functions

BACKGROUND CONDITIONS

Legal, social and economic

CUSTOMERS AND MARKETS

User-oriented strategies for safety and comfort

/// SCIENTIFIC DIRECTOR

Prof. Dr. Dr. Rolf Isermann
TU Darmstadt



/// KINDLY SUPPORTED BY

Continental **ETAS**

ATZ live
Abraham-Lincoln-Straße 46
65189 Wiesbaden | Germany

Phone +49 611 7878-131
Fax +49 611 7878-452
ATZlive@springer.com

MTZ 03|2015 Volume 76

PROGRAM AND REGISTRATION
www.ATZlive.com

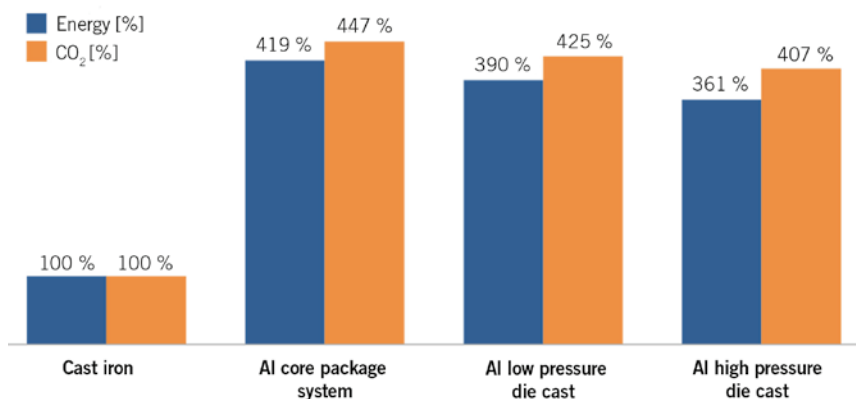


FIGURE 4 Manufacturing phase – energy requirements and CO₂ emissions for the production of a cylinder crankcase (including consideration of the global recycling rate according to GDA)

close-to-production implementation of the prototype manufacture, beginning with the cast part production through to finishing. All prototypes were produced using the new foundry process under production conditions, whereby the first casts already fulfilled all metallurgical requirements and displayed very high dimensional precision. The measured raw component weights corresponded to within 0.4 % of the calculated nominal weights, other positive evaluations were an increase in tensile strength of approximately 5 % and an increase in hardness of approximately 4 %.

ECOLOGICAL SUSTAINABILITY – CO₂ AND ENERGY BALANCE

The increasing interest of end-users in ecological products together with political regulations regarding resource efficiency [4] demand a change in thinking when evaluating environmental impacts: Moving from a purely CO₂ evaluation during the use-phase towards a holistic

view over the entire product lifecycle (“cradle-to-grave”) [5].

MANUFACTURING PHASE

Based on work done by the Institut für Gießereitechnik [6], a comparison of the most important foundry processes could be conducted. All relevant operational and application material such as primary and secondary aluminium, coke, core binders, electrical power together with the energy required for processing and transport were taken into account. The results showed significant differences between the cast iron process and the different casting processes for aluminium, **FIGURE 4**.

USE-PHASE

The calculation methods supplied by the Institut für Gießereitechnik [6, 7, 8] make it possible to evaluate the distance after which the supplementary energy effort in the manufacturing phase is amortised by the weight difference of

1.9 kg and hence via the reduced fuel consumption. The calculation includes the global recycling rate for aluminium published by GDA [9] and the engine’s weight difference of the light weight crankcase, to balance the additional energy demand of an aluminium crankcase, it needs several vehicle lifecycles.

RECYCLING PHASE

The recycling phase represents the stage in the lifecycle of a product where products are fed into the secondary material cycle. In iron foundries, the scrap can be used directly as material without further processing. However, when recycling aluminium, each cycle must remove associated material such as cylinder liners from the scrap and the iron content often must be reduced by adding primary aluminium [10].

COSTS

In price sensitive vehicle classes, the cost pressure on the manufacturer and their suppliers is constantly rising, accompanied by a simultaneous increase in product complexity and requirements.

When compared with other casting methods, cast iron is the most cost-efficient option to manufacture cylinder blocks. If the possible size advantages (reduced component length) and the elimination of cylinder coatings, cylinder liners or singular castings are taken into account then there is an additional potential for cost reduction.

The minimal weight difference comes with a significant cost advantage of approximately 28 % compared to

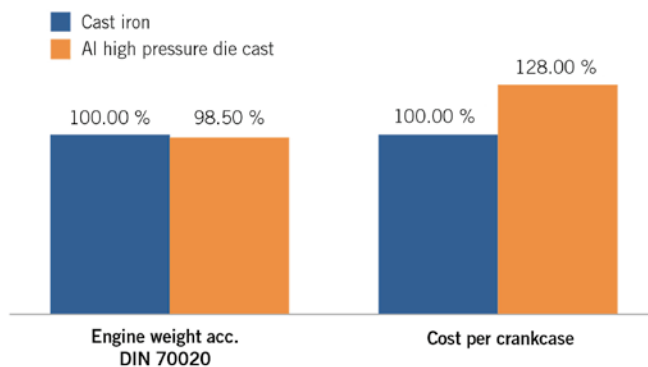


FIGURE 5 Weight and cost comparison of engine variants

an aluminium high-pressure cast,
FIGURE 5. If the manufacturing process described here for cast iron cylinder blocks is compared with CPS (core package system) or low-pressure die-casting, then the cost difference is even greater.

SUMMARY

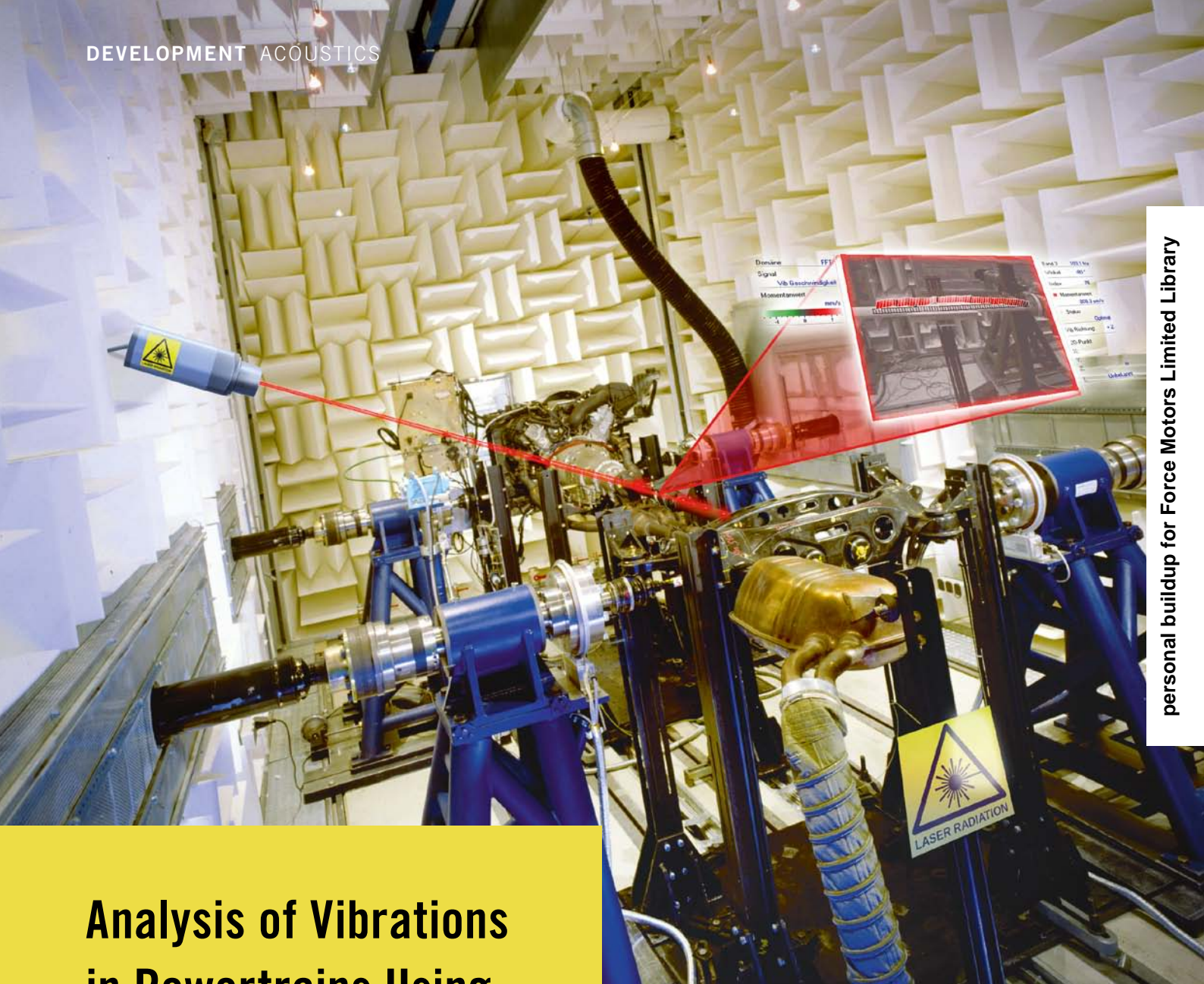
The development project was able to show the potential offered by using cast iron as a material with respect to weight, costs and ecology. The close collaboration between engine developer and foundry was able to reduce the weight difference between engines to a minimum and simultaneously achieve a cost advantage. Furthermore, this new casting and manufacturing technology enables high precision, sustainable and global production.

REFERENCES

- [1] Schöffmann, W.; Weißbäck, M.; Sorger, H. et al.: High specific power and friction reduction – challenge or contradiction? Future diesel and gasoline engines from a common family architecture. 22nd International AVL conference “Engine & Environment”, Graz, 2010
- [2] Schöffmann, W.; Sorger, H.; v. Falck, G. et al.: Lightweight Design, Function Integration and Friction Reduction – the Base Engine in the Challenge between Cost and CO₂ Optimization. 34th International Vienna Motor Symposium, 2013
- [3] Schulze, T.; Wolf, W.; Steinberg, W.; Walz, M: Optimierung aller Entwicklungs- und Herstellprozessen von anspruchsvollen Bauteilen aus Gusseisen. In: Giesserei, 2011
- [4] Comitee, E. E.: Roadmap to Resource Efficient Europe, 2011
- [5] Fritsche, E.: Vergleich der Energieeffizienz und CO₂-Emissionen bei der Herstellung von Zylinderkurbelgehäusen aus Gusseisen oder aus Aluminiumlegierungen. In: Giesserei Rundschau, 2010
- [6] Institut for Foundry Technology: Grundlagen für Energiebilanzen von Zylinderkurbelgehäusen, 2014
- [7] DEKRA: Information regarding CO₂
- [8] Dienhart, M.: Ganzheitliche Bilanzierung der Energiebereitstellung für die Aluminiumherstellung. Aachen, 2003
- [9] GDA: alu.info, statistics 10 21, 2014
- [10] Arte: Xenius aluminium (documentation), broadcasted 11th March 2013

THANKS

With special thanks to Dipl.-Ing. Thomas Schulze and Friedhelm Wieber, Fritz Winter Eisengießerei GmbH & Co. KG at Stadallendorf (Germany), and to Robert Berger, Roland Santner and Christian Seltenhammer, AVL List GmbH at Graz (Austria), for the good and beneficial work.



Analysis of Vibrations in Powertrains Using Simulation Support

AUTHORS



Dr. Josef Girstmair
is Head of the Powertrain Dynamics and Acoustics Group at the Virtual Vehicle Research Center in Graz (Austria).



Univ.-Doz. Dr. Anton Fuchs
is Head of the NVH & Friction Department at the Virtual Vehicle Research Center in Graz (Austria).

Vibrations in the vehicle powertrain not only affect all comfort-relevant vehicle properties but also influence the lifetime of components. In the powertrain, the optimisation of vibration is an increasingly important focus of development aimed at reducing vehicle weight and costs by eliminating heavy and costly secondary measures. Virtual development methods for vibration analysis have become established as a key tool, as shown by the Competence Centre Virtual Vehicle and illustrated by examples.

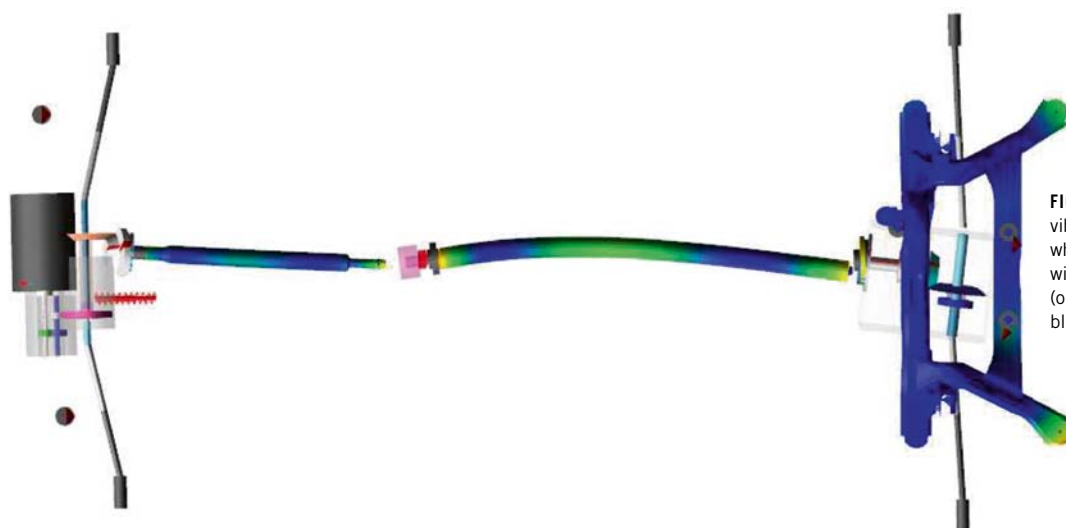


FIGURE 1 Calculated bending vibration of the drive shaft at 103 Hz, which is coupled in fixed body mode with the rear axle transmission (orange/yellow: high bending vibration, blue: low bending vibration)

SIMULATION OF POWERTRAIN VIBRATIONS

The predominantly employed methods of simulating vibro-acoustic scenarios in the development process today are the Finite Element Method (FEM) [1] and Multibody Simulation (MBS) [2]. Detailed, computationally intensive FEM and MBS will be designated as offline simulation methods due to their calculation time.

Realtime simulations are required in diverse applications in the field of powertrains. These are, for example, the evaluation of driveability, models for control unit development using Model-in-the-Loop (MiL) and Hardware-in-the-Loop (HiL) approaches, and applications in the domain of driving simulators. These display sometimes significant differences in the form of the model, the parameter configuration and the degree of detail. Such realtime models are mainly designed to reproduce low frequency vibration phenomena up to a maximum of 30 Hz. The effects on model generation, parameters and the quality of the results for higher frequency phenomena (>30 Hz) has not yet been investigated in sufficient detail. Future applications require the detailed modelling of complex dynamic phenomena, whereby the issues of the simulation of higher frequency vibrations, the question of the impact on calculation efficiency and the quality of the results gain in importance. The following sections describe three relevant application scenarios for powertrain simulation – from detailed offline simulation via reliable realtime simulation to the simulation of mechatronic systems.

DRIVE SHAFT BENDING VIBRATIONS

Drive shaft bending vibrations can influence the vibration behaviour of the rear axle transmission and thus the noise, vibration and harshness (NVH) phenomenon of booming in the passenger compartment. This NVH phenomenon is thus of particular relevance for all rear wheel drive and all-wheel drive vehicles. It is possible to simulate the elastic behaviour of the relevant components with a high degree of reliability using a detailed MBS model, while considering non-linearities such as the elastic drive shaft mounts of the rear-axle transmission. It is critical to consider the non-linear behaviour of the model when simulating the drive shaft bending vibrations, since the entire powertrain is preloaded by the drive torque.

In order to conduct an analysis of the drive shaft bending vibrations using simulation support, the complete test bed configuration was simulated using a detailed offline MBS model. The simulation showed how the non-linear behaviour in the system state, where linearisation occurs, influences the eigenmodes. In order to correctly represent this dynamic behaviour in the simulation, it is crucial to consider the correct dynamic stiffness of the elastomeric bearings in the area of the rear axle drive. For the example shown here, they were calculated experimentally from component tests using the actual levels of preloading. The modified MBS model was linearised under steady-state conditions at constant speed and the eigenmodes were thus calculated. The

prescribed constraints (drive speed and brake torque) corresponded to the values from the test bed.

The calculated bending mode of the drive shaft is coupled with a rigid body mode of the rear axle transmission (Haldex clutch and rear axle differential). The rear axle rotates around the vertical (z) axis and clearly bends in the front elastomeric bearing in the vertical (z) axis, **FIGURE 1**.

For verification purposes, the complete powertrain including the sub-frame, rear axle, rear axle transmission and the bearings was installed on the powertrain test bed. Measurement of the drive shaft bending vibrations was done at constant engine speed, which was selected in such a way that a strong excitation of the first bending mode is given. The probe of a Scanning Laser Vibrometer was focussed diagonally on the drive shaft. The drive shaft executes a superimposed bending movement on the rotational movement. The Scanning Laser Vibrometer only acquires the excursion of the shaft in the direction of the laser beam, **FIGURE 2** [3].

POWERTRAIN REALTIME MODEL

The non-linear behaviour of the model and numerous parameters make it increasingly difficult for the engineer to efficiently improve the product's behaviour. Computer-supported optimisation procedures can be supportive tools, if they deliver reliable results in an adequate timeframe. The connection between level of model detail, result quality and calculation time is shown using the example of an improved real-

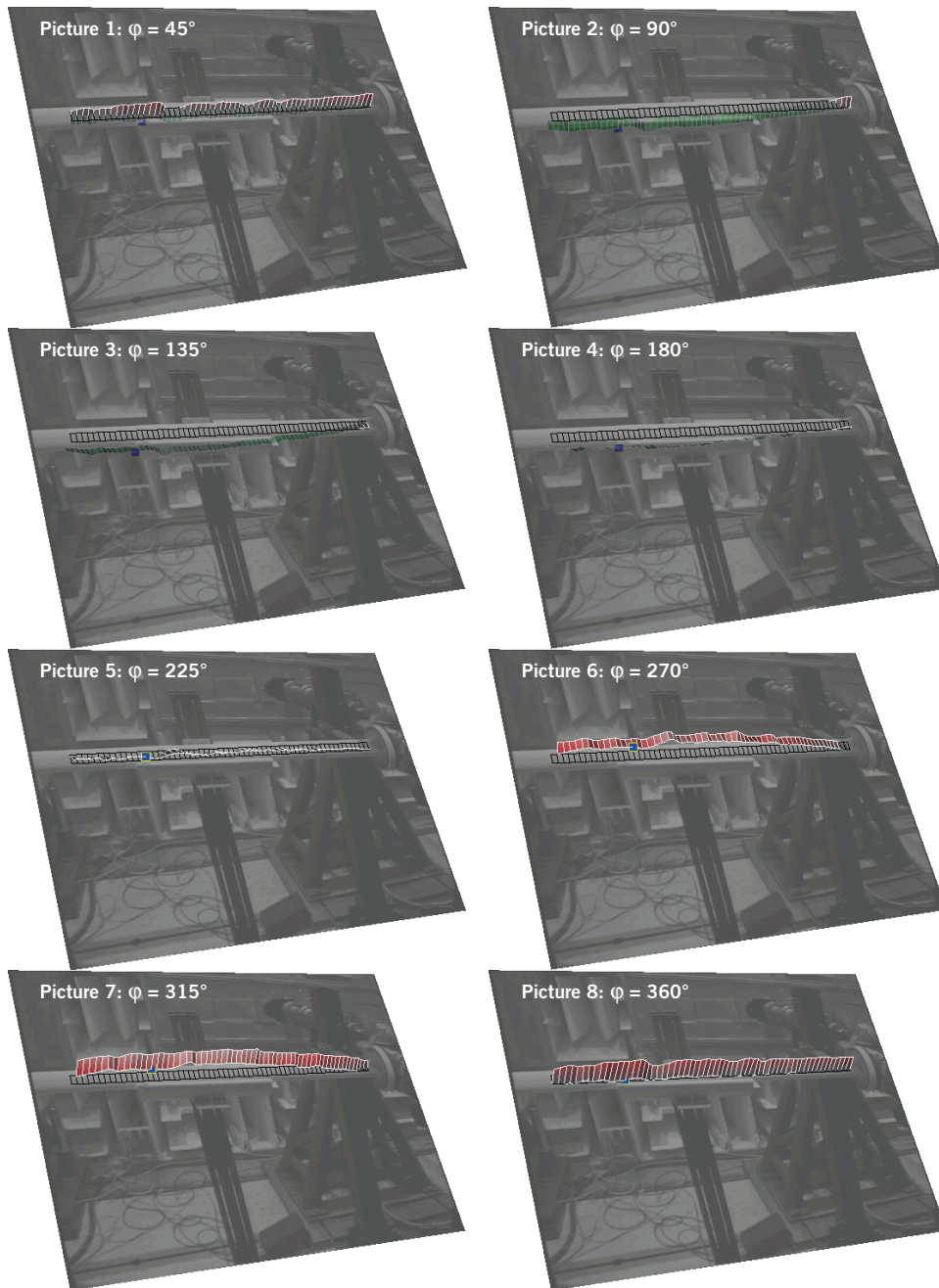


FIGURE 2 Representation of the speed amplitudes measured by the Scanning Laser Vibrometer for one period of the first drive shaft bending mode at 103 Hz

time model for the simulation of powertrain vibrations up to 100 Hz, **FIGURE 3**. The model, constructed in the software environment “Dymola”, displays improvements with regard to quality in the area of engine, drive shaft and tyre models. The engine model simulates the rotational irregularities of the combustion engine via a crank angle dependent mass inertia and a total tangential pressure excitation for all cylinders. The

drive shaft model was extended by a condensed elastic body for the shafts, in order to be able to also consider the influence of the bending vibrations on the excitation of the vehicle’s body. The tyre model includes not only the slip, but also the compliance of the tyre’s footprint via an additional lateral spring, which is also necessary to be able to correctly simulate the vibration behaviour of the wheel and thus the

constraints relative to the road for higher frequencies.

In the following example, optimisation was employed on existing measurement data from the complete vehicle in order to obtain a more exact identification of those model parameters that were associated with uncertainties. A total of nine stiffness and damping parameters were selected in the domains of the transmission, drive shaft and half shafts. It could be demonstrated by the optimisation that the original static stiffnesses of both Hardy discs needed to be increased by approximately 50 % for a frequency range up to 100 Hz. The damping factors also had to be increased compared to the ballpark values that were available in the literature. These model parameters, identified via this measurement, showed good correlation with the measurement results for rotational irregularity of the drive shaft front and rear as shown in the example in **FIGURE 4**.

REDUCTION OF SHUFFLE IN HYBRID POWERTRAINS

The low frequency NVH phenomenon “shuffle” (2 to 4 Hz) is the first eigenmode of the vehicle and the powertrain, whereby the engine oscillates against the vehicle. This shuffle is excited by a sudden change in torque. Vibrations caused by shuffle can be compensated for by adapting the torque via the engine control unit. A parallel hybrid offers the additional possibility of controlling the e-motor according to the principle of disturbance compensation such that longitudinal vehicle oscillations can be compensated for.

A simplified model with four masses was used to design the controller. The integrated tyre model, which converts the wheel torque (rotational) into a longitudinal force (linear) taking the tyre slip into account, uses a speed-dependent damping factor that influences the shuffle frequency. The e-motor in the parallel hybrid was a permanently excited synchronous motor with a maximum power of 15 kW. This is implemented in the model including the corresponding field-oriented control with space vector representation. The necessary DC/AC converter between energy storage and the e-motor is modelled as a simplified

function of pulse width and input voltage. The energy storage consists of supercaps, in order to compensate for the short-term higher power density required from batteries [4].

FIGURE 5 shows a drive-away from rest with gearshift from first into second gear. When pulling away, the clutch is closed slowly, so that no shuffle occurs. When the gear is shifted from first into second, clearly recognisable shuffle vibrations occur, whereby the gearshift is consciously carried out slowly, in order to be able to analyse the vibration behaviour in detail. The first oscillation overshoot after opening the clutch requires high compensatory torque from the e-motor, which cannot be supplied. Even so, the active shuffle compensation, which was designed and evaluated using simulation, can still very effectively reduce the vehicle longitudinal vibrations.

SUMMARY

Simulation methods for the reliable prediction of vibro-acoustic behaviour in powertrains are required in diverse development phases and for the evaluation of development maturity. This results in diverse requirements concern-

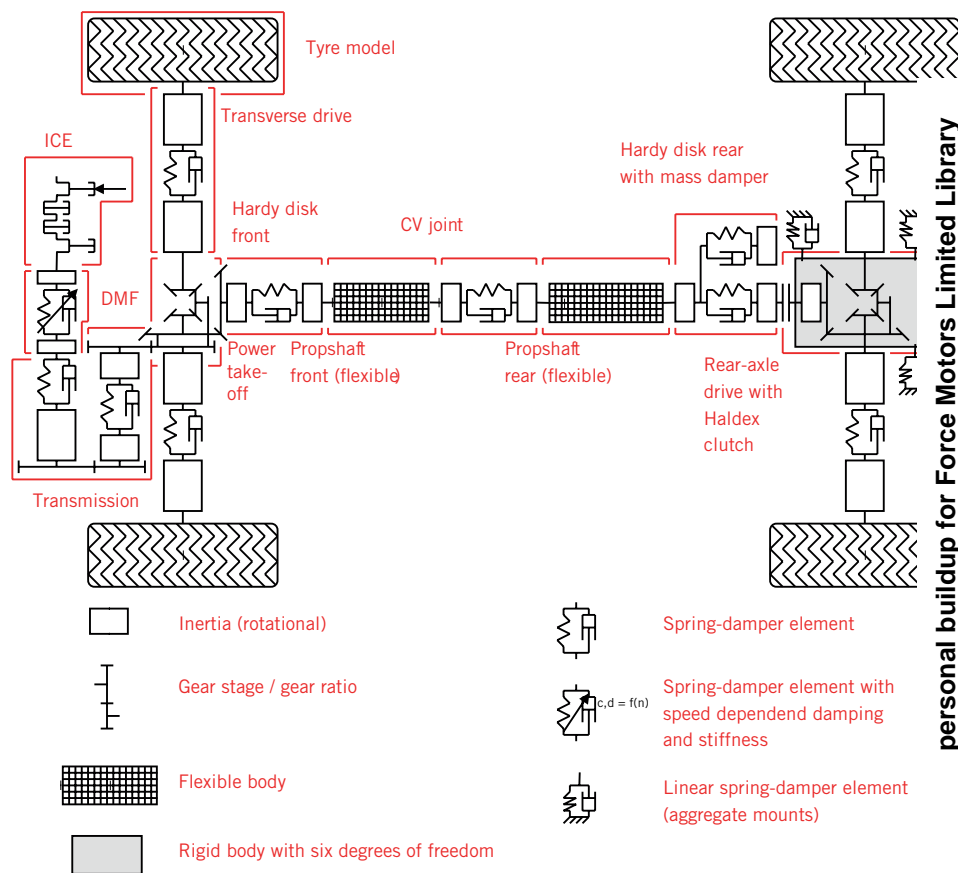


FIGURE 3 Extended powertrain model with elastic bodies for both drive shaft sections and rear axle transmission suspended via three aggregate bearings (ICE: internal combustion engine; DMF: dual mass flywheel)

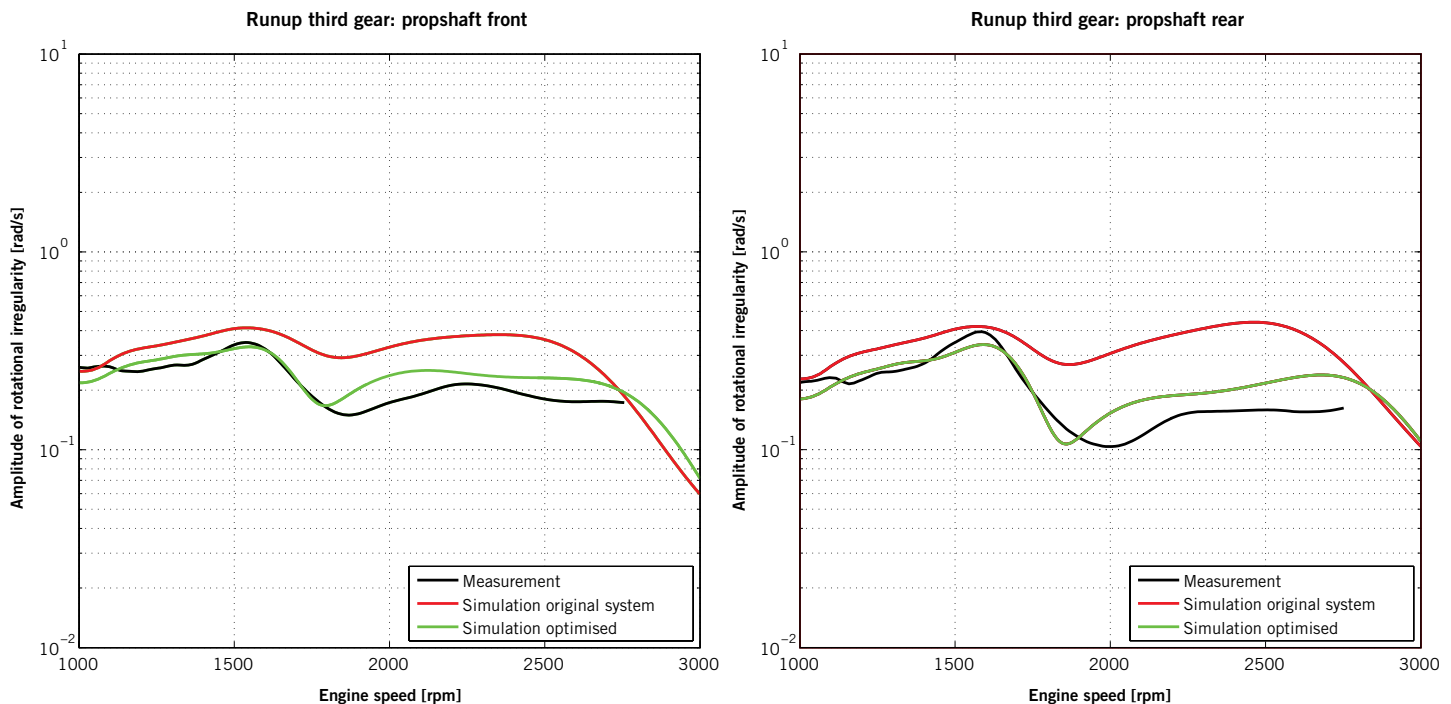


FIGURE 4 Measurement and series comparison of rotational irregularities (amplitude trace 2nd engine order) in the domain of the drive shaft front (left) and drive shaft rear (right)

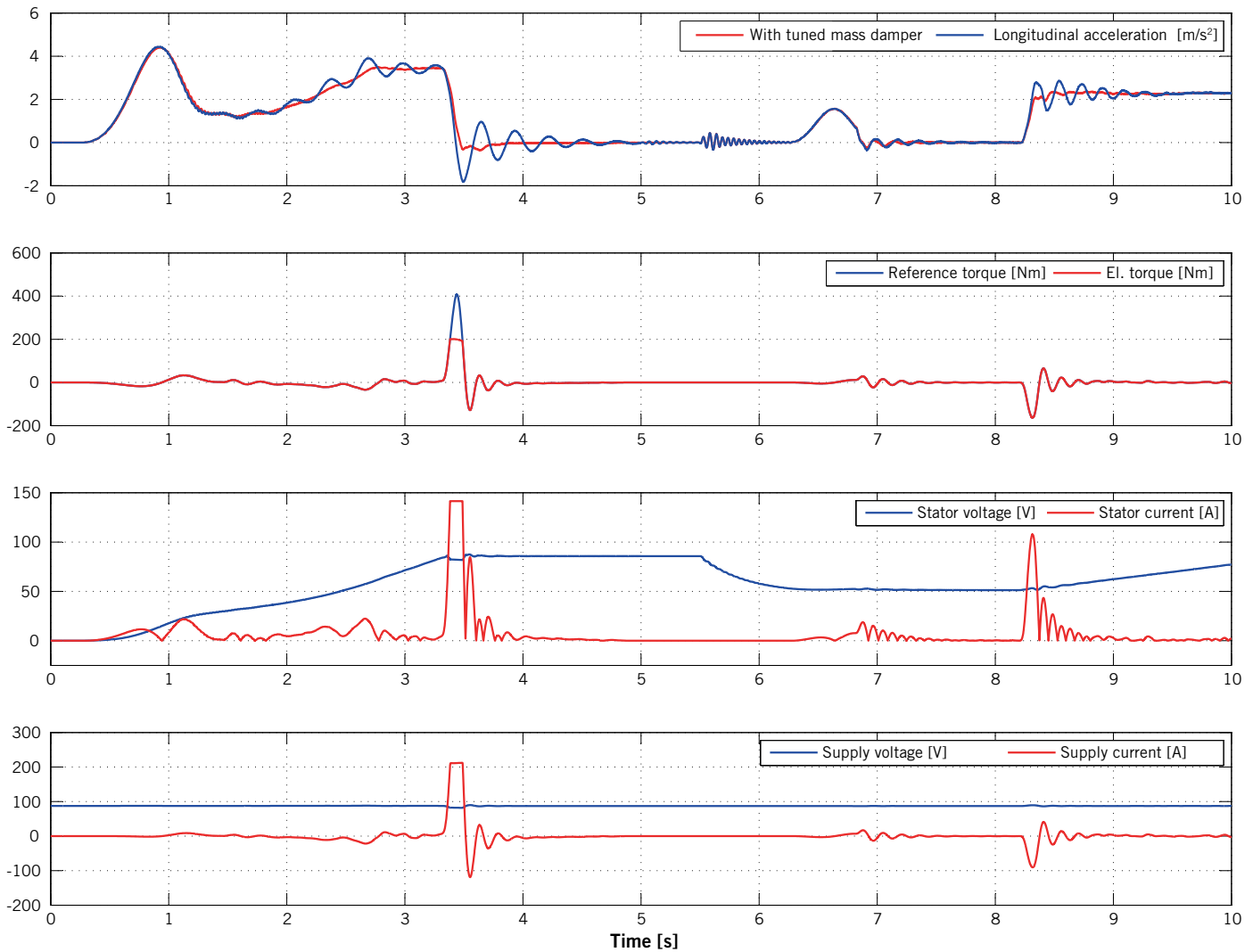


FIGURE 5 Drive-away manoeuvre with active judder compensation: Shown are the vehicle longitudinal acceleration with and without shuffle reduction, the reference torque of the controller, the actual torque of the e-motor, and voltage and current on the stator [4]; shuffle vibrations occur in the uppermost diagram after disengaging of the first gear at around 3.5 s and engaging the second gear at around 8.3 s

ing model design, parametric configuration, quality of results and computational efficiency. This paper shows, using selected examples, that appropriate representation of non-linear model behaviour is crucial for good predictive quality. In the future, the tool and methodology landscape for the NVH design of powertrains will become more widespread and thus support the provision of valid statements in every phase of the development process.

REFERENCES

- [1] Zienkiewicz, O.; Taylor, R.; Zhu, J.: The Finite Element Method: Its Basis and Fundamentals. Elsevier Publishing, 2013
- [2] Shabana, A.: Dynamics of Multibody Systems. Cambridge Publishing, 2013
- [3] Girstmair, J.: Simulation und Verifikation des vibro-akustischen Verhaltens von Pkw-Antriebs-systemen mit Echtzeit und Offline Modellen. Dissertation, Graz University of Technology, 2012
- [4] Girstmair, J.; Priebisch, H.-H.; Nijman, E.: Possibilities for improving the drivability of conventional and hybrid drivetrains. 13th Stuttgart International Symposium Automotive and Engine Technology, 2013

THANKS

The Virtual Vehicle Research Center is supported within the scope of Comet – Competence Centres for Excellent Technologies by the Austrian Ministry for Transport and Technology (BMVIT), the Austrian Ministry for Science, Research and Industry, (BMWFW), the Austrian Research Grant Company mbH (FFG), the province of Styria and the Styrian Business Promotion Agency (SFG). The Comet programme is run via the FFG.

75 YEARS AT THE CUTTING EDGE OF ENGINE TECHNOLOGY.

IT'S OUR BIRTHDAY!



1939



2014

Every month for 75 years, MTZ Motortechnische Zeitschrift has been examining the key issues driving our world: the internal combustion engine and other powertrains. Throughout all those years, our magazine has pulled off the miraculous feat of staying young and fresh while keeping its finger on the pulse of engine technology. And in one point in particular, MTZ has always remained true to itself: in its aspiration to offer our readers the ultimate in quality technical journalism. www.MTZonline.com

MTZ 75
JAHRE



Appearance and Effects of Turbocharger Noise

Almost all modern diesel and gasoline engine concepts rely on the use of turbocharging. As a result, the boundary conditions for the components of the air intake system have also changed. Mann+Hummel has examined the influence of turbocharging on acoustic behaviour and the optimisation measures that can be implemented.

AUTHOR



Robert Hanisch

is System Acoustic Technician in the OEM Unit at the Mann+Hummel GmbH in Ludwigsburg (Germany).

NEW NOISE EXCITATIONS REQUIRE NEW SOLUTIONS

As is commonly known, the emissions regulations for combustion engines in motor vehicles are becoming more stringent. In order to enhance efficiency and performance, forced induction systems have become widely established in the automotive industry. Virtually all current diesel and gasoline engines are equipped with forced induction technology today [1, 2]. As a result of the integrated turbochargers, noises such as whooshing, whistling, whining, hissing or breathing are generated, the characterisations of which are as varied as their causes.

The integration of turbocharging components in the air intake system has thus changed the acoustic framework conditions and consequently the requirements placed on it significantly. On the one hand, these turbomachines act as a reflection and transmission element for the piston-generated pressure pulsations. On the other, regardless of its design, the turbocharger acts as a noise generator. It mainly emits high-frequency tonal sounds and noise which are unrelated to the engine speeds. Owing to the ongoing optimisation of the charging and combustion processes, partly involving significantly higher boost pressures, for

example through full exploitation of the turbocharger map up to the pump limit, it is necessary to implement geometric modifications and e.g. more complex diverter systems. These lead to further, often highly pulsed phenomena such as, for example, load dump noise.

These new noise excitations require new solutions as they have a significant impact on the noise impression of a vehicle both to the outside and in the interior. Owing to their pulse and frequency characteristics, these are neither acceptable for sports cars, nor for comfortable saloons. Because as they are not, as a rule, load dependent throughout the entire engine speed range, they cannot be used for the purpose of acoustic feedback on the driving status.

Conventional air intake system duct geometries which are proven for naturally aspirated engines are not sufficient to cope with this type of acoustic excitation. Eliminating them by means of suitable broadband silencers is therefore essential. Here, it must be ensured that these are installed close to the source. As this is often not possible due to space constraints, new applications, for example multi impedance systems, are used in order to prevent intrusive noise radiation and to achieve a desirable sound characteristic.

FORCED INDUCTION CONCEPTS

A number of forced induction technologies are used in modern engines: Exhaust turbochargers are widely used

and are available in numerous variations. These are implemented singly, as mono-turbochargers, or as multiple turbochargers in a variety of arrangements. These then result in further forced induction concepts, including sequential turbocharging, biturbo/twin turbo, sequential biturbo, multi-stage turbocharging or turbo-compound charging. Furthermore, forced induction can also be achieved using compressors/superchargers. Combinations of the two charger types are also available on the market. These are aimed at ensuring a homogeneous power characteristic throughout the entire engine speed range. A side-effect here, however, is the acoustic challenge that this brings about. The excitation spectra of both charger types often differ, partly owing to the different ways in which they are driven. This often means that more noises have to be dealt with.

THE TURBOCHARGER AS SILENCER

Turbocharger components feature complex geometries. The noise generated by the basic engine (from the pressure pulsations of the reciprocating pistons) is conducted towards the turbocharger through the air intake system components (manifold, charge air cooler, etc.), **FIGURE 1**. During the process, it is already changed through numerous cross-sectional jumps, resonance effects, etc. [3]. The complex turbocharger geometry – particularly noteworthy is the narrow compressor gap and the impeller with its

vane geometry – represent an obstacle to the emitted noise.

Most of the incoming noise is reflected back towards the engine, which occurs with varying intensities for different frequencies. Generally, low frequencies are reflected with particularly great intensity. Depending on the turbocharger map and its geometry, in interaction with the geometry of the immediately adjacent parts, frequency components of the main excitation-generating engine order or multiples thereof pass through the turbocharger. These are then transmitted through the air induction components on the suction side, are modified through known mechanisms and ultimately contribute to the outlet noise, **FIGURE 2**. The influence of the compressor on the acoustic waves emitted by the basic engine, however, still remain largely unknown. No reliable predictions are therefore possible in this regard.

THE TURBOCHARGER AS NOISE GENERATOR

In addition to their properties as low-frequency silencers, turbochargers also generate noise. These noises are caused by a variety of factors which will be outlined below. The noise-generating mechanisms are described, for example in [4]. Common to all these noises are their high excitation frequencies. The frequencies generated by turbochargers are usually above 1000 Hz. They can reach up to 10 kHz. As an initial classification, a distinction can be made between broadband

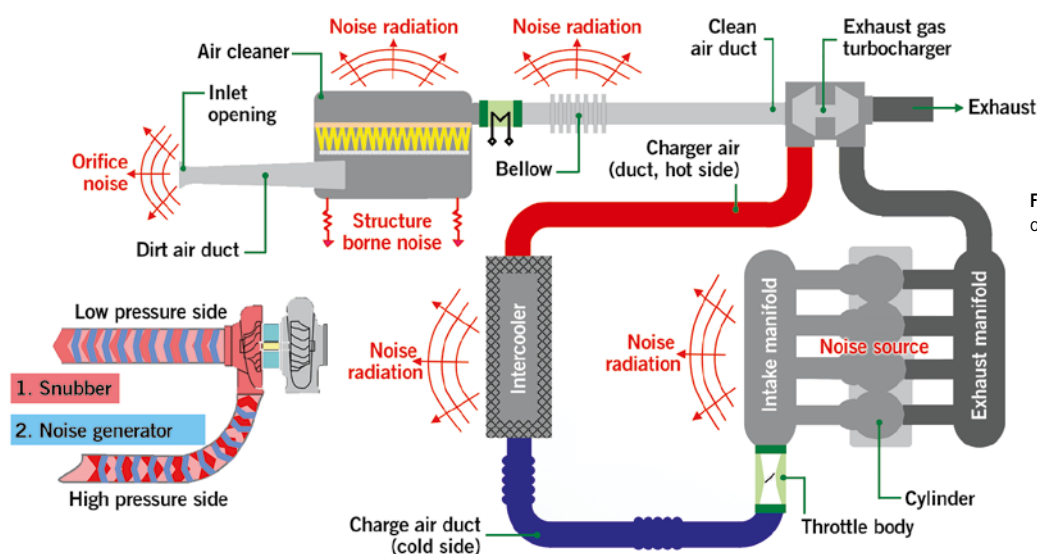


FIGURE 1 Scheme intake acoustic of a turbocharged engine

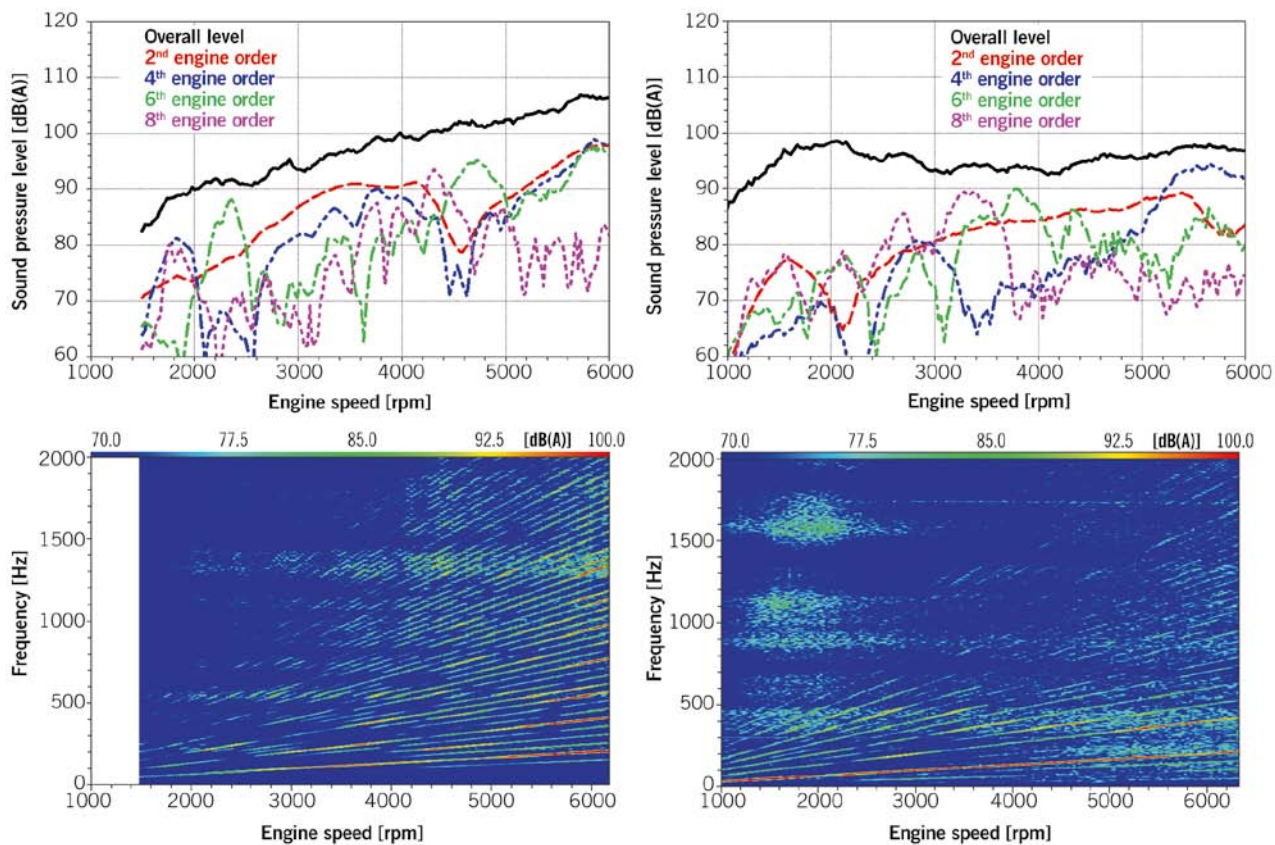


FIGURE 2 Comparison of the outlet noise of a naturally aspirated (left) versus a turbocharged engine (right)

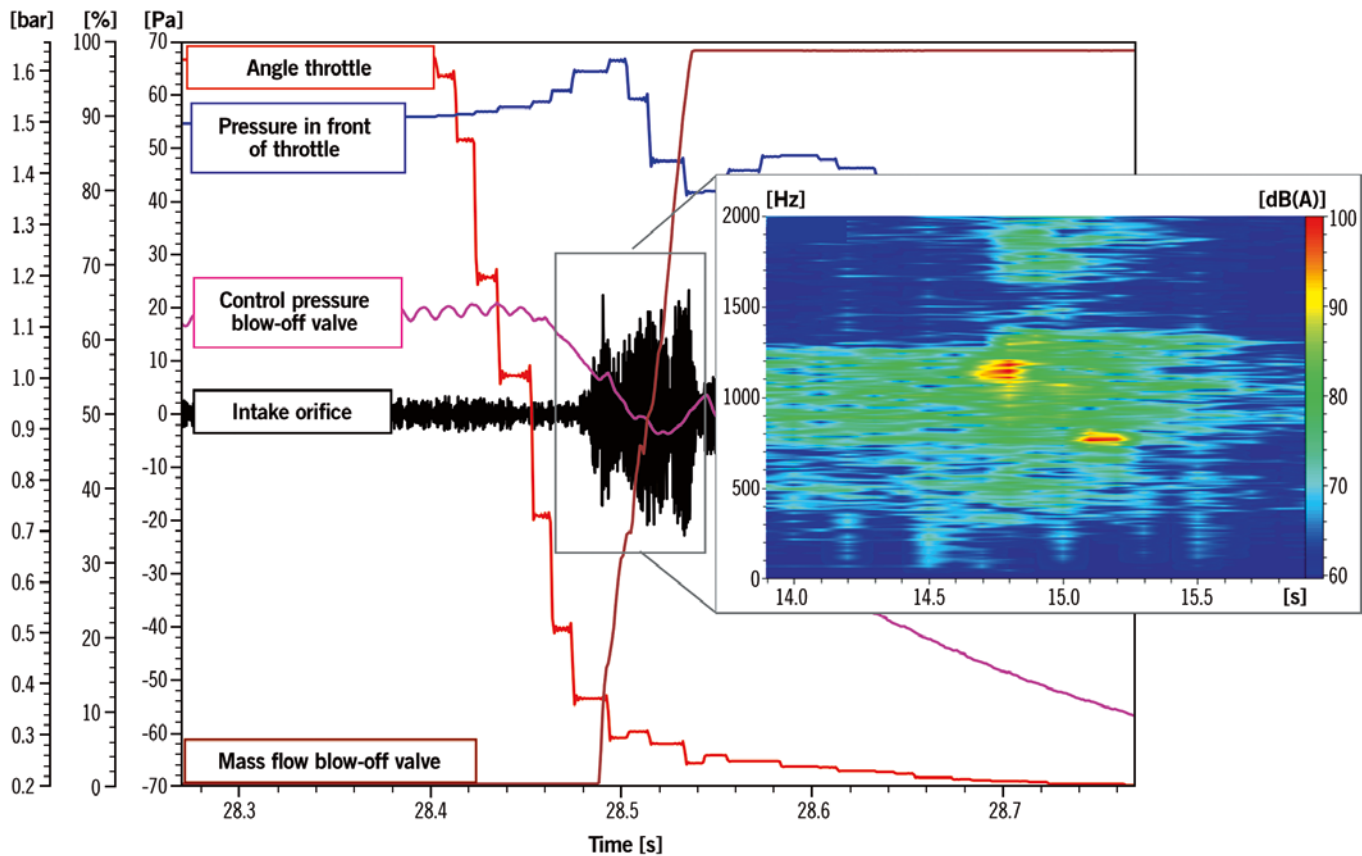


FIGURE 3 Load dump noise of a turbocharged engine

noise and high-pitched tones (e.g. whistling). Constant tones occur, for example due to intrinsic frequencies of the turbocharger shaft in its hydrodynamic oil film bearings. They are independent of the turbocharger speed. Further tonal components often follow the turbocharger order and its multiples, for example the vane orders. The reasons for their occurrence are often imbalances, shaft bearing play, flexural vibrations etc.

Moreover, pulsation noises are emitted, primarily in the intake pipes, which also follow the turbocharger orders and are caused by pressure fluctuations due to alternating forces resulting from asymmetries of the rotor [5].

Whistling noises, as well as whooshing can be caused through the airflow, particularly upstream of the compressor inlet. Here, airflow speeds of up to 0.6 Mach occur. If, for example, a diverter opening is integrated in the compressor

inlet port, turbulent airflows may occur due to vortex shedding. It should generally be noted that from startup until it reaches its operating speed, the turbo engine generates a noise which determines the overall acoustic level, usually at a maximum of 2500 rpm. Explained in simplified terms: until it reaches its ideal operating speed, the engine acts like a naturally aspirated engine drawing the necessary air through the turbocharger. The airflow generated in the compressor is then turbulent.

Depending on the design, further noise phenomena occur in various turbocharger operating states. These include, for example, load dump noises. These can range from “breathing” “hissing” and “cuckoo-like” noises through to highly pulsed, explosive noises. No complete scientific description of the causes has yet been made. It is known that the type and actuation of the wastegate or the variable turbine

geometry, the diverter system with its position and geometry, as well as the throttle valve play a part. Under certain circumstances, the turbocharger, for example, may run on for fractions of a second in the case of a sudden engine load change from full to no load because the frequently vacuum-operated wastegate valve is somewhat “sluggish”. The electrically operated throttle valve, however, closes immediately during this type of load change. If the blow-off valve is also vacuum-operated, it does not open immediately. Owing to run-on of the turbine and of the impeller, a higher pressure then builds up between the turbocharger and throttle valve. From a certain pressure differential and a falling turbocharger speed, this pressure is relieved via the compressor side and back into the low pressure area of the air intake system. This expansion results in the noise phenomena already described, **FIGURE 3**.

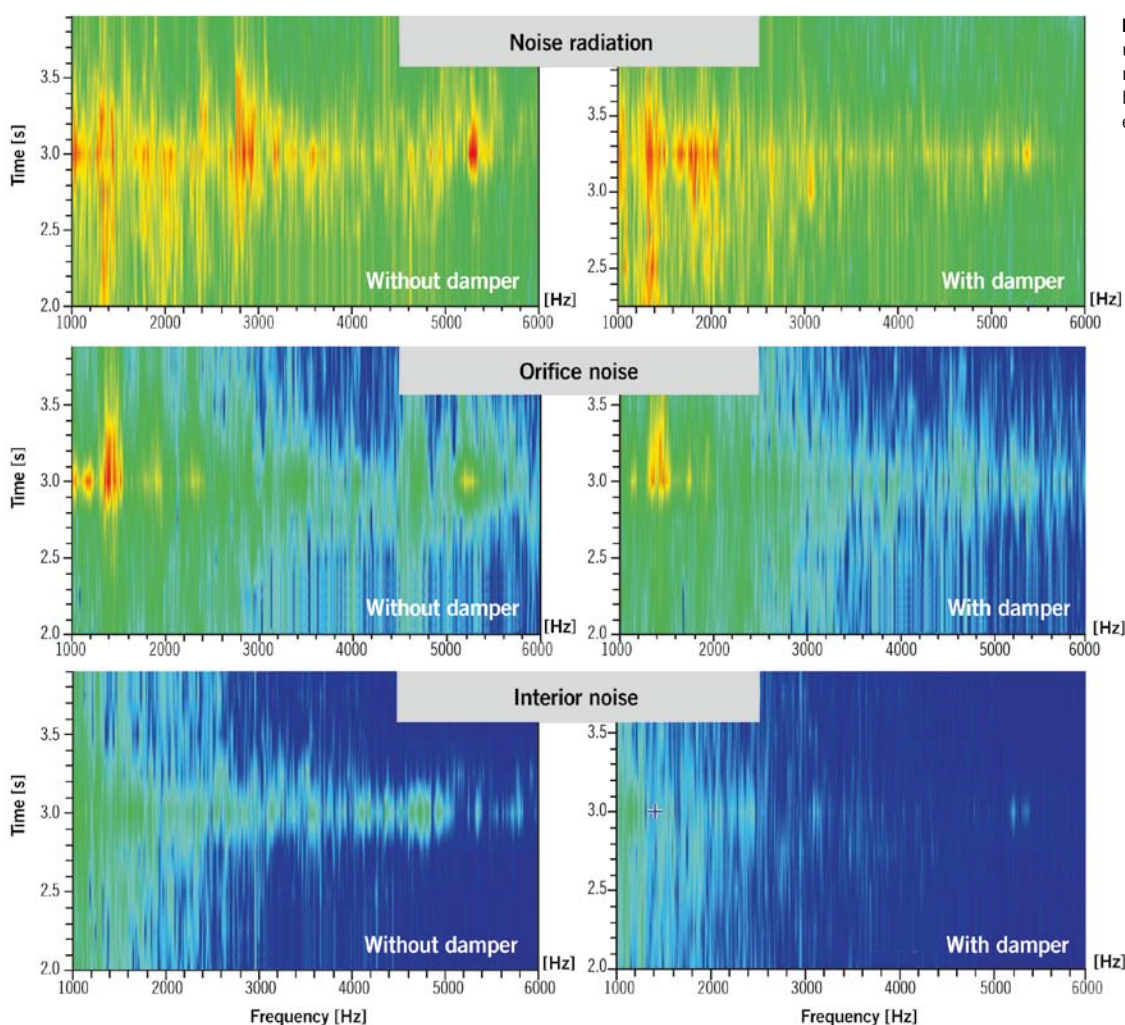


FIGURE 4 Vehicle measurements of a load dump noise (low noise emission blue/green, high noise emission red)

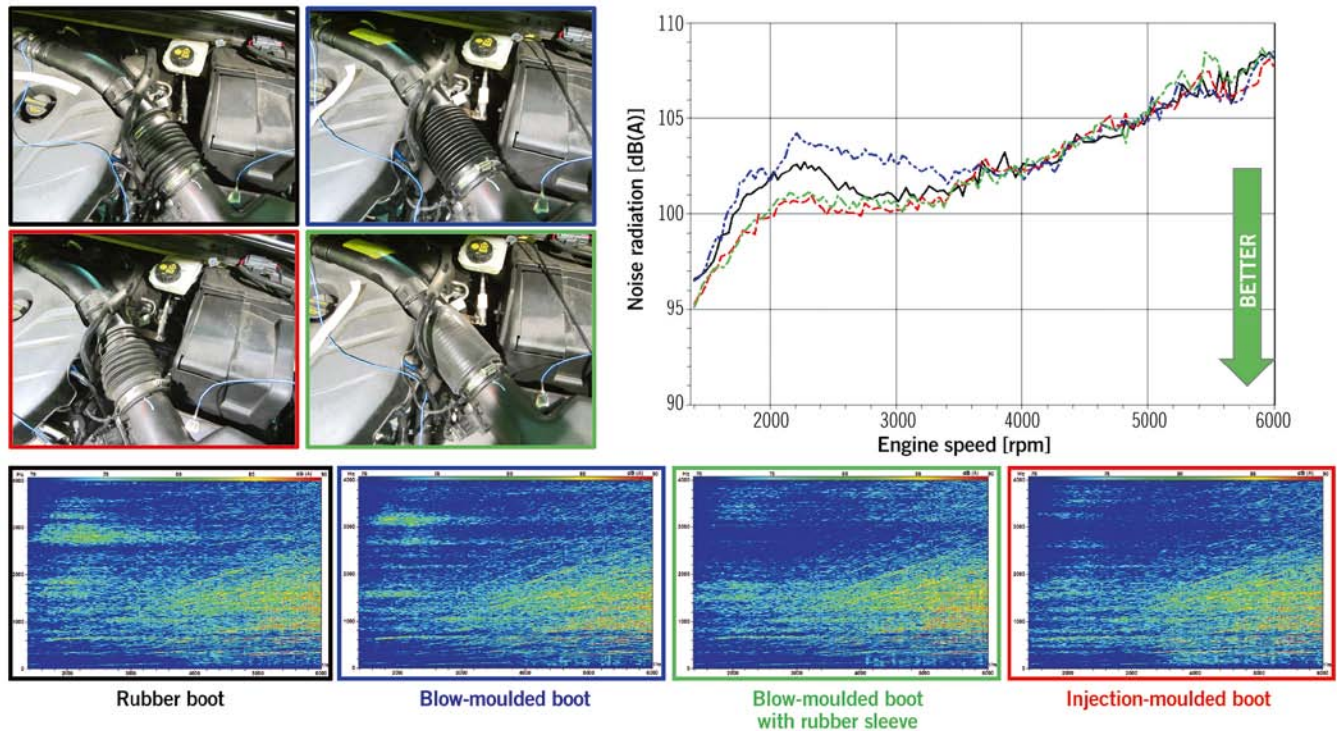


FIGURE 5 Noise radiation behaviour of various clean air ducts (low noise emission blue/green, high noise emission red)

SECONDARY ACOUSTIC MEASURES IN THE AIR INTAKE SYSTEM

Near-source sound absorbers should be used wherever possible to prevent the previously described noises as the intake system ducts do not often represent an adequate barrier to these high frequencies and further radiate the noise. They primarily penetrate into the vehicle interior in this manner. Furthermore, they are transmitted through the air intake system up to the outlet and are perceptible in the external noise. As mentioned previously, owing to their characteristics, these noise emissions are clearly perceived by us humans and are felt to be extremely intrusive. As a near-source solution, broadband absorption silencers and broadband silencers operating according to the Helmholtz resonator principle have proven effective, **FIGURE 4**.

The latter can be used both on the suction and on the pressure side. Combinations of both silencer types are possible, for example to eliminate particularly loud tonal components in addition to the swoosh. Depending on the frequency, $\lambda/4$ pipes can also be very effective. Expansion chambers directly upstream

of the turbocharger compressor inlet, have proven useful.

Where sufficient installation space is available, the silencers can be designed to eliminate the noises completely at source. Unfortunately, this is often not feasible as the available installation space, particularly around the turbocharger, is often very limited and the surrounding conditions challenging. Depending on the type and geometry of the air conveying ducts, it may be necessary to modify these owing to the noise-radiation issues mentioned above. Multi-impedance layers have proven very effective in this context. For this purpose, heavy aluminium-foil clad mats, for example, are fitted onto the ducts. In the area of boots, which are often particularly acoustically transparent, covering with elastomer sleeves is also possible. Both methods are very effective at reducing noise radiation, **FIGURE 5**.

Additional noise attenuation measures can also be implemented in the air filter itself. The integration of absorber layers has, for example, proven successful. It is also possible to install a broadband sound absorber in the air filter, for example an absorption silencer in the clean air connecting piece. Of course, high-fre-

quency sound absorbers can be implemented on the dirty air side. The dirty air duct can also be designed to be porous, i.e. absorbent. This is possible using sintered plastic. Whereas, owing to the high exhaust gas temperatures, the turbocharger cannot easily be encapsulated, this is possible and often advisable in the case of the compressor. Plastic-coated foam parts have proven effective for this purpose.

Above the noise attenuating effect of the turbocharger on the piston-induced pressure waves was described. Because, owing to the turbocharger, these engine orders are now no longer present in the outlet noise, an important component for the interior noise is missing. To date, only weak acoustic load feedbacks can consequently be achieved. With sound measures such as a symposer, it is possible to pick off the excitations of the basic engine upstream of the turbocharger and to direct these into the vehicle interior. By emphasising certain engine orders or frequencies, the interior sound can thus be produced without resorting to sound synthesis. How “dirty”, “racy” or sonorous the sound feedback can ultimately be configured depends, of course, on the engine excitations.

SUMMARY AND CONCLUSION

In the article, the significant influence of forced induction components on combustion engine air intake noise was explained and the sound-attenuating and generating properties of various chargers were also outlined. The main focus was on the turbocharger as a sound generator because the air intake noise characteristic is often intrusively modified by noise emitted from the charger. On naturally aspirated engines, proven components and intake system duct geometries are no longer sufficient for these high-frequency, tonal and often pulsed noises. These are not adequately masked by the turbocharger-attenuated engine order, and thus impair the sound impression of the vehicle. In the article, various secondary acoustic measures, such as absorption and broadband silencers etc. were described. The acoustic components presented represent current, state-of-the-art engine concepts. It remains to be seen, which new challenges will arise out of the further development of the combustion engine, increasing hybridisation etc., and whether they can be countered through purely passive measures.

REFERENCES

- [1] Reif, K.; Dietsche, K.: Kraftfahrtechnisches Taschenbuch. 27th edition, Vieweg+Teubner, 2011
- [2] Mayer, M.: Abgasturbolader. Die Bibliothek der Technik, Volume 103, Verlag Moderne Industrie, 2006
- [3] Munjal, M. L.: Acoustics of Ducts and Mufflers. John Wiley & Sons, New York, 1987
- [4] Stein, M.; Oppermann, N.: Das Aufladesystem im Spannungsfeld zwischen Emissionen, Fahrdynamik und Akustik. Technical book by Haus der Technik, Volume 66, Expert-Verlag, 2006
- [5] Aymanns, R.; Pischinger, S.: Turbo Charger Noise – Development of a Method for Avoiding Whining Noise of Turbo Chargers. FVV report No. 851, Frankfurt/Main, 2008

THANKS

This article is based on the knowledge of the Center of Competence for Acoustics of Mann+Hummel GmbH under the direction of Matthias Alex. The author would like to thank him and his colleagues.

Optimising Thermomechanical Strength of High-load Turbochargers

AUTHORS



Michael Werner M. Sc.
is Simulia Optimisation
Portfolio Technical Specialist,
Simulia Optimisation Strategy,
at the Dassault Systèmes
Deutschland GmbH
in Munich (Germany).



Dr.-Ing. Florian Jurecka
is Director, Strategy Simulia,
at the Dassault Systèmes
Deutschland GmbH
in Munich (Germany).

Modern turbochargers have to withstand high thermal stresses.

Dassault Systèmes has developed a simulation method that enables critical areas on the turbocharger housing to be analysed and optimised quickly and efficiently.

STRESS-BASED DESIGN

In times of increasing performance for fewer emissions and more energy efficiency, turbocharging takes on a large degree of significance in vehicle development. The demand for increased performance in the development of exhaust turbochargers automatically leads to designs approaching their limits in both geometry and material. More and more importance is therefore attached to designing turbochargers capable of sustaining high levels of stress and strain with the aid of simulation and modern optimisation solutions. The right application and positioning of material play a substantial role in influencing the lifetime of a component.

For this purpose, FE analyses with Simulia Abaqus, a Dassault Systèmes

application, are used to simulate thermal fatigue cycles that are known from experiments to be especially critical for the turbine housing. Thermal expansion of the turbine housing reacts locally with different rates to fluctuations of the global exhaust temperature, and the resulting transient thermomechanical stresses plastify the material cyclically, in the worst case until crack initiation. With the calculation of strength, the durability of the turbocharger in the release test is stated in terms of sensitivity to boundary conditions, crack initiation, geometry, thermodynamics, and material.

The use of Dassault Systèmes' Simulia Tosca Structure's optimisation solutions satisfies the necessary premises. Design optimisation automatically improves



FIGURE 1 Spreadsheet evaluation for sensitivity study (screen shot)

details of the component surface to reduce adverse thermomechanical effects, guard against material fatigue, and thus lengthen its lifetime. Local considerations of critical regions are often inadequate, for which reason a two-stage optimisation approach has proved successful. This approach starts by identifying the predominant interactions with a turbocharger in a sensitivity study, enabling utilisation of positive effects and elimination of the negative ones. Based on this globally optimised geometry, detailed improvements that are still necessary are then implemented by a local shape optimisation.

DESIGN OPTIMISATION ON A TURBOCHARGER

To face the challenges in exhaust turbocharger development, a major requirement on the optimisation tool is a maximum possible freedom of design for the surface to be modified. This flexibility for the surface description can be achieved by a non-parametric optimisation tool. Then every single FE node in the design area can be modified directly. The performance objectives cannot be achieved by parametric approaches with resulting housings composed of geometric CAD primitives. Free-form surfaces are needed for adequate and flexible geometric description. Furthermore, the ability to re-use existing simulation models and realistic modeling with nonlinearities such as contacts are essential to create successful optimisation processes. In case of long simulation times the use of optimisation tools based on optimality criteria are beneficial.

GLOBAL OPTIMISATION

The first step of the two-stage optimisation strategy analyses the physical behaviour of the turbine housing exposed to thermomechanical load, and its sensitivity to changes of wall thickness in different regions through a design of experiment (DoE) investigation. In this way it is possible to observe relationships and reciprocal effects that can be utilised and combined to globally optimise the geometry.

MORPHING

Complex mechanical load and boundary conditions (flow, temperature, initial stress) make mathematical derivation of sensitivities unrewarding for an efficient solution with optimisation algorithms. Consequently the DoE chooses a finite difference approach and divides surface geometry into regions that are then grown singly and over a wide area by a uniform amount. This geometry altered (morphed) by Tosca Structure. morph is analysed with the described simulation process to evaluate its performance. Based on these results, the most advantageous combination of variations is sought. The process of geometric changes over a wide surface is also known as shape morphing.

PERFORMANCE EVALUATION OF DESIGN VARIANTS

The individual design variants are evaluated on the basis of equivalent plastic strain (PEEQ). Here, for each design variant, the necessary system responses are observed and evaluated across the individual design and tracking regions, which are the critical areas. Using these

values, the finite difference is then calculated with the results of the unaltered starting geometry. This can be interpreted as follows, taking large-surface growing of 1 mm for example: Positive values in a removed region correspond to improved performance and thus reduced load through the applied change of geometry. Experience demonstrates that the behaviour is virtually linear, and a degradation of performance with growth generally leads to improvement of performance through shrinking (i.e. removing 1 mm of material).

Taking these findings, it is then possible to decide for each region whether it is best to apply additional material or remove it to improve global performance with the observed reciprocal effects of the turbocharger housing. Regions with lots of improving and degrading effects at the same time are best not altered, as even minimal changes of geometry can have an undesirable global result.

MORPHING OF TURBOCHARGER

The optimiser executes the defined geometry changes, starts the analyses in a parallel cluster environment, and generates descriptions of performance. These are then read into a spreadsheet with conditional formatting for clarity in evaluation, FIGURE 1.

COMBINATION FOR GLOBALLY OPTIMISED VARIANT

The DoE analysis determines sensitivities that now serve as guiding information for design decisions. The aim is to use this information so that the global effects are combined advantageously, producing a globally optimised housing design.

This means evaluating the performance of all regions considered for each morphed design variant. First, those variants are sought out that produce solely positive or solely negative effects, because this is where a clear guide to a change of design (grow or shrink) is. The result is a list of surface regions where material is added or removed. This combined morphing variant shows globally improved thermomechanical strength. Considering further design variants that produce improvements for critical regions, for example, and minimally degrade non-critical regions, the globally optimised, combined morphing

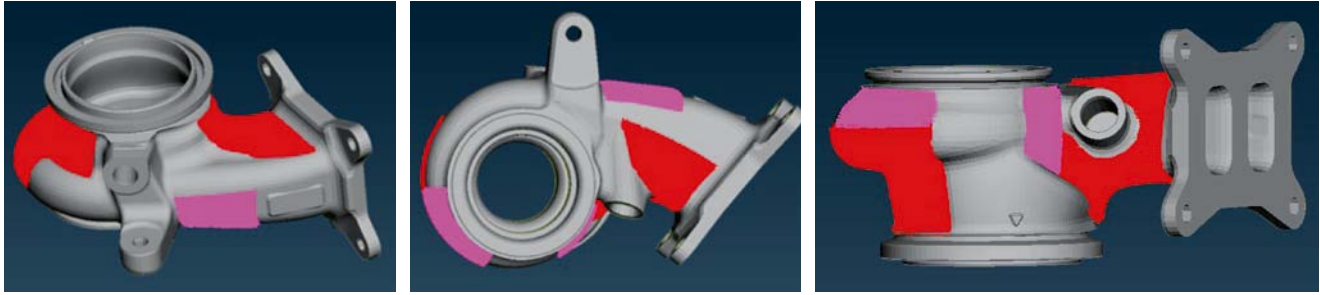


FIGURE 2 Globally optimised design (shrink: red regions, grow: pink regions)

variant can be improved even more. A special focus is on invariant critical regions to improve them by the identified remote effects. This is where experience and engineering expertise count to select and evaluate the variants. Ultimately, within a few variants, you arrive at a global, substantially improved design, **FIGURE 2**.

LOCAL OPTIMISATION

The result of the first optimisation stage is a turbocharger housing design globally improved by large-surface adaptation of wall thickness in which especially critical but invariant regions were optimised by remote effects. The second optimisation stage looks at the remaining critical regions that can be modified directly. This uses the classic shape optimisation in Tosca Structure. The optimisation is intended to minimise PEEQ values in the design areas while ensuring a minimum wall thickness for castability. The non-parametric approach allows maximum design flexibility by shifting every single design node in the design area and thus uses a free-form representation. Thermal and mechanical analyses can directly be used with all modeling details such as contacts and nonlinearities. **FIGURE 3**, **FIGURE 4**, **FIGURE 5** and **FIGURE 6** show the final optimisation results of turbocharger design.

IMPLEMENTATION OF OPTIMISATION RESULTS IN DESIGN ENGINEERING

Ultimate implementation of resulting optimisations in a producible CAD engineering design decides the success of the overall optimisation effort. This calls for close cooperation between the

computational engineer and the design engineer. Globally altered geometric regions are simply worked into the CAD geometry. The results of local design optimisation are exported from Tosca Structure as STL (standard tessellation language) surfaces. Here, the surface is only written in the design areas using

the global engine coordinate system. That enables direct and accurately fitted reading into the original CAD model.

By superimposing the new free-form geometry with the existing model, the design engineer can now use free-form surfaces to match the CAD model to the geometry proposed by the opti-

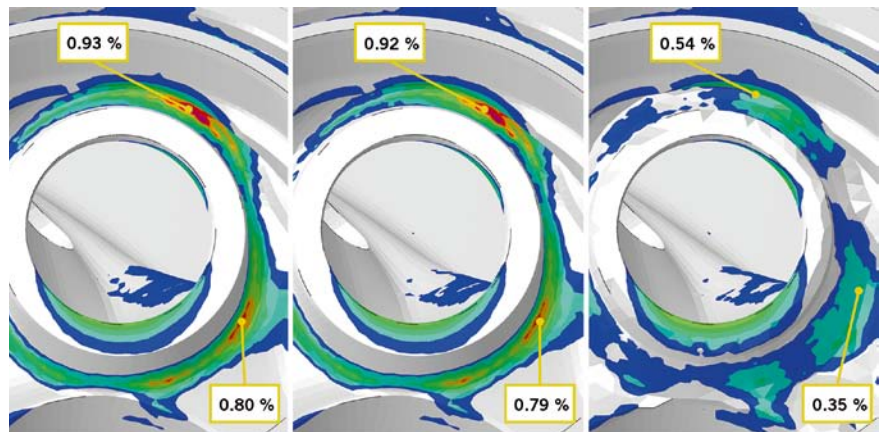


FIGURE 3 Wastegate optimisation (left: original, middle: globally optimised; right: locally optimised; red: high equivalent plastic strain, blue: low equivalent plastic strain)

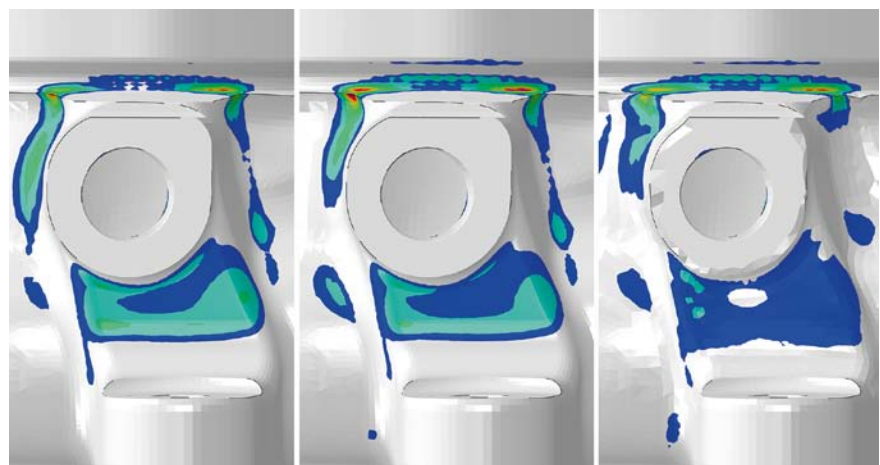


FIGURE 4 Optimised joint between pipe eye and socket head (left: original, middle: globally optimised; right: locally optimised; red: high equivalent plastic strain, blue: low equivalent plastic strain)

miser. Representation of the complex optimised surface geometry by parametric geometric presentations is of no benefit. For high-load turbocharger housings, a tenth of a millimeter can decide on a critical crack initiation. So, a representation of the optimised

geometry with free-form surfaces, as exact as possible, is an absolute must. The process can be simplified significantly, by early preparation of the CAD model for the use of free-form surfaces in the critically loaded regions that are to be optimised.

SUMMARY

Optimisation of thermomechanical strength with Simulia Tosca Structure marks a decisive step towards further improvement in the development of turbochargers. This approach starts by identifying the predominant reciprocal effects in a turbocharger with a sensitivity study, enabling utilisation of positive effects and elimination of the negative ones. Based on this globally optimised geometry, improvements in detail that are still necessary are then implemented by a local shape optimisation. The result are exhaust turbochargers of improved performance and lifetime coupled with more efficient development processes. Trialing and prototyping can be economised on through the consistent application of simulation and optimisation technologies.

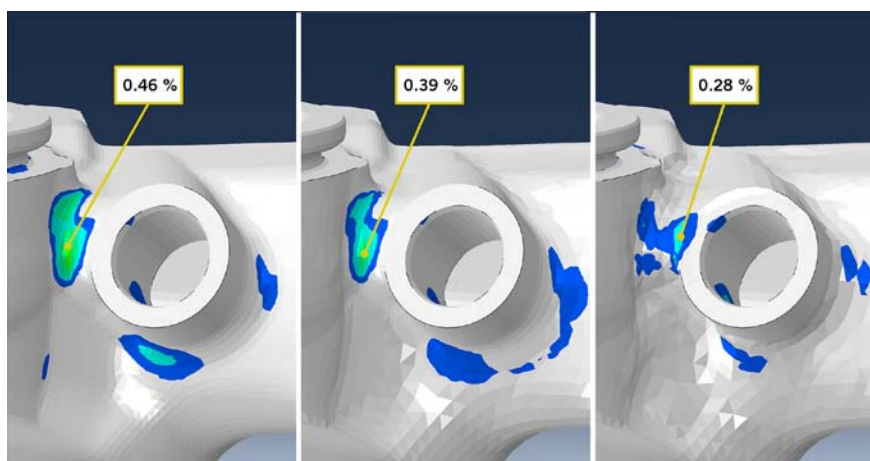


FIGURE 5 Lambda sensor optimisation (left: original, middle: globally optimised; right: locally optimised; green: high equivalent plastic strain, blue: low equivalent plastic strain)

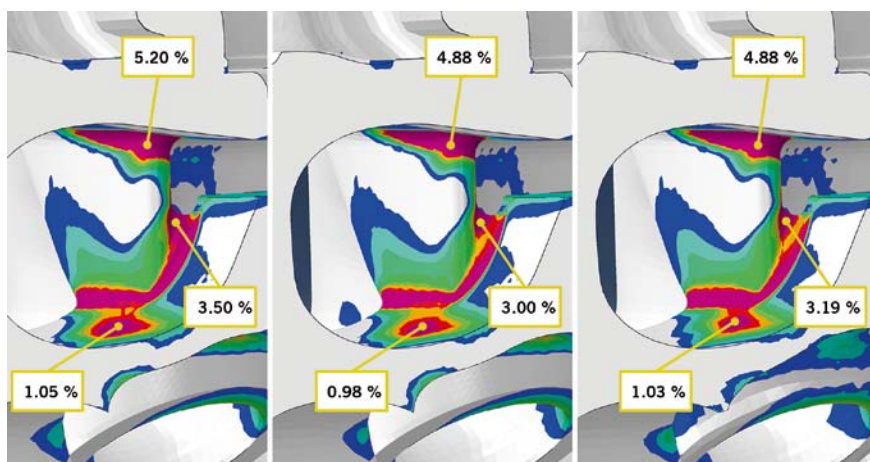


FIGURE 6 Tongue optimisation – improvements without change of geometry (left: original, middle: globally optimised; right: locally optimised; red: high equivalent plastic strain, blue: low equivalent plastic strain)

Founded 1939 by Prof. Dr.-Ing. E. h. Heinrich Buschmann and
Dr.-Ing. E. h. Prosper L'Orange

Organ of the Fachverband Motoren und Systeme im VDMA, Verband Deutscher Maschinen- und Anlagenbau e.V.,
Frankfurt/Main, for the areas combustion engines and gas turbines
Organ of the Forschungsvereinigung Verbrennungskraftmaschinen e.V. (FVV)
Organ of the Wissenschaftliche Gesellschaft für Kraftfahrzeug- und Motorentechnik e.V. (WKM)
Organ of the Österreichischer Verein für Kraftfahrzeugtechnik (ÖVK)
Cooperation with the STG, Schiffbautechnische Gesellschaft e.V., Hamburg, in the area of ship drives
by combustion engine

03|2015 _ Volume 76

Springer Vieweg | Springer Fachmedien Wiesbaden GmbH

P. O. Box 15 46 · 65173 Wiesbaden · Germany | Abraham-Lincoln-Straße 46 · 65189 Wiesbaden · Germany

Amtsgericht Wiesbaden, HRB 9754, USt-IdNr. DE811148419

Managing Directors Armin Gross, Petrus W. J. Hendriks, Joachim Krieger

Managing Director Marketing & Sales Armin Gross | **Director Magazines** Stefanie Burgmaier | **Director Production** Olga Chiarcos

SCIENTIFIC ADVISORY BOARD

Prof. Dr.-Ing. Michael Bargende
Universität Stuttgart

Prof. Dr. techn. Christian Beidl
TU Darmstadt

Dr.-Ing. Ulrich Dohle
Rolls-Royce Power Systems AG

Dipl.-Ing. Markus Duesmann
BMW AG

Prof. Dr.-Ing. Lutz Eckstein
WKM

Dipl.-Ing. Friedrich Eichler
Volkswagen AG

Dipl.-Ing. Dietmar Goericke
Forschungsvereinigung
Verbrennungskraftmaschinen e.V.

Prof. Dr.-Ing. Uwe Dieter Grebe
AVL List GmbH

Jürgen Grimm
Hyundai Motor Europe
Technical Center GmbH

Prof. Dr.-Ing. Jens Hadler
APL

Prof. Dr.-Ing. Jürgen Hammer
Robert Bosch GmbH

Dr. Thomas Johnen
Adam Opel AG

Rainer Jückstock
Federal-Mogul Corporation

Prof. Dr.-Ing. Heinz K. Junker
Mahle GmbH

Prof. Dr. Hans Peter Lenz
ÖVK

Prof. Dr. h. c. Helmut List
AVL List GmbH

Dr.-Ing. Ralf Marquard
Deutz AG

Dipl.-Ing. Wolfgang Maus
Continental Emitec GmbH

Peter Müller-Baum
VDMA e.V.

Prof. Dr.-Ing. Stefan Pischinger
FEV GmbH

Prof. Dr. Hans-Peter Schmalzl
Pankl-APC Turbosystems GmbH

Dr.-Ing. Joachim Schommers
Daimler AG

Prof. Dr.-Ing. Ulrich Seiffert
WiTech Engineering GmbH

EDITORS IN CHARGE

Dr. Johannes Liebl, Wolfgang Siebenpfeiffer

EDITOR IN CHIEF

Dr. Alexander Heintzel
phone +49 611 7878-342 · fax +49 611 7878-462
alexander.heintzel@springer.com

VICE EDITOR IN CHIEF

Dipl.-Ing. (FH) Richard Backhaus
phone +49 611 5045-982 · fax +49 611 5045-983
richard.backhaus@rb-communications.de

MANAGING EDITOR

Kirsten Beckmann M. A.
phone +49 611 7878-343 · fax +49 611 7878-462
kirsten.beckmann@springer.com

EDITORIAL STAFF

Dipl.-Ing. (FH) Andreas Fuchs
phone +49 6146 837-056 · fax +49 6146 837-058
fuchs@fachjournalist-fuchs.de
Dipl.-Ing. Michael Reichenbach
phone +49 611 7878-341 · fax +49 611 7878-462
michael.reichenbach@springer.com
Stefan Schlott
phone +49 8726 9675-972
redaktion_schlott@gmx.net
Markus Schöttle
phone +49 611 7878-257 · fax +49 611 7878-462
markus.schoettle@springer.com
Martina Schraad
phone +49 611 7878-276 · fax +49 611 7878-462
martina.schraad@springer.com

PERMANENT CONTRIBUTORS

Andreas Burkert, Prof. Dr.-Ing. Stefan Breuer,
Hartmut Hammer, Detlef Krehl, Dipl.-Ing.
Ulrich Knorra, Roland Schedel

ENGLISH LANGUAGE CONSULTANT

Paul Willin

ONLINE | ELECTRONIC MEDIA

Portal Manager Automotive
Christiane Brüninglinghaus
phone +49 611 7878-136 · fax +49 611 7878-462
christiane.brueninglinghaus@springer.com
Editorial Staff
Katrin Pudenz M. A.
phone +49 6172 301-288 · fax +49 6172 301-299
redaktion@kpz-publishing.com

SPECIAL PROJECTS

Managing Editorial Journalist
Markus Bereszewski
phone +49 611 7878-122 · fax +49 611 7878-462
markus.bereszewski@springer.com
Editorial Staff | Coordination
Dipl.-Reg.-Wiss. Caroline Behle
phone +49 611 7878-393 · fax +49 611 7878-462
caroline.behle@springer.com
Christiane Imhof M. A.
phone +49 611 7878-154 · fax +49 611 7878-462
christiane.imhof@springer.com

PROJECT MANAGEMENT | ASSISTANCE

Yeliz Konar
phone +49 611 7878-180 · fax +49 611 7878-462
yeliz.konar@springer.com

ADDRESS

Abraham-Lincoln-Straße 46 · 65189 Wiesbaden
P. O. Box 1546 · 65173 Wiesbaden, Germany
redaktion@ATZonline.de

ADVERTISING

SALES MANAGEMENT

Volker Hesedenz
phone +49 611 7878-269 · fax +49 611 7878-78269
volker.hesedenz@best-ad-media.de

MEDIA SALES

Frank Nagel
phone +49 611 7878-395 · fax +49 611 7878-78395
frank.nagel@best-ad-media.de

KEY ACCOUNT MANAGEMENT

Rouwen Bastian
phone +49 611 7878-399 · fax +49 611 7878-78399
rouwen.bastian@best-ad-media.de

DISPLAY AD MANAGER

Nicole Brzank
tel +49 611 7878-616 · fax +49 611 7878-78164
nicole.brzank@best-ad-media.de

AD PRICES

Advertising ratecard from October 2014.

MARKETING | OFFPRINTS

HEAD OF MARKETING

JOURNALS + EVENTS
Jens Fischer

PRODUCT MANAGEMENT

AUTOMOTIVE MEDIA
Jens Fischer
phone +49 611 7878-340 · fax +49 611 7878-407
jens.fischer@springer.com

OFFPRINTS

Martin Leopold
phone +49 2642 907-596 · fax +49 2642 907-597
leopold@medien-kontor.de

PRODUCTION | LAYOUT

Heiko Köllner
phone +49 611 7878-177 · fax +49 611 7878-78177
heiko.koellner@springer.com

SUBSCRIPTIONS

Springer Customer Service Center GmbH
Haberstraße 7 · 69126 Heidelberg · Germany
phone +49 6221 3454-303 · fax +49 6221 3454-229
Monday to Friday, 8 a.m. to 6 p.m.
springervieweg-service@springer.com
www.my-specialized-knowledge.com/automotive

SUBSCRIPTION CONDITIONS

The eMagazine appears 11 times a year at an annual subscription rate 199 € for private persons and 333 € for companies. Special rate for students on proof of status in the form of current registration certificate 98 €. Special rate for VDI/ÖVK members on proof of status in the form of current member certificate 172 €. Special rate for studying VDI members on proof of status in the form of current registration and member certificate 71 €. Annual subscription rate for combination MTZworldwide (eMagazine) and MTZ (print) 399 €. All prices include VAT at 7%. Every subscription comes with access to the online archive. However, access is only available for the individual subscription holder. To obtain access for your entire company/library/organization, please contact sales@springerprofessionals.de or phone +49 611 7878-686. The subscription can be cancelled in written form at any time with effect from the next available issue.

YOUR HOTLINE TO MTZ

Editorial Staff

+49 611 5045982

Customer Service

+49 6221 3454-303

Advertising


+49 611 7878-395

HINTS FOR AUTHORS

All manuscripts should be sent directly to the editors. By submitting photographs and drawings the sender releases the publishers from claims by third parties. Only works not yet published in Germany or abroad can generally be accepted for publication. The manuscripts must not be offered for publication to other journals simultaneously. In accepting the manuscript the publisher acquires the right to produce royalty-free off-prints. The journal and all articles and figures are protected by copyright. Any utilisation beyond the strict limits of the copyright law without permission of the publisher is illegal. This applies particularly to duplications, translations, microfilming and storage and processing in electronic systems.

© Springer Vieweg |
Springer Fachmedien Wiesbaden GmbH,
Wiesbaden 2015

Springer Vieweg is part of
Springer Science+Business Media.

 Springer Vieweg

PEER REVIEW

Peer Review Process for Research Articles
in ATZ, MTZ and ATZelextronik

STEERING COMMITTEE

| | | |
|-------------------------------------|-------------------------------------|-----------------------------------------------------|
| Prof. Dr.-Ing. Lutz Eckstein | RWTH Aachen University | Institut für Kraftfahrzeuge Aachen |
| Prof. Dipl.-Des. Wolfgang Kraus | HAW Hamburg | Department Fahrzeugtechnik und Flugzeugbau |
| Prof. Dr.-Ing. Ferit Küçükay | Technische Universität Braunschweig | Institut für Fahrzeugtechnik |
| Prof. Dr.-Ing. Stefan Pischinger | RWTH Aachen University | Lehrstuhl für Verbrennungskraftmaschinen |
| Prof. Dr.-Ing. Hans-Christian Reuss | Universität Stuttgart | Institut für Verbrennungsmotoren und Kraftfahrwesen |
| Prof. Dr.-Ing. Ulrich Spicher | MOT | |
| Prof. Dr.-Ing. Hans Zellbeck | Technische Universität Dresden | Lehrstuhl für Verbrennungsmotoren |

ADVISORY BOARD

| | |
|-------------------------------------------------|----------------------------------------|
| Prof. Dr.-Ing. Klaus Augsburg | Dr. Malte Lewerenz |
| Prof. Dr.-Ing. Michael Bargende | Prof. Dr.-Ing. Markus Lienkamp |
| Prof. Dipl.-Ing. Dr. techn. Christian Beidl | Prof. Dr. rer. nat. habil. Ulrich Maas |
| Prof. Dr. sc. techn. Konstantinos Boulouchos | Prof. Dr.-Ing. Markus Maurer |
| Prof. Dr. Dr. h.c. Manfred Broy | Prof. Dr.-Ing. Martin Meywerk |
| Prof. Dr.-Ing. Ralph Bruder | Ao. Univ.-Prof. Dr. Gregor Mori |
| Dr. Gerhard Bruner | Prof. Dr.-Ing. Klaus D. Müller-Glaser |
| Prof. Dr. rer. nat. Heiner Bubb | Dr. techn. Reinhard Mundl |
| Prof. Dr. rer. nat. habil. Olaf Deutschmann | Prof. Dr. rer. nat. Peter Neugebauer |
| Prof. Dr.-Ing. Klaus Dietmayer | Prof. Dr. rer. nat. Cornelius Neumann |
| Dr. techn. Arno Eichberger | Prof. Dr.-Ing. Nejila Parspour |
| Prof. Dr. techn. Helmut Eichseder | Prof. Dr.-Ing. Peter Pelz |
| Prof. Dr. Wilfried Eichseder | Prof. Dr. techn. Ernst Pucher |
| Dr.-Ing. Gerald Eifler | Dr. Jochen Rau |
| Prof. Dr.-Ing. Wolfgang Eifler | Prof. Dr.-Ing. Konrad Reif |
| Prof. Dr. rer. nat. Frank Gauterin | Prof. Dr.-Ing. Stephan Rinderknecht |
| Prof. Dr. techn. Bernhard Geringer | Prof. Dr.-Ing. Jörg Roth-Stielow |
| Prof. Dr.-Ing. Uwe Dieter Grebe | Dr.-Ing. Swen Schaub |
| Dr. mont. Christoph Guster | Prof. Dr. sc. nat. Christoph Schierz |
| Prof. Dr.-Ing. Holger Hanselka | Prof. Dr. rer. nat. Christof Schulz |
| Prof. Dr.-Ing. Horst Harndorf | Prof. Dr. rer. nat. Andy Schürr |
| Prof. Dr. techn. Wolfgang Hirschberg | Prof. Dr.-Ing. Ulrich Seiffert |
| Prof. Dr. techn. Peter Hofmann | Prof. Dr.-Ing. Hermann J. Stadtfeld |
| Prof. Dr. rer. nat. Peter Holstein | Prof. Dr.-Ing. Karsten Stahl |
| Prof. Dr.-Ing. Volker von Holt | Prof. Dr. techn. Hermann Steffan |
| Prof. Dr.-Ing. habil. Werner Hufenbach | Prof. Dr.-Ing. Wolfgang Steiger |
| Prof. Dr.-Ing. Armin Huß | Prof. Dr.-Ing. Peter Steinberg |
| Dr. techn. Heideinde Jetzinger | Dr.-Ing. Peter Stommel |
| Prof. Dr.-Ing. Roland Kasper | Dr.-Ing. Ralph Sundermeier |
| Prof. Dr.-Ing. Prof. E. h. mult. Rudolf Kawalla | Prof. Dr.-Ing. Wolfgang Thiemann |
| Prof. Dr.-Ing. Tran Quoc Khanh | Prof. Dr.-Ing. Dr. h.c. Helmut Tschöke |
| Dr. Philip Köhn | Prof. Dr.-Ing. Georg Wachtmeister |
| Prof. Dr.-Ing. Ulrich Konigorski | Prof. Dr.-Ing. Jochen Wiedemann |
| Prof. Dr. Oliver Kröcher | Prof. Dr. rer. nat. Gerhard Wiegler |
| Prof. Dr.-Ing. Peter Krug | Prof. Dr. techn. Andreas Wimmer |
| Dr. Christian Krüger | Prof. Dr. rer. nat. Hermann Winner |
| Prof. Dr. techn. Thomas Lauer | Prof. Dr. med. habil. Hartmut Witte |
| Prof. Dr. rer. nat. Uli Lemmer | Dr.-Ing. Michael Wittler |

Scientific articles of universities in ATZ Automobiltechnische Zeitschrift, MTZ Motortechnische Zeitschrift and ATZelextronik are subject to a proofing method, the so-called peer review process. Articles accepted by the editors are reviewed by experts from research and industry before publication. For the reader, the peer review process further enhances the quality of the magazines' content on a national and international level. For authors in the institutes, it provides a scientifically recognised publication platform.

In the Peer Review Process, once the editors has received an article, it is reviewed by two experts from the Advisory Board. If these experts do not reach a unanimous agreement, a member of the Steering Committee acts as an arbitrator. Following the experts' recommended corrections and subsequent editing by the author, the article is accepted.

In 2008, the peer review process utilised by ATZ and MTZ was presented by the WKM (Wissenschaftliche Gesellschaft für Kraftfahrzeug- und Motorentechnik e. V./ German Professional Association for Automotive and Motor Engineering) to the DFG (Deutsche Forschungsgemeinschaft/German Research Foundation) for official recognition. ATZelextronik participates in the Peer Review since 2011.



AUTHORS



**Dipl.-Ing.
Thorsten Krenek**

is Project Assistant at the Institute for Powertrains & Automotive Technology at the Vienna University of Technology (Austria).



**Dipl.-Ing.
Christopher Bacher**

is University Assistant at the Algorithms and Data Structures Group at the Vienna University of Technology (Austria).



**Prof. Dipl.-Ing. Dr.
Günther Raidl**

is Associate Professor Algorithms and Data Structures Group at the Vienna University of Technology (Austria).

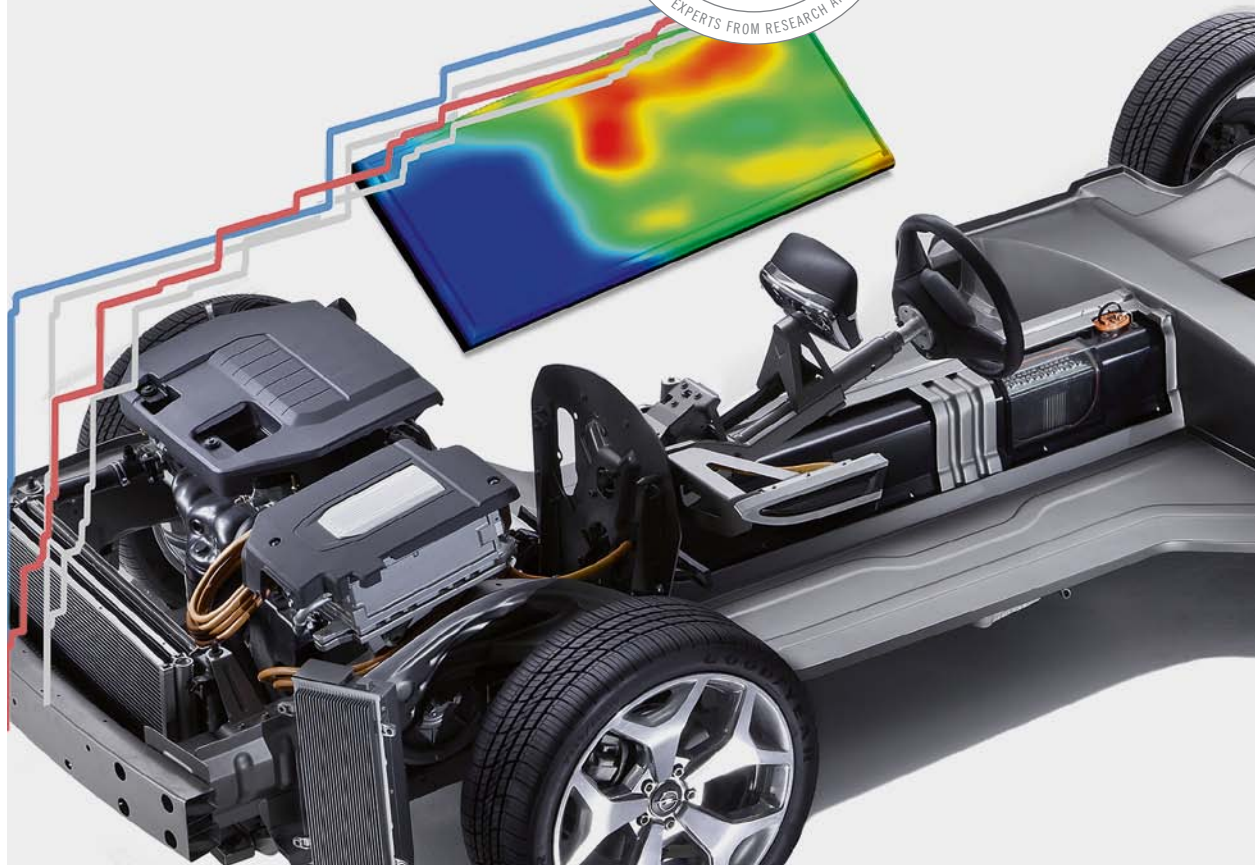


**Prof. Dipl.-Ing. Dr.
Thomas Lauer**

is Associate Professor at the Institute for Powertrains & Automotive Technology at the Vienna University of Technology (Austria).

Numerical Optimisation of Electro Hybrid Powertrains

In the future, the number of plug-in hybrid electric vehicles will further increase in order to fulfil CO₂ legislation. The complexity of electrified powertrains makes it difficult to optimise the vehicle performance and the thermal management efficiently due to the high number of degrees-of-freedom. Therefore, a tailor-made optimisation tool was developed at the Vienna University of Technology to optimise the efficiency of an electrified powertrain while considering comfort functions like the heating of the driver cabin.



1 MOTIVATION

Hybrid electric vehicles (HEVs) are a promising further development of conventional powertrain concepts in terms of fuel consumption and CO₂ emissions. Nevertheless, they have a higher complexity with respect to the dimensioning of the powertrain components, the operation strategies and the thermal management. Appropriate numerical simulation models allow the analysis of the powertrain and its interfaces to the vehicle. Thus, the experimental efforts on vehicle testing can be reduced.

In the following the optimisation of the thermal management of a hybrid electric vehicle at low ambient temperatures is described. Therefore, a comprehensive numerical vehicle model, based on the Opel Ampera powertrain, has been created and analysed for two driving cycles with different power demand (NEDC and US06). The electrified powertrain's high number of degrees of freedom makes the optimisation process difficult and time consuming. However, this process can be supported by the numerical optimisation. For this, an optimisation approach has been developed that is based on meta-heuristic algorithms and neural networks. It was employed to find an operation strategy that minimizes the fuel efficiency without losing thermal comfort during the driver cabin's heat-up period.

2 DEVELOPMENT OF THE NUMERICAL POWERTRAIN MODEL

The numerical vehicle model, as depicted in **FIGURE 1**, has been created using the simulation environment GT-Suite. The model includes the main components of the Opel Ampera powertrain [1], that is to say the two electric machines, the internal combustion engine (ICE), the planetary gear set and the clutches for switching between the driving modes. Additionally, for investigating heat-up strategies the ICE coolant circuit and the driver cabin were also modelled. The driving resistance was calculated using the frontal area, the drag coefficient, the rolling resistance and the weight of the car.

The driving mode is chosen in dependency of the most influential parameters like the vehicle speed, axle-torque or the battery state-of-charge (SOC). The battery is implemented with a static model based on open-circuit voltage and internal-resistance maps. The electric machines are represented by efficiency and maximum torque maps. A detailed thermodynamic model of the ICE has been created in order to take the influence of combustion parameters, like ignition timing, on the heating of the cooling water into account. The necessary data for calibrating the model were determined by engine dynamometer tests. In order to improve the calculation time for the optimisation process a simplification of the ICE model was necessary. Therefore, a mean-value model was derived that calculates the mean flow and a mean high-pressure cycle whereas the specifics of the gas exchange and the combustion are considered with trained neural networks. Details, also for the coolant circuit model are given in [2].

In order to define a reference state for the following optimisation and to verify the model assumptions for the operation strategies,

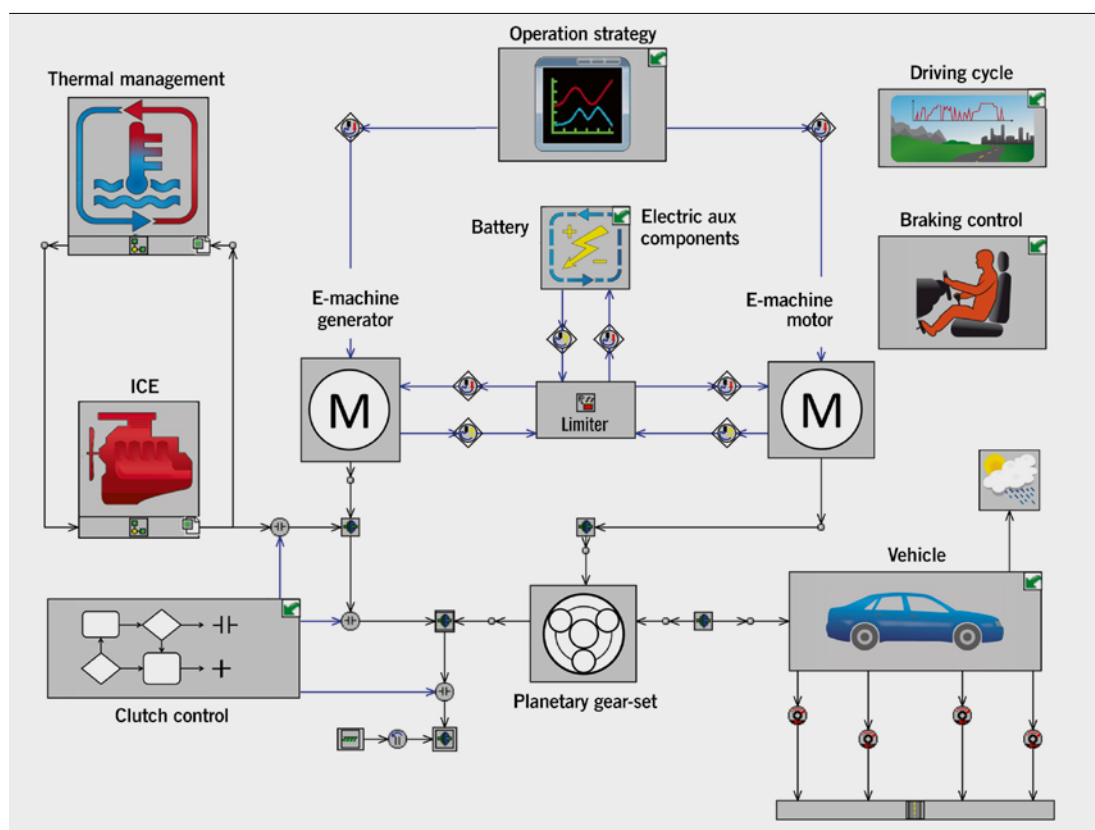


FIGURE 1 Schematic illustration of the GT-Suite vehicle model

the coolant circuit and the electric components, an Opel Ampera was measured on a dynamometer. Details of the engine and vehicle dynamometer tests are also given in [2].

3 OPTIMISATION SCHEME

For reducing the fuel consumption of the described HEV model, variants of well-known population-based metaheuristic algorithms are used. These types of algorithms are known to find sufficiently good solutions, although in general no performance guarantee can be given. The algorithms are implemented in a modular optimisation framework specifically designed for simulation optimisation [3]. Typically, population-based metaheuristics rely on a large number of objective function evaluations, which correspond in our case to simulation runs to determine the fuel consumption of a particular model configuration. Running a large number of simulations is not feasible, due to the high computation times of the HEV model for specific driving cycles (about 20 min/simulation for the NEDC). This is compensated by relying on neural networks to approximate the simulation results for unknown model configurations. How the neural networks are finally used by the optimisation software depends on the design of the optimisation algorithm. The number of simulations is restricted further, by discretising possible parameter configurations to points on a regular grid. This approach allows for caching simulated configurations, despite the continuous nature of the search space, efficiently

avoiding their recomputation. For a more in-depth explanation of these techniques see [4]. Related approaches are described in [5].

The neural networks are built on the fly during the optimisation and are used in so called “bagging ensembles” [6]. This technique builds multiple neural networks from the simulation results and averages their predictions, usually resulting in a lower generalisation error if compared to standard neural networks. The generalisation error is tried to be reduced further, by never considering an absolute objective value for comparing configurations, but rather their relative order. Therefore, the neural networks are not required to predict the objective value, but the ordering of configurations is deemed to be easier achieved.

The optimisation process splits into three phases, each with a different optimisation intent. Further the number of grid points is increased in each consecutive phase by introducing a new point between any two adjacent points in each dimension. Below a description of the optimisation scheme is given. An overview of the scheme is depicted in **FIGURE 2**. Note that the description already provides concrete values for settings of the optimisation algorithms e.g. number of iterations, or the values of the constants influencing the algorithm behaviour. The concrete settings depend on the problem and have been chosen for the specific use case due to previous experiences with the algorithms.

In the first phase a simple genetic algorithm (GA) is used to generate an initial diverse set of simulation results for neural network training. Genetic algorithms are inspired by the principles of evolution and natural selection. They operate in iterations/generations of sets of possible solutions to the simulation – so called populations. More specifically, in each iteration a population of size six is created by sampling two configurations randomly and obtaining the remaining four by recombination. Recombination creates a new configuration by randomly selecting two pairs of configurations from the previous generation and selecting the best configuration from each pair. The selected solutions then form the opposite corner points of a hypercube wherein a new configuration is sampled randomly. The GA is executed two times for 50 iterations each.

The second phase is the main part of the optimisation. This phase starts using bagging ensembles of 24 neural networks, regenerated every 3 iterations to include the data from newly generated configurations. In every iteration a particle swarm optimisation (PSO) [7] is executed – a metaheuristic which mimics the behaviour of bird flocks on food search. For the optimisation process the particle swarm is represented by 20 configurations which are evaluated with the bagging ensemble. The PSO then executes a step, where each configuration moves towards the globally best configuration and towards its own best configuration from previous steps. Again all configurations are evaluated with the bagging ensemble and this step repeats 200 times. At the end of the last step the best six configurations generated by the PSO are evaluated with the simulation model. The intent of this procedure is to execute time-intensive simulations for promising configurations only.

The last phase of the optimisation is used to further improve already discovered solutions. To this end an Evolution Strategy (ES) with Active Covariance Matrix Adaption [8] is used. The algorithm basically uses a normal distribution to generate new configurations and adapts the distribution over time. The mean of the distribution is estimated averaging the thirty best configurations and ten random configurations. Additionally the covariance matrix of the normal distribution is estimated from the selected configurations. In every iteration 100 new configurations are sampled by using the normal distri-

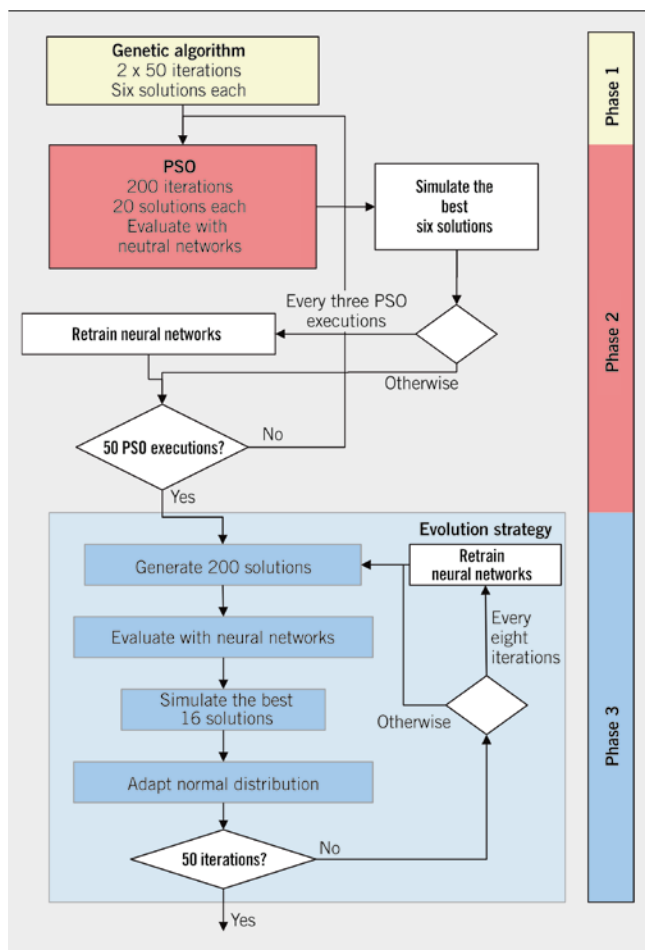


FIGURE 2 Overview of the optimisation process scheme

bution with the calculated covariance matrix and mean. These configurations are then evaluated with the bagging ensemble. Of those the best 6 configurations are evaluated with the simulation model. That way the neural networks act as filter for the current set of configurations. Afterwards the covariance matrix and the mean are adapted so good configurations become more likely. The concrete adaption scheme is explained in [8]. The optimisation ends after executing 50 iterations of the active covariance matrix adaption. For a more detailed explanation of the optimisation algorithms see [3].

4 ANALYSIS OF THE POWERTRAIN OPTIMISATION

For the optimisation of the powertrain eleven parameters have been chosen. The most important ones are listed in **TABLE 1** including their boundaries. The parameters were used to vary the displacement of the ICE, the operation and charging strategy, the gear ratio and the electric heat demand. A detailed analysis of the results in terms of ICE operating point distribution and energy flow analysis is shown in [2]. In the following mainly the optimisation process is described. In **FIGURE 3** the optimisation process is illustrated by the number of calculated configurations and the best known improvement found so far in comparison to a reference configuration measured on the chassis dynamometer. In the US06 and the NEDC driving cycle there is a large improvement in the first phase of the algorithm, whereas in phases 2 and 3 further low potentials were found. Unfortunately, a full statistical analysis of the optimisation is not applicable due to the high computation times of the simulation. To illustrate the process in more detail a qualitative approach is applied. For analysis purposes self organising maps (SOM) have been derived. SOMs are a machine learning method which projects a high-dimensional space – the space of configurations and their associated fuel consumption – onto a two-dimensional grid in a non-linear way. Each point in the grid is represented as so called unit. A unit is associated with a position in the high-dimensional space, which is determined by a training algorithm. Each computed configuration is then projected onto the closest unit.

The SOM can be overlayed with different visualisations. First a smoothed data histogram (SDH) [10] is used which gives insight into

| Parameters | US06 Boundaries | | NEFZ Boundaries | |
|---------------------------------------------------|-----------------|---------|-----------------|---------|
| | Minimum | Maximum | Minimum | Maximum |
| ICE displacement multiplier [-] | 0.7 | 1 | 0.5 | 1 |
| Maximum generator power [kW] | 30 | 60 | 15 | 45 |
| Maximum coolant temperature for electric heat [K] | 283 | 313 | 283 | 313 |
| Maximum electric heat power [kW] | 0 | 7 | 0 | 7 |

TABLE 1 The main optimised parameters with boundaries for the US06 and the NEDC

the distribution of the configurations over the map. This allows to analyse which regions of the map have been searched by the optimisation algorithm. Second a component planes [11] visualisation is used. It shows for each parameter of the HEV model its value's distribution over the map. Visualising multiple component planes side-by-side gives hints about correlations between fuel consumption and parameter values for configurations evaluated by the algorithm. It should be noted that this view does not provide correlations between fuel consumption and parameter values in general, as the optimisation algorithm will not explore all areas of the search space equally.

In **FIGURE 4** the maps of the distribution of the calculations and of the fuel consumption are shown. The maps in the first column depict the aforementioned SDHs. On these maps yellow-to-white coloured clusters can be observed, which correspond to the areas where most of the solutions have been calculated. In combination with the fuel consumption maps it can be seen that these clusters coincide with areas of low fuel consumption (blue colouring). Most of these configurations have been calculated in the second and third phase of the algorithm. The areas of the higher fuel consumption (red colouring) are mainly caused by the first phase of the algorithm, where many random configurations have been calculated. This means that the optimisation algorithm has worked, as a lot of configurations with low fuel consumption have been calculated especially in the last two phases. In **FIGURE 5** and **FIGURE 6**

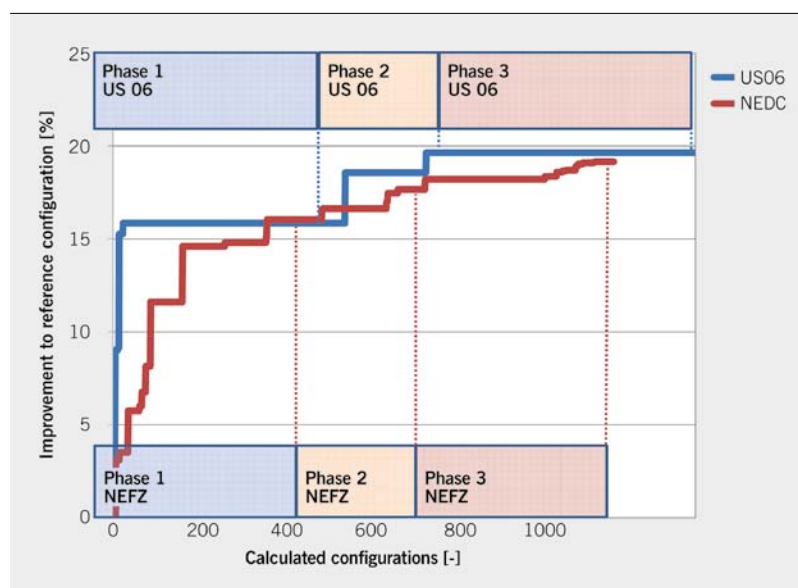


FIGURE 3 Illustration of the optimisation process in the US06 and NEDC

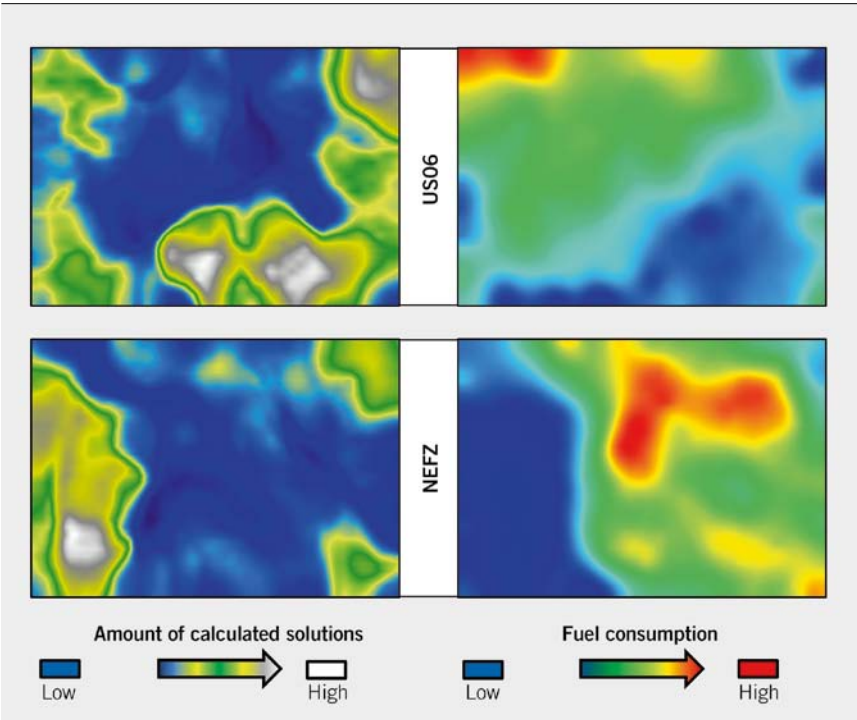


FIGURE 4 Self Organising Maps of the calculation distribution and the fuel consumption

the maps for the most important parameters of the configurations listed in **TABLE 1** are shown for the US06 and NEDC. These maps must be interpreted in combination with the SOMs shown in **FIGURE 4**. For further explanations promising configurations are marked as blue coloured areas in the fuel consumption maps shown in **FIGURE 3**. The map left above in **FIGURE 5** and **FIGURE 6** shows the scaling of the ICE displacement. For promising configurations in the US06 it can be seen that areas with low, mid and high multipliers exist, that is to say there is no direct relation between the ICE displacement and configurations with high efficiency. This is due to the high average power demand of the driv-

ing cycle. In contrast, a significant relation between configurations with low fuel consumption and small ICE displacements is obvious for the low power demand of the NEDC. The small displacement allows a continuous engine operation with high efficiency as illustrated in **FIGURE 7**. The map right above in **FIGURE 5** and **FIGURE 6** shows the maximum generator power to charge the battery. In the US06 the promising configurations show low to medium powers. The limitation is necessary to prevent operation points at high engine speeds, enriched mixture and low fuel efficiency. **FIGURE 8** shows the operation point distribution of the engine for the reference and optimised state for the US06. It can be noticed that due

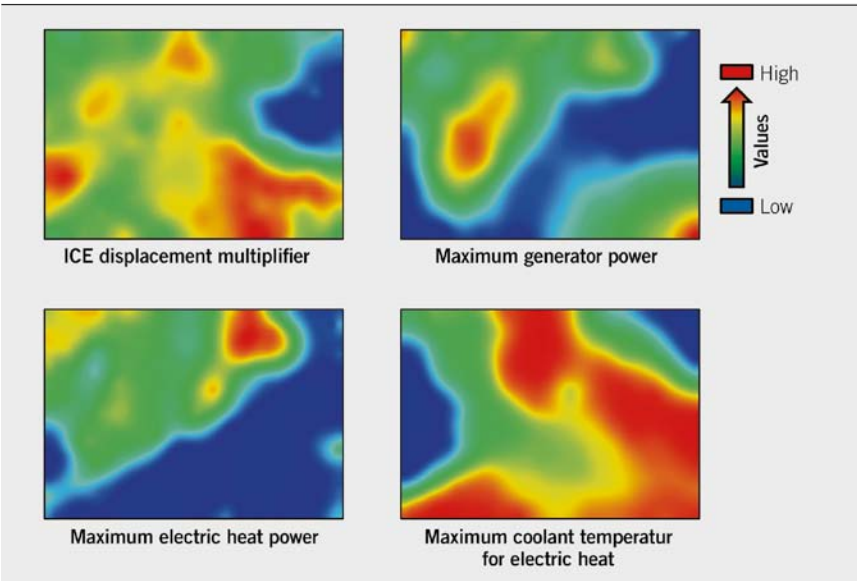


FIGURE 5 Self Organising Maps of the most important parameters in the US06

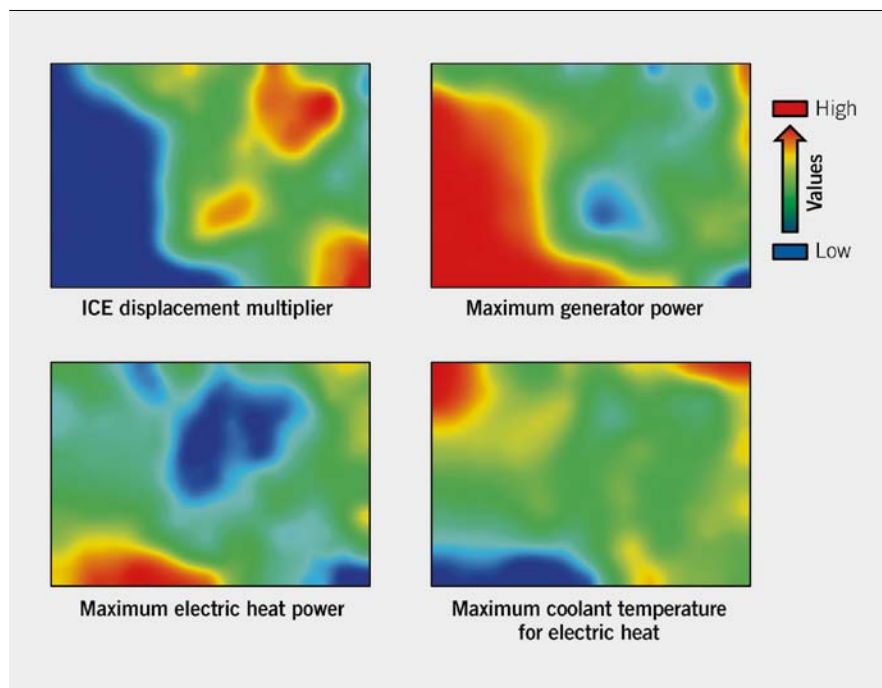


FIGURE 6 Self Organising Maps of the most important parameters in the NEDC

to the limitation of the power the engine speed decreases to more efficient areas in the fuel map. In contrast, all promising configurations have a high maximum generator power for the NEDC. This initially unexpected result is due to the optimised small displacement of the engine (two-cylinder instead of four-cylinder) and the generator power that scales similarly. The high amount of generator power is necessary for the power demand during the extra-urban part of the NEDC. The lower maps in **FIGURE 4** and **FIGURE 5** show the electric heating power and the coolant temperature threshold for electric heating. As it becomes clear from the maps, electric heating is not necessary for promising configurations for

the US06. Therefore, the temperature threshold has no effect. For the NEDC it is not possible to deactivate the electric heater completely, but as depicted in **FIGURE 7** and **FIGURE 9**, the electric energy heat demand can be reduced. For the promising configurations this is achieved by either reducing the electric heating power and a higher maximum coolant temperature or by reducing the maximum coolant temperature and increasing the electric heating power. In the first case the coolant is electrically heated with low power, but for a longer time range. In the second case the coolant is electrically heated with high power, but only for a short time range. In the end, both cases consume a similar amount of electric energy.

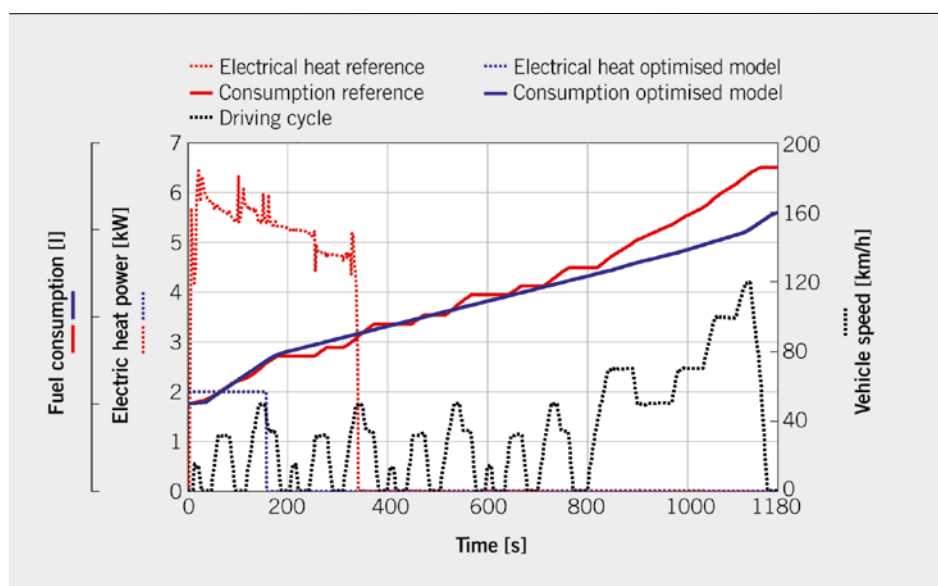


FIGURE 7 Vehicle speed and comparisons between the optimised and reference configuration of the fuel consumption and the electric heater power in the NEDC

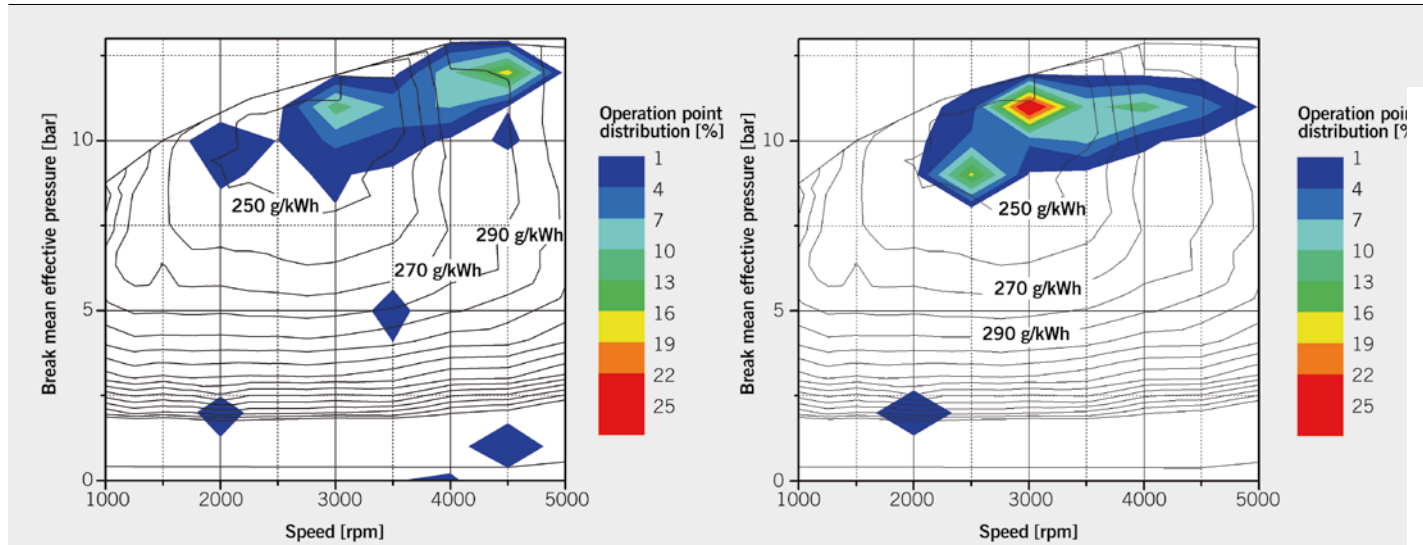


FIGURE 8 ICE Operation point distribution of the reference (left) and the optimised (right) configuration in the US06

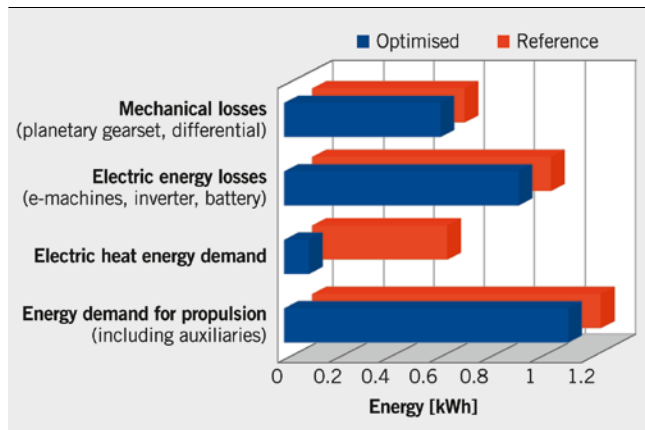


FIGURE 9 Comparison between the optimised and reference configuration of the energy demand in the NEDC

5 SUMMARY AND OUTLOOK

An optimisation algorithm has been presented and applied to a comprehensive numerical HEV model. It could be shown that the optimisation software is able to find good configurations in a complex search space with eleven parameters within approximately 1000 simulation calculations. It should be noted that the optimisation results are specific solutions of the two driving cycles. The dependence on the current driving cycle is illustrated by the significant differences between the optimisation results.

For a further performance improvement it is planned to split the specific driving-cycle in smaller periods and predict the target function value with neural networks for each period instead of the whole cycle. Due to the expected improved prediction of the neural networks they can be increasingly used, so the calculation time is shortened and extended real driving cycles can be calculated. Thus the optimisation should be more relevant to the current driving situation.

REFERENCES

- [1] Grebe, U.; Nitz, L.: Electrification of General Motors Vehicles – A Portfolio of Solutions. 32. Internationales Wiener Motorensymposium, 2011, VDI-Fortschritts-Berichte, row 12, No. 735
- [2] Krennek, T.; Lauer, T.; Bobicic, N.: Investigations on Heat Up Strategies of a Hybrid-Electric Powertrain Using a Comprehensive Vehicle Model. 16. MTZ-Fachtagung VPC.plus, 2014
- [3] Bacher, C.: Metaheuristic Optimization of Electro-Hybrid Powertrains using Machine Learning Techniques. Vienna: Vienna University of Technology, Master Study, 2013
- [4] Bacher, C.; Krennek, T.; Raidl, G. R.: Reducing the Number of Simulations in Operation Strategy Optimization for Hybrid Electric Vehicles. Lecture Notes in Computer Science, Springer (2014), Vol. 8602, pp. 553-564
- [5] Jin, Y.; Olhofer, M.; Sendhoff, B.: A Framework for Evolutionary Optimization with Approximate Fitness Functions. Evolutionary Computation, IEEE Transactions on, Vol. 6, pp. 481-494
- [6] Breiman, L.: Bagging predictors. Machine Learning, Vol. 24, No. 2, pp. 123-140
- [7] Kennedy, J.; Eberhart, R.: Particle Swarm Optimization. IEEE International Conference on Neural Networks, 1995, Vol. 4, pp. 1942-1948
- [8] Jastrebski, G.; Arnold, D.: Improving Evolution Strategies through Active Covariance Matrix Adaptation. IEEE Congress on Evolutionary Computation, 2006, pp. 2814-2821
- [9] Kohonen, T.: Self-organized Formation of Topologically Correct Feature Maps. In: Biological cybernetics (1982), Vol. 43, pp. 59-69
- [10] Pampalk, E.; Rauber, A.; Merkl, D.: Using Smoothed Data Histograms for Cluster Visualization in Self-Organizing Maps. Berlin Heidelberg: Springer, 2002, pp. 871-876
- [11] Vesanto, J.: Som-Based Data Visualization Methods. In: Intelligent Data Analysis (1999), pp. 111-126

THANKS

The authors thanks the Austrian Ministry for Transport, Innovation and Technology (BMVIT) which funded the project within the program "Future Mobility". Further thanks go to the Opel Wien GmbH and Adam Opel AG for their active support of the project.